Creating a local residual curvature during S-lay pipeline installation by lowering the stinger

M.Sc. Graduation Thesis

Alexandra Kalpakoglou

Delft, November 2020

Creating a local residual curvature during S-lay installation by lowering the stinger

by

Alexandra Kalpakoglou

Dipl. Civil Eng., Aristotle University of Thessaloniki

Thesis submitted in partial fulfillment of the requirements for the degree of

Master of Science
in Offshore and Dredging Engineering
at Delft University of Technology

Author name:	Alexandra Kalpakoglou
Student number:	4934369

Thesis committee:	Prof. dr. A. Metrikine	TU Delft
	Dr. ir. J. M. de Oliveira Barbosa	TU Delft
	Ir. T. Dronkers, Unit Head- Pipeline Engineering	Allseas Engineering B.V.

Delft, November 2020

A digital version of this document is available at `http://repository.tudelft.nl/`

'Cogito, ergo sum'

I think, therefore I am

René Descartes

Acknowledgements

This MSc Thesis was something more than just a prerequisite for the accomplishment of my studies in TU Deflt. It was an opportunity for learning, development and growth. Learning, due to the specific topic of research and the cooperation with specialised engineers. Development and growth, due to the completely new experience which considerably pushed me past my comfort zone.

During this journey, the support and guidance from the supervisors was invaluable. First of all, I would like to thank the chairman of the committee Prof. dr. Andrei Metrikine for his enlightening feedback during the progress meetings which contributed to the improvement and understanding of the research. Thanks to Thomas Dronkers, the Unit Head of Pipeline Engineering, for giving me this opportunity to be part of the Allseas group, and most importantly for undertaking the role of a mentor providing his guidance and expertise for the realization of this research. Furthermore, I feel grateful for having Dr. João Barbosa as a daily supervisor. João, thank you for the continuous support and patience, but most of all, thank you for being available for discussion during trying times. Finally, I should not fail to mention and thank all the staff of Allseas Pipeline Department and especially Robby van Vliet for the cooperation and for providing such a friendly and inspiring working environment.

Last but not least, I would like to thank my family, for giving me the opportunity to go abroad, grow as a person and engineer and for making me feel secure through their continuous and unconditional support. Of course, I cannot forget about my friends in Greece and the beloved people I met in Rijswijk and Delft who were always there to bring joy and unforgettable moments.

This is the closure to my MSc studies in the Netherlands and my student life in general. This has definitely been a happy ending due to your contribution. Thank you!

A. Kalpakoglou
Delft, November 2020

Abstract

Marine pipelines are often operated at high internal pressure and temperature. This loading condition results in the development of axial compressive force which can cause the pipeline to buckle globally. Global buckling occurs when significant lateral motion is present in the pipeline and excessive feed-in occurs at that specific location, which in turn forms into a sharp curve that can initiate destructive structural failure. Research has been conducted addressing the control of buckle development.

The ”buckle initiation” techniques were invented to mitigate the uncontrolled buckling of the pipelines on the seabed. These techniques involve the creation of less stiff sections in the pipeline (imperfections), so that buckling occurs in these locations. The most common buckle initiation techniques used in S-lay installation so far, are the ”snake lay” method, the ”artificial vertical out-of-straightness” and the ”distributed buoyancy” method. However, these techniques require the addition of subsea structures on the seafloor or larger pipeline length, which can increase the pipelaying cost dramatically.

A beneficial buckle initiation technique is the ”residual curvature” method. The residual curvature method (RCM) principle is based on creating intermittent residual curvature sections in the pipeline so that buckling can be initiated at these locations. The curvature sections are created by adjusting the settings of the already existing installation equipment. So far, this method is only used in reel-lay installation. It is particularly urgent to examine if the local residual curvature method can successfully be applied in pipelines laid by S-lay vessels, since S-lay is considered the most common and frequently used technique due to its adequacy on different water depths and pipe diameters.

The scope of this master thesis is to assess the feasibility of creating local residual curvatures in the pipeline by lowering the stinger during S-lay. The assessment is accomplished by simulating numerically the pipelaying process and the creation of the residual curvature, by analysing the behaviour of the pipeline while being lowered (in particular, looking at its twist/rotational behaviour) and by verifying if the alterations to the normal pipelaying procedure still respect the integrity of the pipeline and installation equipment.

Keywords: *offshore pipeline; S-lay method; overbend; sagbend; deep water; residual curvature; stinger inclination; bend moment- curvature diagram; static analysis; dynamic analysis; limit states; DNVGL; pipeline rotation; stinger integrity, OrcaFlex;*

Contents

List of Tables

List of Figures

Abbreviations

API	American Petroleum Institute
DCC	Displacement Controlled Conditions
DFF	Design Fatigue Factor
DNV- GL	Det Norske Veritas (Norway)- Germanischer Lloyd (Germany)
DP	Dynamic positioning
EA	Axial Stiffness
EI	Bending Stiffness
GI	Torsional Stiffness
HPHT	High Pressure High Temperature
ID	Inner Diameter
JIP	Joint Industry Project
LCC	Load Controlled Conditions
OB	Overbend
OD	Outer Diameter
ROV	Remotely Operated Underwater Vehicle
RCM	Residual Curvature Method
SB	Sagbend
SMYS	Specified Minimum Yield Stress
TDP	Touchdown point
VAS	Virtual anchored spacing
VIV	Vortex Induced Vibrations

Definitions

Terms frequently used in this report, constitute the basic terminology in the offshore pipelaying industry. Some of them are summarised and described here, to avoid potential misunderstanding.

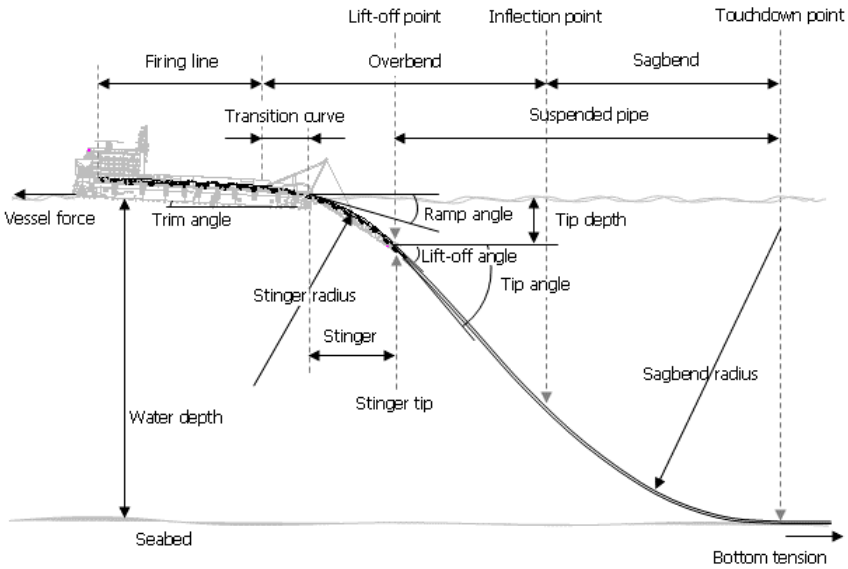

- **Stinger:** This is the main item in this report. Frame structure hanging from the pipelaying vessel. Its function is to prevent the pipeline from buckling when it is bent from a nearly horizontal position on the vessel through the first bend of an S-curve towards the seabed.
- **Pipe support:** Pipe supports can be track type or roller box types. Their function is to support the pipeline vertically and allow the pipe string to travel in the longitudinal direction of the vessel. Roller boxes contain a set of rollers in pairs. Track type supports are made of tracks similar to tensioner tracks. Both types of supports can be adjusted in height. Pipe supports are installed approximately every 12 m in the firing line and every 5 m to 12 m on the stinger (roller boxes only).

Figure 1: Pipeline on stinger supported by rollerboxes (visible in their white frame).

- **Stinger radius:** The stinger radius is the radius of a circle formed by the pipe supports on the stinger.

- **Overbend:** The overbend is the section of the pipeline where the pipeline is curved concave-down.
- **Inflection point:** At the inflection point the moment in the pipeline is zero. It is the transition point between the overbend of the pipeline and the suspended pipeline in the sagbend.
- **Touchdown point:** The touchdown point is the point where the pipeline touches the seabed.
- **Sagbend:** The sagbend is the pipeline section where the pipe is curved concave–upward. This is between the inflection point and the touchdown point.
- **Bottom tension:** The bottom tension is the axial tension in the section of the pipeline where it touches the seabed.
- **Lift-off angle:** The lift-off angle (or departure angle) is the angle, relative to the horizontal plane, of the pipeline at the point where the pipeline is no longer in contact with the rollers on the stinger.
- **Lift-off point:** The lift-off point is the point from where the pipeline is no longer in contact with rollers on the stinger.
- **Suspended pipe:** The suspended pipe is the part of the pipeline in suspension. This is from the lift-off point to the touchdown point. The radius of this part of the pipeline is not constant.
- **Tensioners:** Tensioners are the central element of most pipelay systems. Their function is to hold the pipe in suspension between the end of the stinger and the seabed, by applying a constant tension to the pipe. This tension is applied by exerting a controlled pressure of the tensioners' tracks on the pipe. When the barge is stationary the tension is kept constant, compensating e.g. for the effect of barge motions. When the barge moves forward, the tension in the pipe increases until a set limit. At the limit the tensioners start paying out.

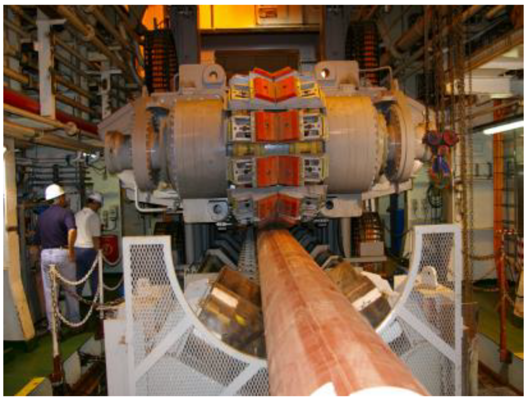

Figure 2: Picture of the tensioner with the clamped pipe.

- **Welding stations:** In the welding stations the lined-up pipe is welded onto the pipeline. The welding can take place in several welding stations; in each welding station the weld is filled with a number of layers, until the weld is completed. The welding can be done manually or with automatic welding machines.

Figure 3: Joint welding system.

Chapter 1

Introduction

Pipelines in Europe account for 85% of the natural gas [11], a rate currently increasing, due to the growing need for improvement of the current gas network and diversifying of supply routes [11]. Concerns in relation to the environment such as greenhouse gas emissions, air quality, oil spills, accidents amplify the idea that construction of new pipelines can contribute with environmentally viable alternatives [11]. Although pipelines already dominate over other means of oil and gas transportation, offshore industries are striving towards continuous improvement of the pipeline installation techniques and the reduction of the CO_2 emissions [1].

Gas transmission by pipeline is the transportation of gas over large distances and under high pressure and temperature [11]. Marine pipelines utilized for this purpose are the so-called high- pressure high- temperature pipelines. The high pressure and temperature differences are the main cause of structural failure of pipelines (unburied pipelines in deep water) due to lateral buckling [21]. In particular, when a pipeline is operated at high internal pressure and temperature it will attempt to expand and buckle laterally due to the compressive forces that are generated [30]. Research has been conducted addressing the control of buckle development, the stresses and the strains in the pipelines laid on the seabed.

1.1 Background

Previous studies have identified the buckle initiation techniques as a method to manage lateral buckling. The principle is based on creating sections with less stiffness at constant intervals in the pipeline, so that extension in axial direction due to temperature may occur in a distributed and controlled manner [37]. Comparison among several techniques demonstrates that the local residual curvature method is the most beneficial when it comes to simplicity, efficiency and cost-effectiveness. This method, patented by Statoil (2002) [12], involves the creation of local curvature in the pipeline during its installation and up to this time it is applicable to all steel pipelines installed from reel (reel –lay vessels), Figure 1.1. For example, one of the most significant and successful application of this method has been conducted in "Skuld project" 2012 (Statoil) [15].

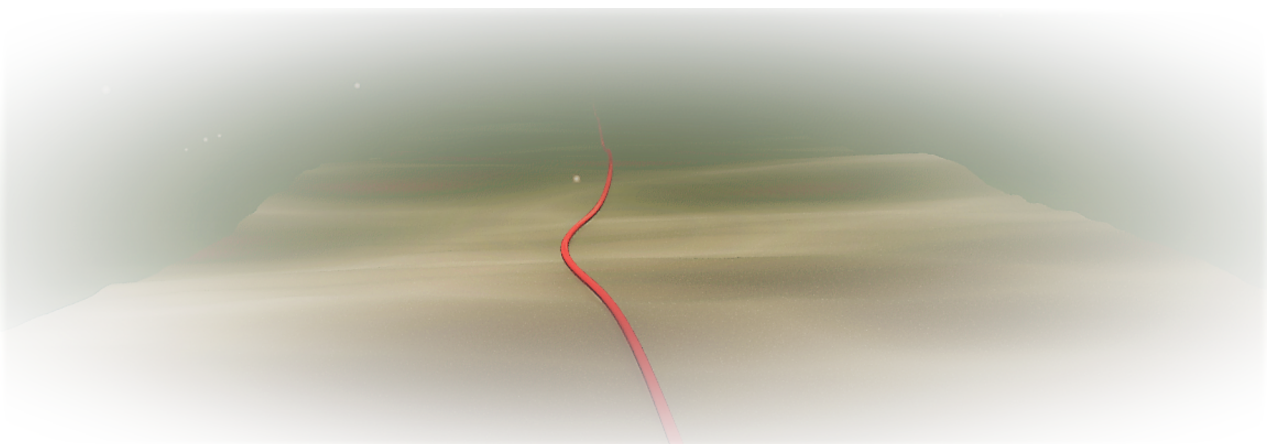

Figure 1.1: Typical configuration of the residual curvature on the seabed.

The invention of the local residual curvature method added value to the pipeline installation procedure due to multiple benefits. From a structural point of view, it is proven that this method is superior in triggering buckling at low axial compressive force [13], minimizing the risk of pipeline failure. In addition, the pipeline installation is independent of additional seabed structures and the pipeline length is shorter, introducing the cost-effective aspect of this method [13],[26]. Last but not least, the route of the vessel is remarkably shorter compared to snake-lay and so is the fuel consumption, since it sails on a straight path, contributing to the reduction of the environmental impact.

Although the local residual curvature method is a proven technique for reel-lay installation method, there is an absence of research concerning the S-lay installation method. It is particularly urgent to examine if the local residual curvature method can successfully be applied in pipelines laid by S-lay vessels, since S-lay is considered the most common and frequently used technique due to its adequacy on different water depths and pipe diameters. More specifically, S-lay installation method is named after the 'S' shaped curve that the pipeline forms during laying, Figure 1.2. This shape is achieved by two components on the vessel: the tensioner system and the stinger system. The stinger system guides the pipeline along its way to the seabed while the tensioner system applies an axial force to the pipeline to prevent buckling of the pipeline [28]. This effect increases with larger water depths and therefore larger tension must be applied to the pipeline [28].

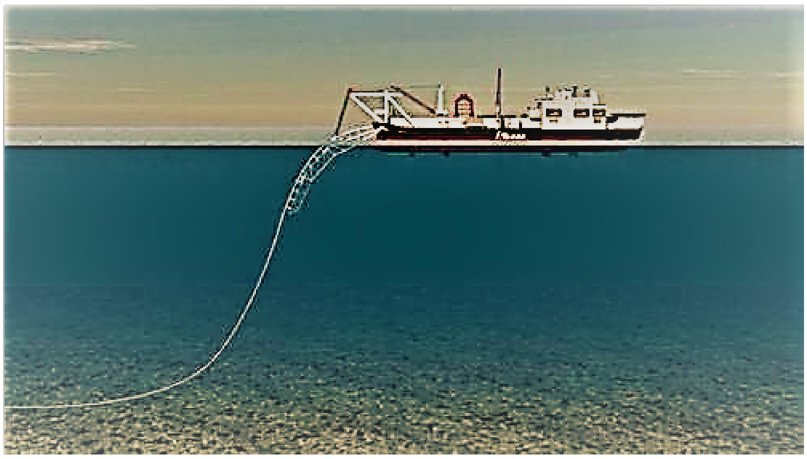

Figure 1.2: Side view of the S-lay installation method.

1.2 Thesis aim and approach

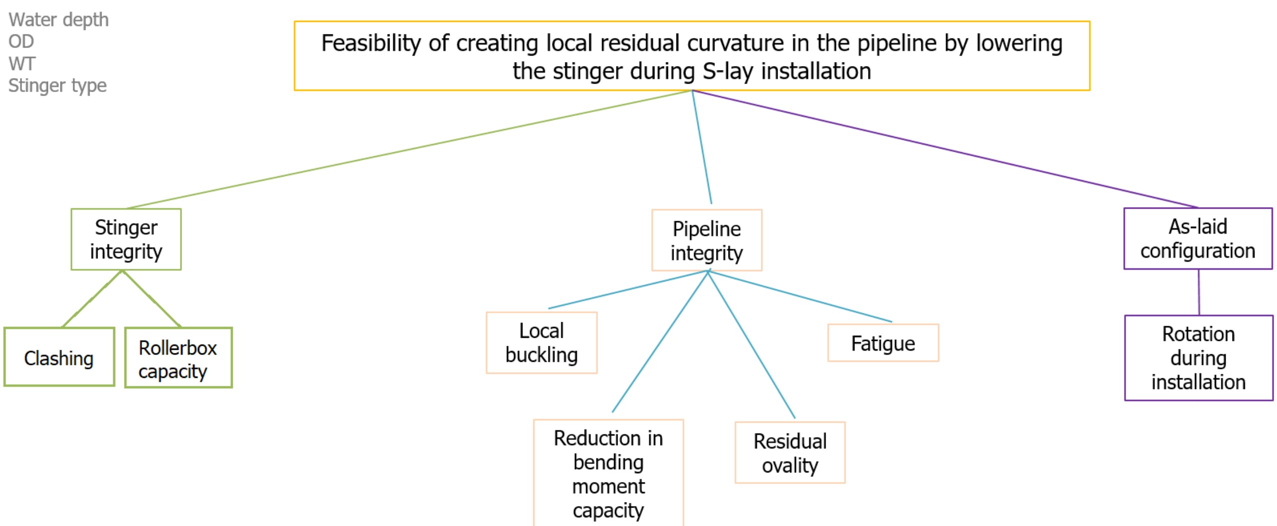

Figure 1.3: Schematic representation of thesis approach.

The lack of knowledge concerning the application of the local residual curvature method during S-lay installation leads to questions.

- *How can the local residual curvature method be incorporated in the S-lay installation method?*
- *Which adjustments are required in the procedure of normal pipe laying?*
- *Which are the effects of such alternations on the pipeline structural integrity?*
- *Which is the behavior of the residual curvature while suspended in the catenary area?*

These research questions will be addressed in collaboration with Allseas Group S.A.

Allseas is a pioneering company with leading figure in offshore pipeline installation, heavy lift and subsea construction. Founded in January 1985 by Edward Heerema, Allseas' vessels sail worldwide performing more than 275 projects. The invention of paramount importance for the pipelaying method was the concept of pipelaying on dynamic positioning (DP) vessels. Today, Allseas operates eight ships able to execute challenging projects that the increasingly demanding market imposes.

In addressing the research questions, this master thesis will investigate the effectiveness of lowering the stinger in order to create a local residual curvature in the pipe during installation. Firstly, a comprehensive literature study will be performed regarding the behavior of the pipelines with residual curvature. Furthermore, the report consists of two main parts (Figure 1.3). The first part is the methodology for the creation of residual curvature due to sufficient stinger inclination. The limit state checks to ensure pipeline integrity, as well as the calculations for the stinger integrity are presented too. For a given set of inputs (water depth, stinger radius, pipe properties) and for different stinger inclinations iterative static and dynamic analyses were conducted in OrcaFlex software. The assessment of the created residual curvature was based on the bend moment- curvature diagram. All the integrity checks were conducted in accordance with the DNV GL standards.

The second part refers to the pipeline behaviour during installation. Marine pipelines with residual curvature tend to rotate during installation. In this research, a comparative study has been done to define the differences in the pipeline rotation during common installation procedure and installation with residual curvature. Finally, it was examined whether the residual curvature met the requirements, when landed on the seabed, to act as buckle initiator. As a whole, this master thesis provide a guidance about the steps that need to be made in order to install pipelines with residual curvature during S-lay method.

1.3 Overview of chapters

Chapter 2 presents the literature review related to the research topic. Chapter 3 enlightens the reader about the theory, the methodology and the results of the required stinger inclination after conducting static and dynamic analyses in OrcaFlex 10.3d software for deep water installations. The corresponding effects on the pipeline integrity are addressed in Chapter 4. Additional integrity (safety) checks that need to be examined under dynamic conditions are presented in the same chapter. Chapter 5 describes the rotational analyses conducted for the assessment of the behaviour of the residual curvature before landing on the seabed as well as the as-laid configuration of the curved pipe section. The checks regarding the integrity of the stinger are presented in Chapter 6. Lastly, an updated version of the installation procedure is presented in Chapter 7 based on the conclusions highlighted from the outcomes of the said research study. A summary of all conclusions can be found in Chapter 8 while recommendations for further work are given in the Discussion section (Chapter 9).

Chapter 2

Literature Review

2.1 S-lay installation method

As described in Allseas' Installation file [3], offshore pipeline installation with S-lay method involves the attachment of a stinger to the stern of a lay barge to launch the pipeline from the deck to the seabed. The stinger is attached to the vessel either rigidly or with a hinge. Over the course of the time, pipelaying projects have become more demanding due to the ever-increasing water depth. The stinger configuration has had to evolve to cope with this change. The stinger's final formation is composed of several segments connected in series by special hinge joints, on the top of which there are adjustable rollers. In this way, the S-lay method became remarkably efficient to install long pipelines under extreme conditions. Tensioners control the laying of the pipeline and the rollers support the pipeline by forming a curvature. Hence, as the pipeline is being laid from the barge to the seabed under pre-tension, it forms an "S" shape, by which the name of the method is inspired.

The S-lay installation is characterized by three sections: the firing line, the overbend, and the sagbend (Figure 2.1). Firstly, in the firing line, the separate pipe joints are positioned in line and welded onto the pipeline elements. Several welding stations may occur to complete the welding faster. Each weld is checked in the following station, the non-destructive testing station. The final station of the firing line is the field joint coating station, where a protective coating is applied on the welded ends of the pipe. The welded, inspected and coated pipeline is driven in the water, controlled by the stinger and the tensioner. The upper curved part of the suspended pipeline is called the overbend while the lower curved part on the seabed is called sagbend. The transition point between the overbend and sagbend where the curvature of the pipe becomes zero, is known as the inflection point.

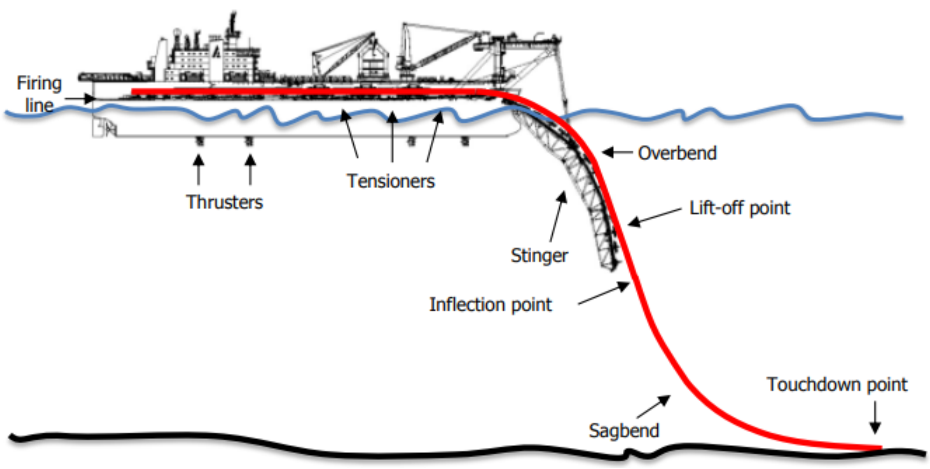

Figure 2.1: Schematic representation of the terminology used in the S-lay technique. Illustration of the "S" shaped pipeline installation [3].

The S-lay installation procedure is briefly described based on Allseas' Introduction file [3]. Initially, the barge is kept stationary by a mooring system or a DP system (dynamic position). The duration of immobility is determined by the time needed for a layer of weld to be completed in a welding station. As each pipe segment (joint) passes through one station of the firing line, the vessel moves forward. The pipeline, supported by the stinger and pulled by the tensioners, is introduced into the water and reaches the touchdown point on the seabed. Hence, every time the vessel moves forward, a length of pipeline equal to the length of a single pipe segment is installed.

The S-lay method contributed to the evolution of the marine pipeline installation due to its flexibility and capabilities. As enumerated by Tewolde [33], the adjustment of the stinger radius and departure angle combined with the use of tensioners, made the installation in deep waters feasible. Notwithstanding, it is suitable for shallow and intermediate waters as well. In addition, the S-lay method is the best method for installing large diameter single pipelines since a minimum modification is required to its system to suit varying diameter pipe. The production rates are higher compared to J-lay installation method, due to the simultaneous work been done in different stations of the firing line [24]. Lastly, the operation is often completed with the least amount of shore support and the method is beneficial for routing and minimizing spans.

2.2 Global buckling of marine pipelines on the seabed

Global buckling of a pipeline implies buckling of the pipe as a bar in compression and it has become a serious issue at present [37]. Moving from shallow to deep waters and nowadays to ultra-deep waters, pipeline operation has become more challenging than ever due to the higher environmental effects. Buckling is a form of instability, meaning that there is a change in the configuration of the structure in order to find a new equilibrium position. There are different types of global buckling shape. Downward buckling appears when the pipeline passes above a free span. Lateral (horizontal) buckling is experienced by pipelines laid on the seabed. Upheaval (vertical) buckling is usually observed at buried pipelines [37]. By performing small scale experiments, it was proven that lateral (horizontal) bucking is dominant, provided that there is no lateral restraint to the pipeline [17].

Global buckling of ”High- Pressure High- Temperature” (HPHT) pipelines is caused mainly due to a high compressive axial force. The pipelines have ambient temperatures after installation, but operate at higher temperatures [4]. This temperature difference leads the pipeline to expand its length. However, this expansion is restricted by the presence of constraints such as subsea facilities, rock dumping, and soil friction resistance in the longitudinal direction [4]. As a consequence, a compressive axial load is present, and when its magnitude exceeds a critical value (the so-called critical buckling load [20]) the pipeline experiences buckles. The effective axial load is characterized by the following equation [5]:

$$S_{\text{eff}} = N - P_i A_i + P_e Ae \tag{2.1}$$

where,

N	-pipeline axial steel- wall force
P_i	-pipeline internal pressure
A_i	-pipeline internal cross-sectional area
P_e	-pipeline external pressure
A_e	-pipeline external cross-section area

During operation, the effective axial force takes this form [5]:

$$S_{eff} = H - \Delta P_i A_i (1 - 2v) + A_s E \alpha \Delta T \tag{2.2}$$

where,

H	-residual lay tension
ΔP_i	-internal pressure difference relative to as-laid
v	-Poisson Ratio
A_s	-cross- sectional area of the pipe
E	-Young’s Modulus of Elasticity
α	-thermal coefficient of expansion
ΔT	-temperature difference relative to as-laid

The axial compressive force depends on the factors distinguished below, according to "DET NORSKE VERITAS" (DNV) Standards [37].

- Pipe cross sectional properties
- Lateral resistance
- Imperfection (out- of- straightness) on the pipeline
- Lateral buckling triggering force ([9], [4])

Therefore, global buckling may occur when one of the following conditions is present ([4], [37]).

- High effective compressive stress
- Low compressive capacity of pipeline
- Low pipe-soil resistance
- Light weight pipelines

In retrospect, global buckling is not a failure mode in itself. It is a load response instead. However, if the axial compressive force is left unmitigated, the resulting "rogue" buckles (Figure 2.2) are of an uncontrolled shape and uncontrolled strain [26]. Hence, global buckling entails other failure modes such as local buckling, fracture, fatigue [4] and decreases the axial carrying capacity of the pipe ([4], [9], [37]). Such failure modes affect the longevity and the functionality of the pipeline [26]. For this reason, it is vital to implement techniques where the peak loads and stresses remain within acceptable design limits.

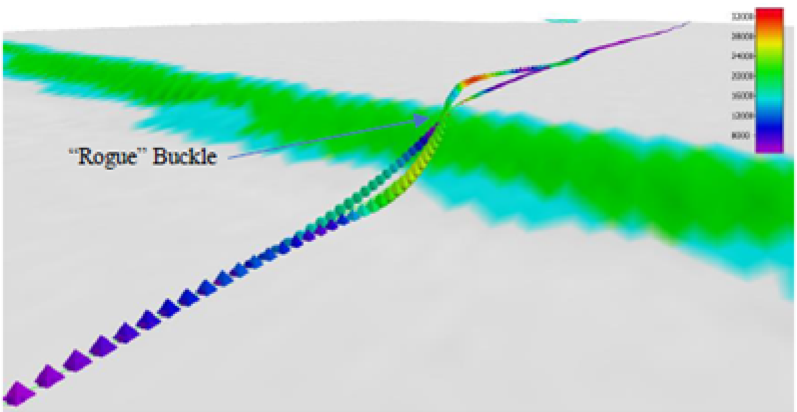

Figure 2.2: Rogue buckle forming at a free span shoulder [26].

2.3 Buckle initiation techniques

To ensure the pipeline longevity, the development of "rogue" buckles should not be left uncontrolled. Several techniques have been invented: "engineered buckling" or "buckle initiation" techniques. The principle is based on creating sections in the pipeline with less stiffness, so that extension in the axial direction (due to temperature) may occur in a distributed and controlled manner. In this way, pipe deflections are caused without producing large compressive forces. This is explained in Figure 2.3 below, where it is illustrated that as the curvature in a column increases, the level of axial force required to buckle reduces [37].

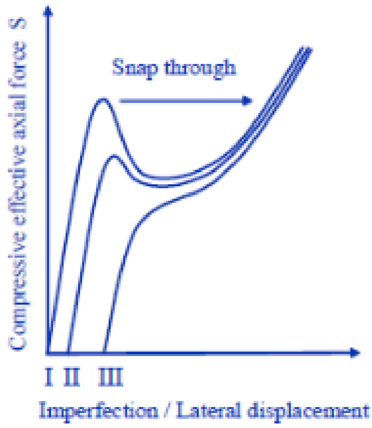

Figure 2.3: Load response of a globally buckling pipeline [37]

When the temperature and pressure in the pipe increase, the effective axial compressive force goes beyond the residual lay tension. The less stiff pipe sections are characterised by less capacity to compressive load. As a consequence, when the effective axial compressive force reaches the capacity of the first imperfection, buckling is initiated at this location, resulting in an instant drop of the compressive force. If the temperature and pressure keep increasing then the adjacent imperfection will buckle once its buckling capacity is exceeded. If the increase of the axial compressive force is not sufficient then buckling of the second imperfection is not triggered and localisation of axial feed-in into the first imperfection will occur [37]. For this reason, a safety margin should be documented during the design phase to avoid excessive feed-in [37]. Figure 2.4 illustrates the different stages of the axial compressive force. Initially, the force increases up to the point which causes the first imperfection to buckle ($S_{G,1}$). Afterwards, the load drops and again increases with a further increase in the pressure and temperature in the pipeline. A sufficient increase (ΔS) is required to trigger the second imperfection to buckle. The same behaviour is expected for the rest adjacent imperfections.

The most common buckle initiation techniques by which the pipeline is installed with imperfection, are snake-lay, artificial vertical out-of-straightness, distributed buoyancy and the local residual curvature method. The common aim of all these techniques is to impose relatively large out-of-straightness features at known locations [33].

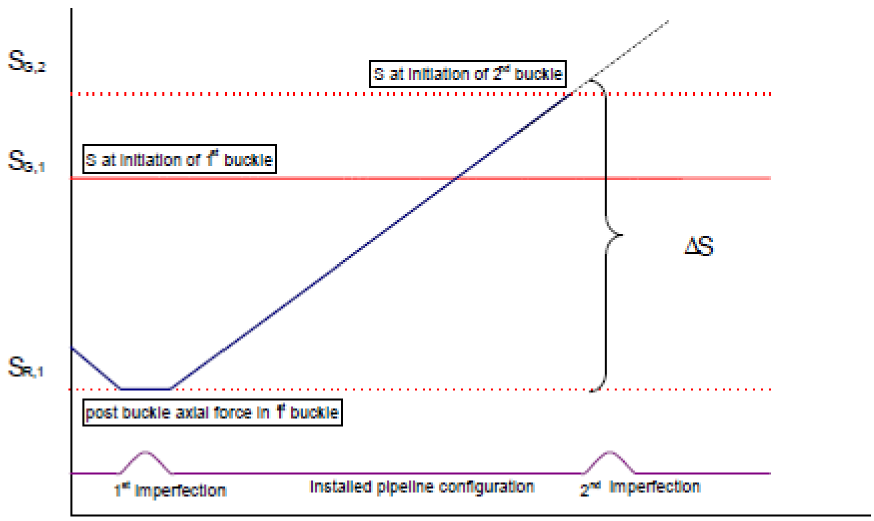

Figure 2.4: Sharing of buckles. Basic principle [37].

2.3.1 Snake- lay

The snake lay method is a procedure in which the pipeline is laid in a series of gentle curves in a zig-zag formation with the use of counteracts [33], [15]. The key parameters in the snake lay method are the snake pitch, offset and the bend radius [33]. The lay bend radius is typically 500-1500 m as shown in Figure 2.5 [15]. Under operating conditions, these regions absorb axial feed-in and lateral displacement occurs in a controlled way [15], [4].

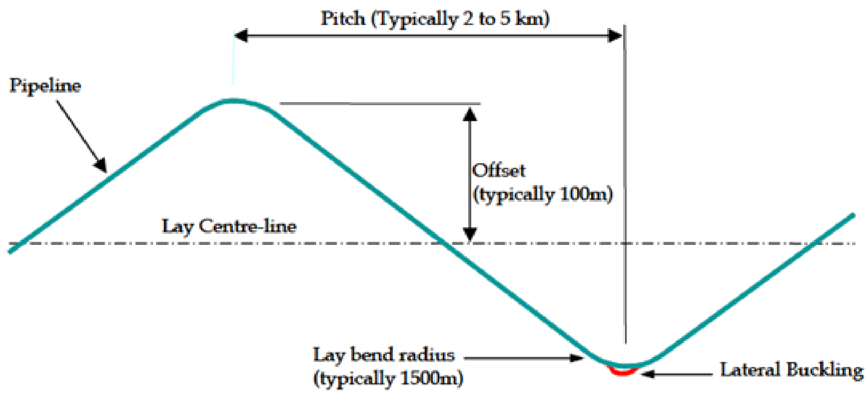

Figure 2.5: Schematic representation of the snake lay method [33].

2.3.2 Vertical out-of-straightness or vertical trigger berm method

The vertical out-of-straightness (vertical trigger berm) method is a procedure in which artificial vertical imperfections are produced [33], [15], [5]. These imperfections are usually produced by sleepers, concrete or rock berms which are placed on the seabed at a predetermined number of locations [33], [15], [4], [39]. This method takes advantage of the fact that pipeline buckling can be initiated in either the vertical or horizontal direction [33]. In principle, the imperfections raise the height of the pipe and the buckling is preferentially happening at these locations [33], [15], [39]. Unfortunately, these imperfections are expensive to install and free spans are susceptible to VIV induced fatigue and trawl-gear interaction. An illustration of the vertical out- of- straightness method can be seen in Figure 2.6.

Figure 2.6: Schematic representation of the vertical out-of-straightness method [33].

2.3.3 Distributed buoyancy

The distributed buoyancy method involves the installation of additional buoyant pieces on the pipeline in order to reduce weight. This buoyancy is installed in specific lengths of typically 60 to 200 m and act as buckle initiation sites [33]. The typical spacing between these modules is 2 to 3 km and its primary aim is to reduce the operational submerged weight of the pipeline at about roughly 10% of the normal submerged weight (Figure 2.7) [33]. This results in the creation of a natural out-of-straightness at the chosen locations thus the buckle initiation force is reduced. This effect increases the likelihood of buckling happening at the locations the buoyancy is applied [4]. Unfortunately, the same problems that arise in the vertical out-of-straightness method appear in this method as well [33].

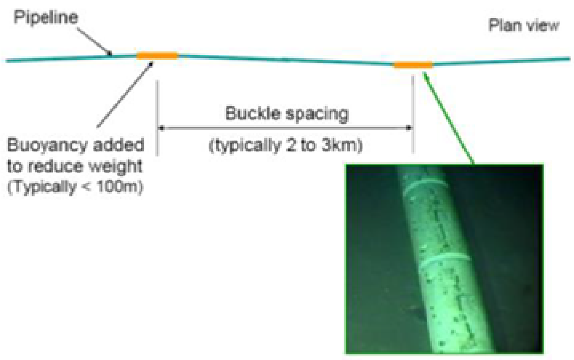

Figure 2.7: Buckling initiation by using distributed buoyancy [33], [4].

2.3.4 Residual curvature method

The residual curvature method (RCM) principle is based on creating intermittent residual curvature sections in the pipeline so that buckling can be initiated at these locations [33], [5], [4]. This concept was proposed by Geir Endal, patented by Statoil (2002) [12] and first applied offshore in 2012 [5]. More specifically, the patent mentions the term "thermal expansion loops". Sharing of expansion into adjacent buckles means that the expansion potential is released into imperfections in the pipe configuration at various locations [37], [4]. The geometry of the pre-bent curves of the thermal expansion loops should be such that the stiffness in the longitudinal direction will be substantially less than the axial stiffness for a straight pipe [12], [5]. As shown in Figure 2.8 below [5], the ratio of the stiffness of the pre-deformed pipe section to the stiffness of a straight pipe decreases as the applied axial force increases. In addition, the ratio $P_{ax}/(K_p * L_w)$ increases as the axial force is increased. This happens due to the reduction of the stiffness of the deformed pipe section [5].

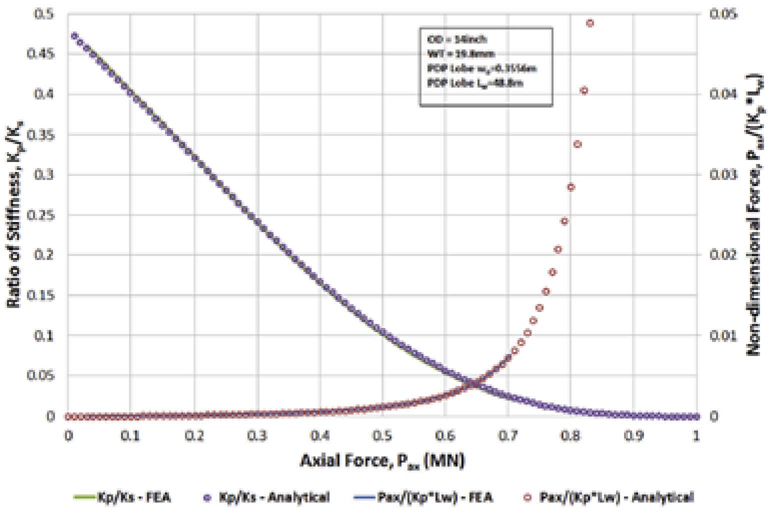

Figure 2.8: Stiffness ratio (K_p/Ks) and $P_{ax}/(K_p * L_w)$ ratio plot [5].

So far, this method is only employed in reel-lay installation technique. The typical RCM geometry consists of 0.20-0.25% residual strain over a short length (usually 20-60m) every km or so, meaning that this method makes use of plastic deformations instead of elastic out-of-straightness [33], [15], [5]. There are also transition sections on either side of the central curvature section as illustrated in Figure 2.9. The straightener system in reel-lay normally employs a three- point bending system whose positioning settings are hydraulically adjustable [26], [33]. In a typical reel-lay vessel, the pipe leaves the reel, naturally wanting to curl. The straightener will then produce a straight pipe by bending the pipe in the opposite way. During reel lay, several quick adjustments in the straightener system create sections of residual curvature by not straightening the pipeline (under-straight sections) [4]. Detailed review regarding the creation of residual curvature in the pipe during reel-lay procedure can be found in Section 2.4.1. Figure 2.10 taken from Endal's patent [12] represents the creation of residual curvature during reel-lay.

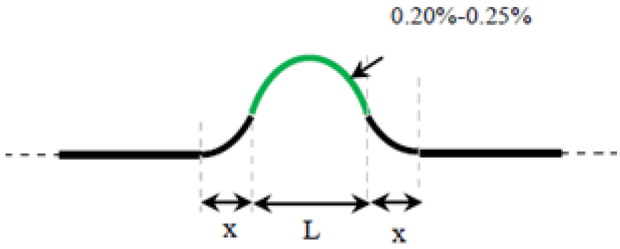

Figure 2.9: Residual curvature and transition sections [33], [15], [5].

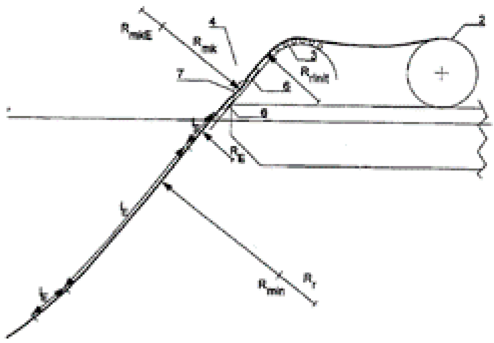

Figure 2.10: Side view of a vessel provided with a pipeline reel and a straightening means for the pipeline. Preferred embodiment of the residual curvature method to the reel-lay installation [12].

2.3.5 Comparison of the techniques

A detailed comparison between the conventional techniques and residual curvature technique is presented in Table 2.1.

Table 2.1: Comparison between residual curvature method and other methods.

Conventional Techniques		**Residual Curvature**	
Pros	Cons	Pros	Cons
• Proven method	• Additional measures at the seabed, hence more expensive methods	• No additional measures required, hence more economical and robust technique	• Only for reeling so far
• Used in S-lay	• Pay-out stops to install the buckle initiation equipment, hence more time consuming method	• Adjustments in the straightener system take 10-20 minutes per location and the pay-out is continuous, hence faster method [2]	• No track record for S-lay
	• More space on the seafloor due to larger offset and bend radius	• Less footprint, hence increased flexibility for routing of future lines	
	• Longer route	• Shorter route (5% route length reduction is achieved)	
	• Detailed route planning required, hence significant impact to the schedule of the project in case something needs to change	• Allows for the late design stages as no additional procurement or logistics are required	
	• Larger critical buckling force	• Superior in triggering buckling at low axial compressive force (50% lateral buckling force is achieved)	
	• Higher utilization of the bending moment	• Post-buckle strains are lower, hence no risk of overstressing and no need of special welding	

2.4 State of the art- Local residual curvature method

In this section, all the important insights of the research for the suitability and the applicability of the local residual curvature method are presented. There is sufficient background information about the implementation of this method during reel-lay installation technique, which can constitute the basis for the understanding, the development and the utilization of the method in future projects.

2.4.1 Creation of Residual Curvature during reel-lay installation

The reel-lay installation method is named after the reeling and unreeling process that the pipeline experiences during installation. It is a cost-effective method since most of the welding operations are conducted onshore [23], [15]. The steps of the standard reel-lay installation are the following [15], [16], [23], [19] : The already welded pipeline is reeled onto a large diameter reel on the vessel for transportation, a procedure which involves loading of the pipeline beyond the elastic limit of the material. During installation, the pipeline is unreeled and driven into the water through the installation equipment, namely the aligner and the straightener. The pipeline is under tension between the reel and the aligner ("overbend" in Figure 2.11) where it experiences second bending. The plastification of the pipe by the reel results in a residual ovalisation which is a critical parameter for the collapse resistance of the pipeline, especially in deepwater applications. To prevent or control such a transformation of the pipeline shape, the pipeline goes through a hydraulically adjustable straightener system, Figure 2.12. The pipeline is subjected to a reverse plastic bend in the straightener (three-point bending). Thus, the pipeline leaves the vessel in a straight shape.

Installation of the pipeline with residual curvature is successfully done by changing the settings of the straightener system [29], [16]. The pay-out procedure stops every time the upper and lower track of the straightener need to be relocated to the desired level. This level is determined by whether or not the pipeline needs to be left with a residual curvature [16]. Over-straightening of the pipe can be achieved by pushing the upper track closer to the pipe, while a curvature can be maintained in the pipe if the upper track is retracted away from it [16]. Hence, the contact force between the pipe and the upper track reduces, allowing for the creation of pipe sections with residual curvature [19].

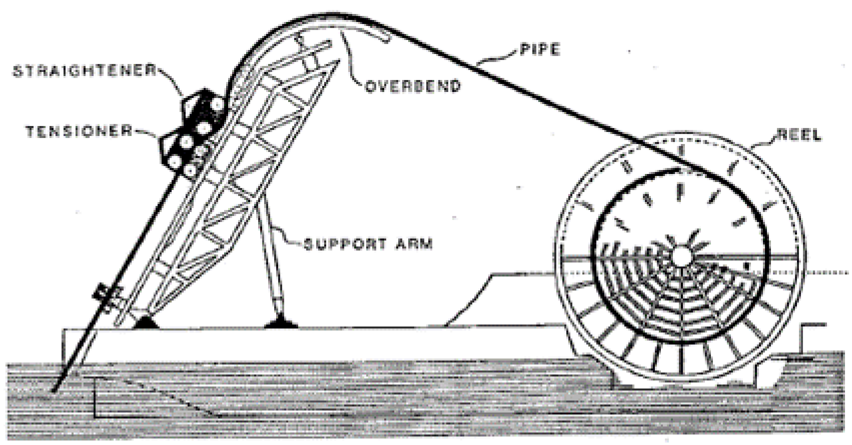

Figure 2.11: Schematic representation of reel-lay installation technique [23].

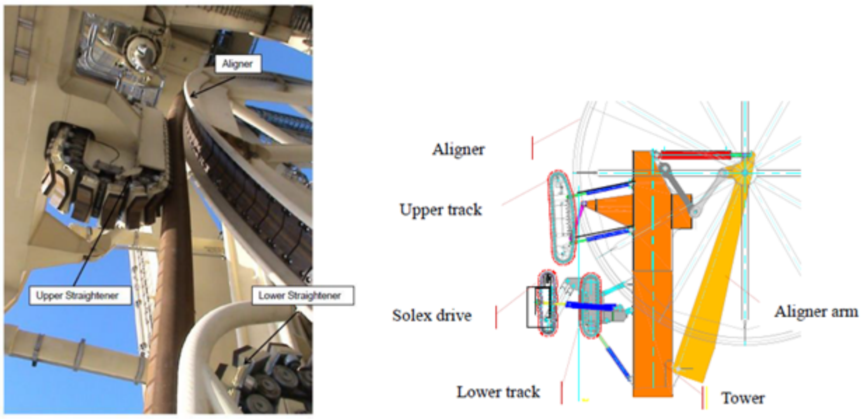

Figure 2.12: The straightener equipment comprises the aligner, the upper and lower straightener (tracks) [29], [16], [19].

Numerous analyses were conducted to investigate the interaction between residual curvature and the tensioner. In the paper of Karjadi et al [19] a full reeling model was created which included the effects of the reeling-off procedure from the transportation vessel. Initially, it was proven that variations of the pipe material strength do not impede the creation of sufficient residual curvature in the pipe. After performing separate analyses, one including and one excluding the tensioner loads, for given straightener settings, it was concluded that the impact of the tensioner (squeeze load and top tension) on the achievement of the desired residual curvature is negligible.

2.4.2 Applications

When it comes to the efficiency of the said method, research studies provide guidance, but the experience is fundamental. The local residual curvature method has already been applied in a few projects, described below.

Skuld project

Statoil's project in the Norwegian Sea in 2012 which first used the local residual curvature method during reel-lay installation [15], [16]. An approximately 26 km long 14”-16” dual- diameter pipeline was installed using Subsea 7's reel ship “Seven Oceans” [15]. The residual curvature strain was 0.2% approximately of 40 m length surrounded by a 15 m long transition section. The 0.2% residual curvature corresponds to 100 m bending radius [15].

Significant conclusions driven from this project are [15]:

- It is not necessary to perform straightening trials to verify the residual curvature level.
- The pipeline response is little sensitive to the residual strain variations (0.15%, 0.20%, 0.25%).
- Little sensitivity of the pipeline utilization to a relatively large variation of soil-pipe interaction model. Therefore, the residual curvature dominates the response.
- The load-controlled condition (LCC) utilisation at the buckle locations was within the acceptance criteria, including trawl pull-over load.
- Efficient offshore installation with the reeling ship. Additional vessel time was 10-20 minutes per location.
- Pipeline rotated typically 90° during installation so that the residual curvature locations ended in the horizontal plane.
- ROV surveys showed that global buckling had been triggered at all the residual curvature sections, see Fig 2.13, so that sharing of thermal expansion and acceptable pipe utilization was confirmed.

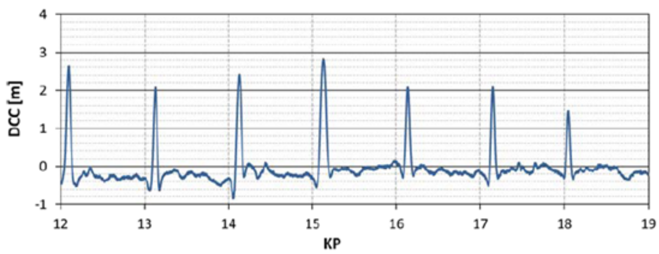

Figure 2.13: Results from Skuld ROV survey. Measurement of the lateral displacement of a part of the pipeline. Residual curvature sections created at one km intervals (KP12.1, KP13.1 etc) [15].

Edradour Production Pipeline

The Edradour field is located to the North West of the Shetland Islands on the UK continental shelf [6]. A 1.2 km long cooling section was installed by Technip using the residual curvature method lateral buckling initiator, as part of a 12" production pipeline [6], [16]. The water depth is approximately 300 m. The results of the in- place analysis show that the RCM effectively mitigated the risk of the pipeline buckling elsewhere within the cooling section. The method demonstrated to be a robust and reliable approach to trigger pipeline buckling. A schematic representation of the RCM section of the pipeline can be seen in Figure 2.14. A key takeaway from this project is that following calibration, the RCM buckle initiator shapes from the simplified method compare very well to those predicted by the detailed reeling model [6].

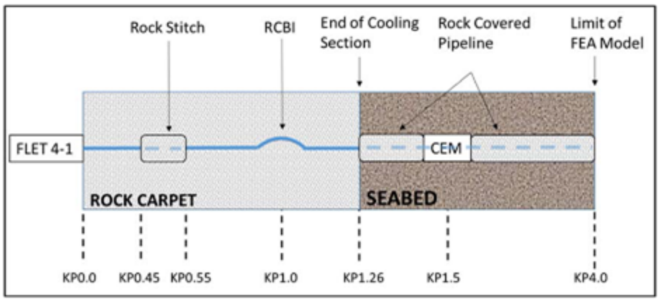

Figure 2.14: Schematic view of the Edradour Cooling Section – FEA model [6].

Other projects such as the pipe-in-pipe flowline in the Norwegian Sea designed by the IKM Ocean Design confirmed the numerous benefits of the local residual curvature method compared to the other buckle initiation techniques (snake-lay).

2.4.3 Rotation of the pipeline before landing on the seabed

The first investigation of the pipeline twist while suspended was conducted in 1995 by Geir Endal [14], the advisor of Statoil for pipeline technology matters. More specifically, Endal tried to quantify the roll angle of the pipeline and to examine the effect of the plastic strains developed in the overbend during installation on the as-laid configuration. It must be noted that the goal was to install a straight pipeline on the seabed and not a curved configuration, as it is currently under research.

Firstly, a simplified analytical model was conducted. The roll angle resulting from this approach was the one which gave the minimum total work in the sagbend area (the structure should end up to a position where the total potential energy of the system is lessened). The total work was assumed to consist of a roll contribution and a bending contribution, see equation 2.3. The roll was assumed to happen between the inflection point and the touchdown point and the angle was dependent on the corresponding pipeline length between these two points, the residual curvature caused from the stinger configuration in the overbend area, and the nominal curvature in the sagbend. Secondly, a 3D non-linear finite element analysis was done in Abaqus software. The model represented an S-lay installation procedure where the lay barge and the seabed were modelled as rigid surfaces while the pipeline was modelled based on the 3D beam theory. After testing for different depths (shallow waters) and the combination of stinger radius and pipe tension, he showed that for large stinger radius, the pipe rolled with a rapid increase. The roll was initiated after the inflection point where the reversed bending of the sagbend area occurs. In addition, it was proved that low plastic strains in the overbend (maximum 0.3%) did not influence the straight configuration of the pipeline on the seabed.

Lastly, the role of the tension was examined as well. Two contradictory phenomena were observed. On the one hand, an increase in the tension resulted in a decrease of the sagbend curvature and subsequently, the roll was decreased too. On the other hand, a further increased tension caused a reduction in the torsional resistance which allowed for a growing roll. Therefore, it can be concluded that the initiation of pipeline roll is dependent not only on the combined plastic strains over the stinger and the reversed bending in the sagbend, but on the pipe tension as well.

$$W_{tot} = W_R + W_B = \int_0^L M_R(x) * \phi(x)dx + \int_0^L M_B(x) * \kappa(x)dx \tag{2.3}$$

Where,
$M_R(x) = GI_T \frac{d\phi}{dx}$, the roll-momentum
$M_B(x) = EI * \kappa(x)$, the bending moment

A few years later, more research upon the pipeline twist was conducted by Damsleth et al in 1999 [8]. In this paper, the focus is on the relation between the minimum potential energy and the phenomenon of rotation. More precisely, when the pipeline is plastically bent due to the curvature of the stinger, the equilibrium of the system will be found in the sagbend area where a balance between three different energies (torsional, potential, bending strain) is reached. In the catenary area, where the pipeline is suspended, the twist will just lead the pipeline to a lower potential energy situation. On the contrary, an elastically bent pipeline already has the minimum potential energy, hence no twist is initiated. Therefore, the paper concludes that pipeline rotation is induced by the minimization of the potential energy [8].

To validate the aforementioned conclusion, Damsleth et al [8] created 3D models of three different cases. A straight pipe, an overbend pre-bent pipe (R=571 mm, 0.1% residual strain) and an underbend pre-bent pipe (R=571 mm), as seen in Figure 2.15. The one end of the pipeline was fixed and the other pinned, but both were at the same height. The loads were applied in two steps, firstly a horizontal current was applied which caused an out-of-plane bending and secondly, the submerged weight and the horizontal tension. Analyses of the rotation at the midpoint of the pipe with respect to the lateral force showed that the straight pipe had zero rotation, the underbend pipe had a very small rotation, and lastly, the overbend pipe showed a significant rotation, see Figure 2.15. In addition, it was proved that the angle of rotation is linearly dependent on the lateral force, meaning that the pipeline twist is a “stable process” [31], [8].

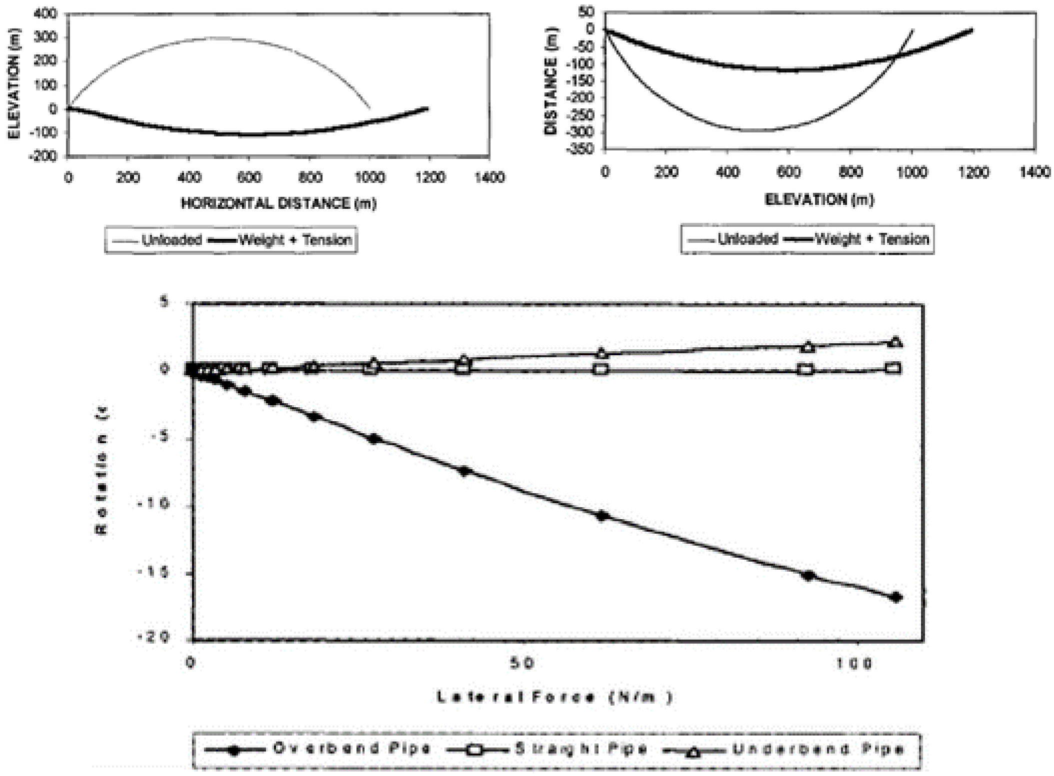

Figure 2.15: Left: The pre-curved overbend model in its free and loaded conditions. Right: The pre-curved underbend model in its free and loaded conditions. Bottom: Rotation profile of the overbend, straight and underbend pipe [8].

The issue of pipeline twist came back to the fore in 2016, in the context of a master thesis conducted in Delft University of Technology [31]. More specifically, the pipeline twist was assessed during lowering and lay operations in shallow waters with the reel-lay method, due to plastic deformations developed in the pipeline by the straighteners. Both cases were analyzed by using the Endal's analytical equations [14] and finite element models. It was proven that the lack of considering the out-of-plane bending due to horizontal currents, in the analytical equations, resulted in inaccurate twist approximation, especially for large residual curvature (small radius of residual curvature) for which the out-of-plane bending becomes dominant [31], [19]. In addition, inspired by Damsleth et al paper [8], it was established that when the pipe is understraighten (overbend) it rotates significantly before reaching the touchdown point, while for an overstraighten (underbend) pipe the twist is negligible. Thus, the pipeline twist can be controlled by selecting the appropriate straightening direction or by managing the magnitude of the residual curvature itself.

At the same period, companies from the oil and gas industry showed an insatiable interest to investigate more about the pipeline rotation when applying the residual curvature method. As a continuation of the previous studies, Karjadi et al [19] examined the twist of the residual curvature in deep waters by creating 3D numerical models in Flexcom software. Four different cases for the pipe end on the seabed were modelled, shown below:

1. Free end
2. End with twist constraint
3. Twist constraints at three different locations on the seabed
4. Twist constraint next to the touchdown point

The conditions for all cases were the same, namely a small lateral distributed force (1 N/m) was applied on the residual curvature and the seabed was modelled as a rigid surface without friction [19]. The results from the analyses revealed that the residual curvature section can achieve a sufficient rotation when it is located at least 400 m from a twist constraint. Moreover, it was proven that even a small lateral force (for example a current) can force the residual curvature to overturn.

The relation between the length of the residual curvature and the pipeline twist has been examined as well [33]. Based on the analytical equations of the energy approach [14], it was assessed that for long residual curvatures (50 m- 150 m) the roll angle for which the total work was minimum, was larger than 90 degrees. Other parameters that influence the pipe roll angle are the pipe diameter and the pipe D/t ratio. When the diameter is large or the D/t ratio is reduced, the system finds its equilibrium for small twist angles [33]. Lastly, the roll angle is growing for increasing water depth [33], [36].

In retrospect, the rotation of the pipeline in the catenary area exists and is dependent on several parameters. The pipe properties, the plastic strains induced in the pipeline and the length of the corresponding residual curvature, the conditions during installation and the presence of constraint on the seabed, all affect the behaviour of the pipeline. As a conclusion, the prediction of the angle of rotation is a difficult and complicated task.

2.4.4 On- seabed behaviour of the pipeline with residual curvature

The final area of research regarding the feasibility of the local residual method as a lateral buckling mitigator, is the investigation of the behaviour of the bent pipe sections during operation. Cooperation of researchers and industry gave rise to the consolidation of the characteristics of the on-seabed pipeline response to buckling. The key findings are presented in this section.

Teigen and Ibrahim [32], developed a 3D finite element model in Abaqus software, which represented a reel-lay induced imperfection (0.2% residual strain) in an 14" pipeline. After exposing the pipeline to particular operational loads (in 360 m water depth), they verified that the maximum lateral deflection occurred at the location of the imperfection (Figure 2.16). This means that indeed the creation of residual curved sections act as means of triggering buckling in known locations. The shape of the residual curvature on the seabed was affected by the residual lay tension. However, this residual lay tension has no impact on the buckling behaviour (Figure 2.17 [1]); the buckling behaviour depends on the built-in residual strain and not on the shape of the imperfection. The higher the residual strain, the smaller the effective axial force (Figure 2.17). The effective axial force is influenced by the length of the residual curvature as well. For longer imperfections, the axial force decreases (Figure 2.18). An additional parameter which influence the effective axial force, is the soil friction. By testing for different axial and lateral soil friction coefficients, it was concluded that the larger the soil resistance to pipeline movement, the larger the effective axial force required to make the pipe section with residual curvature to buckle (Figure 2.18). Lastly, the development of the axial effective force is independent of the presence or not of the transition sections in the model.

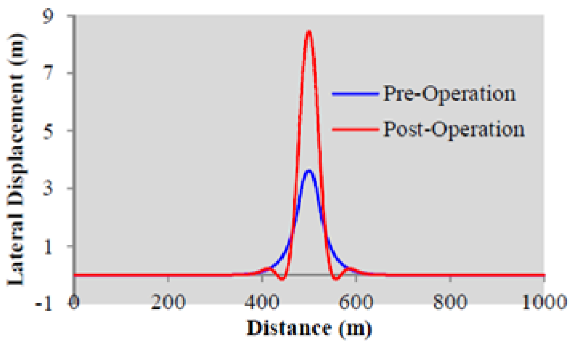

Figure 2.16: Significant lateral displacement at the location of imperfection after the application of operating loads [32].

[1] axial feed-in is considered the "maximum axial pipeline displacement from the one side of the imperfection"[32]

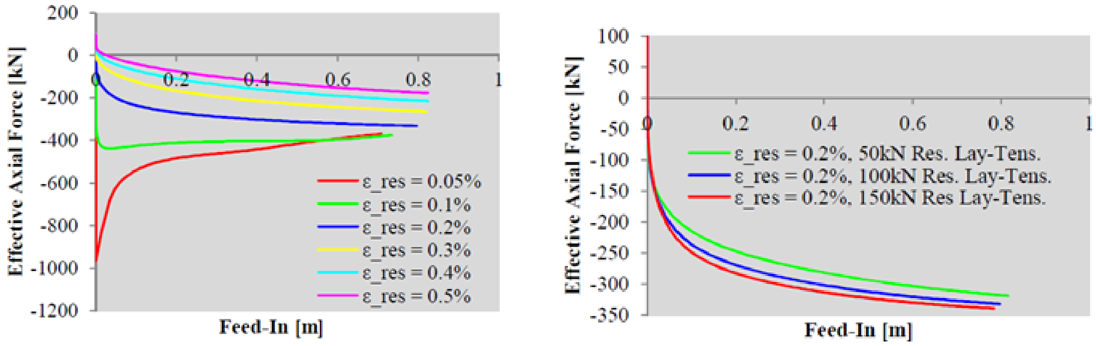

Figure 2.17: Left: Impact of the magnitude of residual curvature on the effective axial force. Right: Negligible effect of the residual lay tension on the induced effective axial force [32].

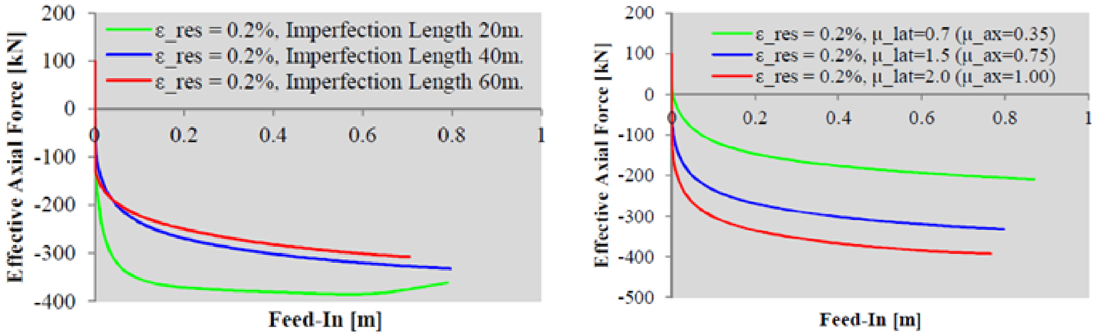

Figure 2.18: Left: Sensitivity of the effective axial force to the length of the imperfection. Right: Induced effective axial force in the imperfection for different values of soil friction coefficient [32].

On top of the aforementioned insights, Gallegillo et al. [16] tested whether the complicated full-reeling modelling can be replaced by a simple monotonic bending model. After creating the two models (complex and simplified approach), they performed a comparison of the results of basic limit state checks from each case. They used the same pipe diameter as Teigen and Ibrahim [32] and approximately the same water depth (300 m). Regarding the on-seabed behaviour of the pipeline under operational loads, they were driven to the same conclusions as the previous research [32]. Regarding the simplification of the model, it was observed that the model of simple monotonic bending can efficiently represent the creation of residual curvature in the pipeline. Such a conclusion proved to be helpful for the researchers after Gallegillo, since the analysis from the simplified model is significantly faster and can be easily used for the creation of a series of imperfections along the whole pipeline.

The post buckle strain state has been assessed, encountering for the impact from the anchored point in deep water conditions [7]. For the case examined it was proved that when using the residual curvature method, the peak strain from the buckle smoothly increases with the distance from a fixed point, while for a straight pipeline, the increase follows a higher slope, reaching high and sometimes unacceptable strain values (Figure 2.19). It is clearly illustrated that at a virtual anchored spacing of 3km, the peak strains induced in the curved section are less than 0.4%, while for a straight pipeline, the peak strains in the “rogue” buckle that appears, reach the extreme value of 1.0%. This constitutes a validation that the residual curvature method is superior at delivering “benign” buckles at pre-determined positions [7].

Another parameter which affects the buckling behaviour of the residual curvature on the seabed is the twist angle. Possibly the curvature rotates 180 degrees, therefore it lands on the seabed with the crown oriented downwards [7]. In such a case, the soil contact pressure as well as the lateral friction, increase. The final configuration of the residual curvature can be seen in Figure 2.20. The lateral displacement of the middle point of the residual curvature resulted smaller than the displacement of the lobes of the section (transition sections). In this way, the bending strains are shared to three points rather than being concentrated to the crown of the curvature. This behaviour reveals that even an inverted residual curvature section (rotated by 180 degrees), shows a favourable response under operational loads [7].

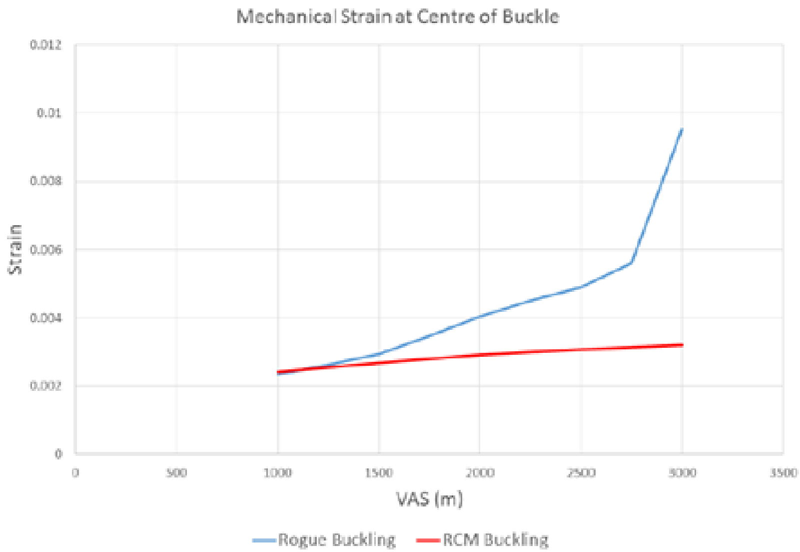

Figure 2.19: Peak strain in buckle [7].

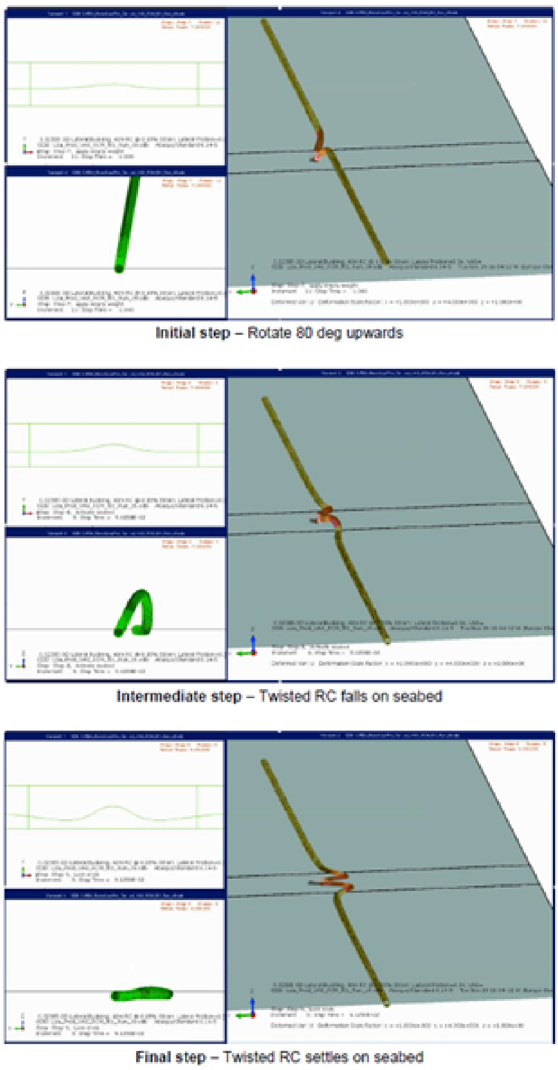

Figure 2.20: A step-wise presentation of an inverted curved section, as it falls on the seabed [7].

A year later, a sensitivity study was conducted to assess the behaviour of a perfectly- straight and perfectly-pre deformed pipe section in comparison to the behaviour of an imperfectly-straight and imperfectly-pre deformed pipe section [5]. In reality, the creation of residual curvature may involve some variation in the amount of deformation (tolerances). Initially, for a 14” pipe, it was confirmed that for increasing operational loads, the induced effective axial force is smaller in a pre-bent pipe rather than in a straight pipe (Figure 2.21). This results from the reduced stiffness of the pre-bent section.

When the lobes are perfectly designed or when the pipeline is perfectly straight, the effective axial force continuously increases as the operational loads increase. On the other hand, when an imperfection is introduced in the design of the curved section or the straight pipeline, there is a significant drop in the effective axial force, see Figure 2.22. This drop characterises the occurrence of buckling. As seen, when the pipeline contains curved sections, buckling occurs for higher operating loads. For the case examined, the first buckle appeared at 75% of the operating load.

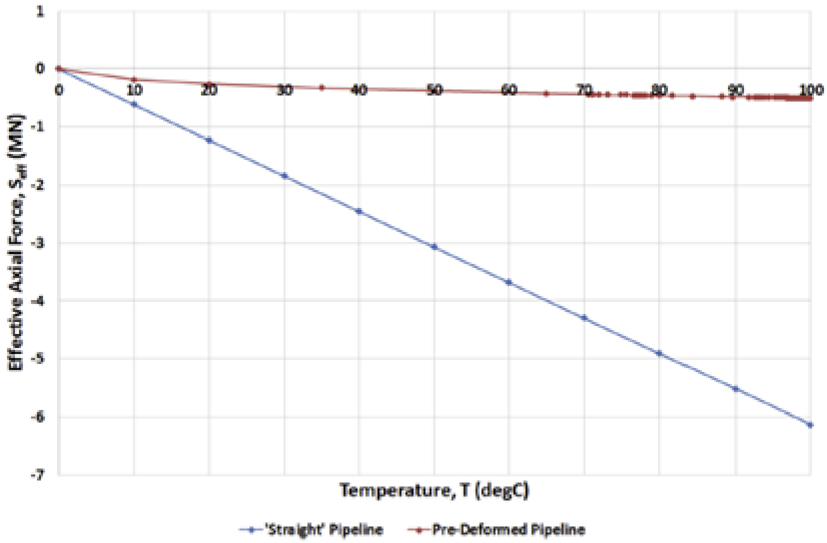

Figure 2.21: Effective axial force significantly smaller for a pre-deformed pipeline and a straight pipeline [5].

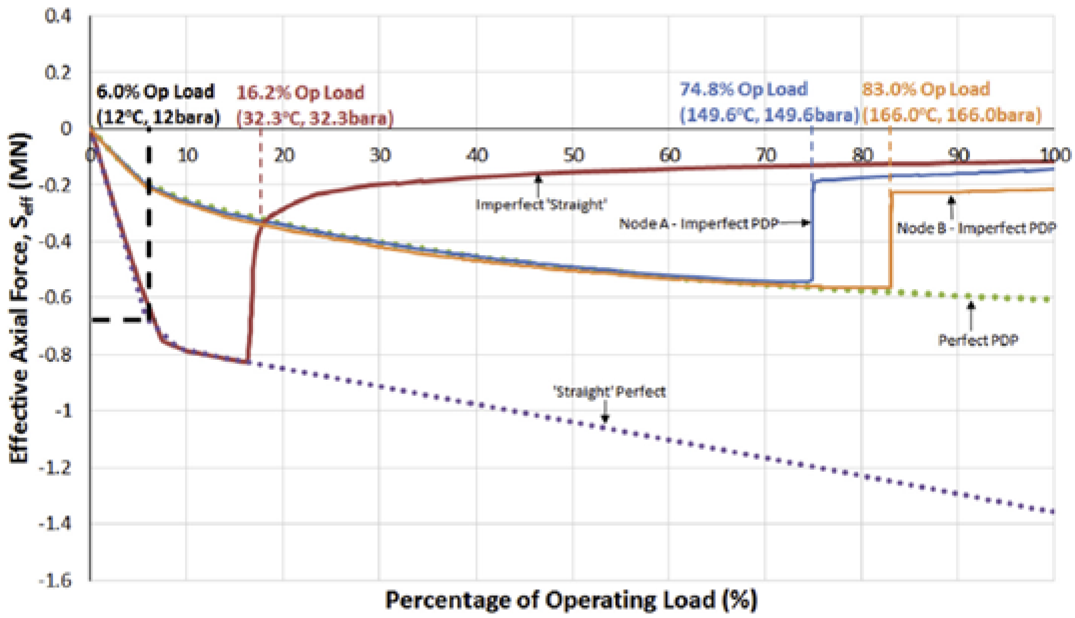

Figure 2.22: The plot of the effective axial force as a function of the percentage of operating load induced in a perfect and imperfect straight pipeline and in a perfect and imperfect pre- deformed pipeline [5].

In retrospect, the buckling behaviour of the residual curvature on the seabed is beneficial since buckling is driven to occur in the residual curvature section with a smaller axial compressive force. The axial compressive force is sensitive to the magnitude of the residual strains, the length of the curved section, the soil friction, the twist angle of the pipeline as well as the distance from an anchored point. The modelling of the transition sections does not influence the magnitude of the buckle initiation force obtained from a finite element analysis.

2.5 Creation of residual curvature during S-lay

Keeping in mind the limitations of the reel-lay method, this section focuses on the S-lay method. To think of alternatives of how imperfection can be created in the pipeline, one should pay attention to the equipment of the S-lay method. During this installation procedure, the pipeline is driven to the water through a stinger, supported by rollerboxes. The pipeline geometry is controlled by the position of the rollerboxes along the stinger [25]. This geometry determines the strains induced in the pipe [25]. Therefore, a residual curvature can possibly be created by adjusting the stinger inclination or the level of the rollerboxes (Figure 2.23) [13]. However, no research has been done so far to prove the feasibility of these two possible ways of creating a residual curvature.

Proposed ways:

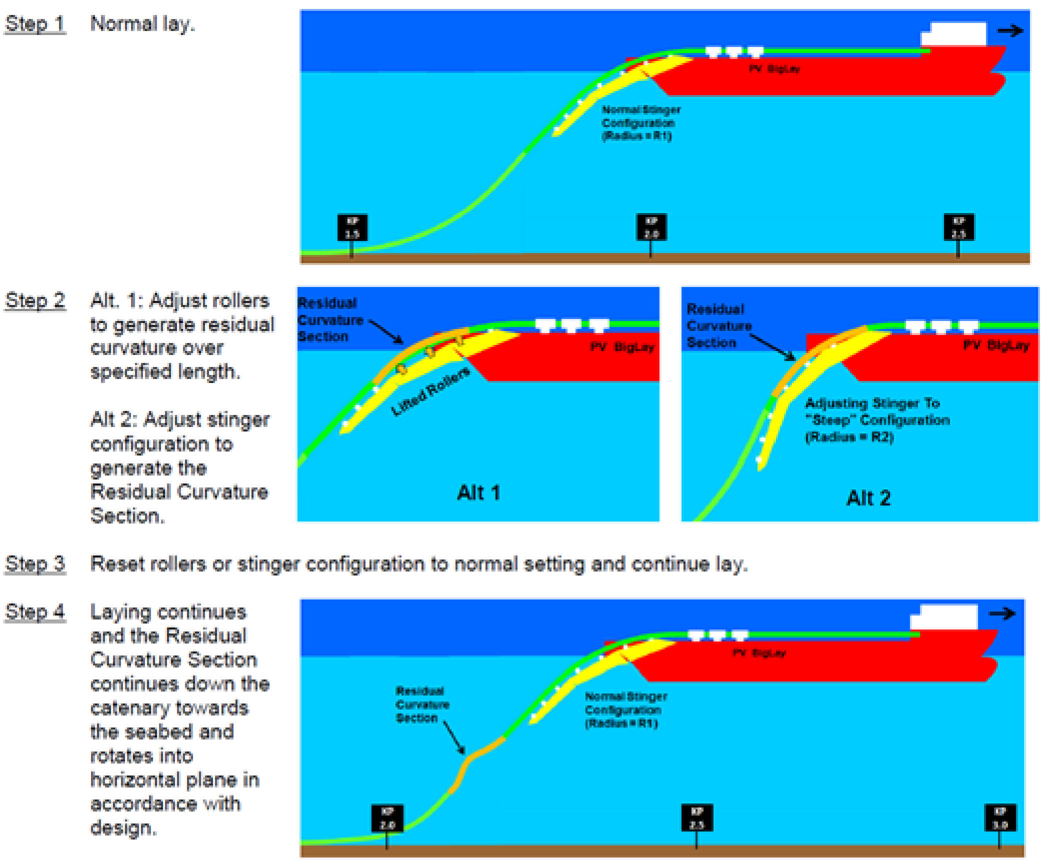

Figure 2.23: Ways of creating a residual curvature in S-lay installation [13].

To get an indication of what may happen in the pipeline when lowering the stinger or rising the rollerboxes, a useful correlation is to search for the pipeline behaviour during S-lay installation in deep waters. Installation in deep waters involves large departure angles of the pipeline from the stinger, the so-called "Steep S-lay" [25]. As a consequence, the pipeline experiences high strains in the overbend. Hence, it is vital to collect information about the strain criteria for deepwater installation, as they might be relevant also for the residual curvature method.

To begin with, it is known that during reel-lay method, the maximum strain levels in the reel are 2.0% approximately [25]. The increased strains in the overbend during S-lay can reach values just beyond 0.2%. Therefore, the pipe integrity per se is not in risk.

The increased bending strains in the overbend may have an impact on other features of the pipeline: the ovality of the cross section, the weld defects, the fatigue crack growth, out-of- straightness [25]. For this reason, it is vital to check if the aforementioned aspects stay within allowable limits when we want to take advantage of the pipe stain capacity in the overbend.

To conclude, although there is broad knowledge regarding the creation of residual curvature during reel-lay installation method, the feasibility of the incorporation of this buckling initiation technique into the S-lay method is still unknown. Since S-lay method is proven to be beneficial for the accomplishment of the challenging deepwater pipeline installations, supporting the installation of large diameter and long- distance pipelines, it cannot be denied that S-lay method will remain an attractive pipeline installation method in the future projects. Therefore, research upon improving and optimizing the laying procedure must be made, in order to meet the requirements of the future.

Chapter 3

Assessment of stinger angle

Local residual curvature is created in the pipeline by lowering the stinger during installation. In order to achieve the desirable plastic strain in predetermined intervals of the pipeline, a suitable inclination must be designed for the stinger. All the topics examined in this research study refer to specific pipe and stinger properties (the stinger of Audacia vessel), shown in Table 3.1.

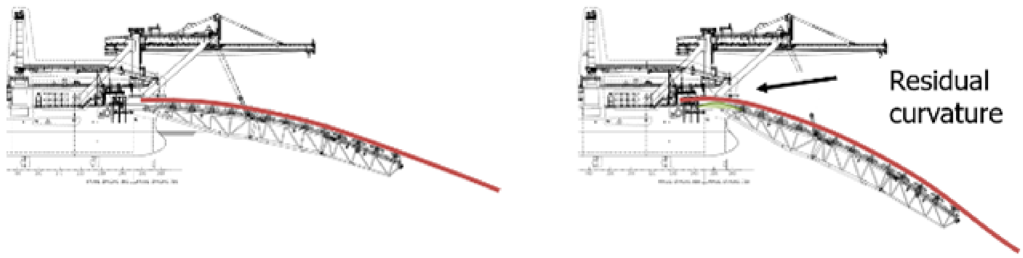

Figure 3.1: Residual curvature creation by lowering the stinger.

Table 3.1: Input data for the assessment of the suitable stinger inclination.

Pipe OD	18	[in]
Wall thickness	28.5	[mm]
Water depth	1925	[m]
Young's modulus	2.07E+11	[Pa]
Stinger length	110	[m]
Stinger radius	85	[m]
Material	X65	
Yield stress	448	[MPa]
Tensile strength	530	[MPa]

OrcaFlex 10.3d software is used for the accomplishment of the static and dynamic analyses, which provide an indication about the structural response of the pipeline during installation.

3.1 Model in OrcaFlex 10.3d

OrcaFlex, developed by Orcina, is a 3D nonlinear finite element software. It is designed to perform static and dynamic analysis for offshore systems, including pipelines. OrcaFlex' typical applications are for modelling of riser systems, mooring systems, installation planning with capabilities across the full range of scenarios, towed systems etc. This software meets the industry standards and it is widely used due to its users friendly environment. A representation of the graphic environment of modelling in OrcaFlex is depicted in Figure 3.2.

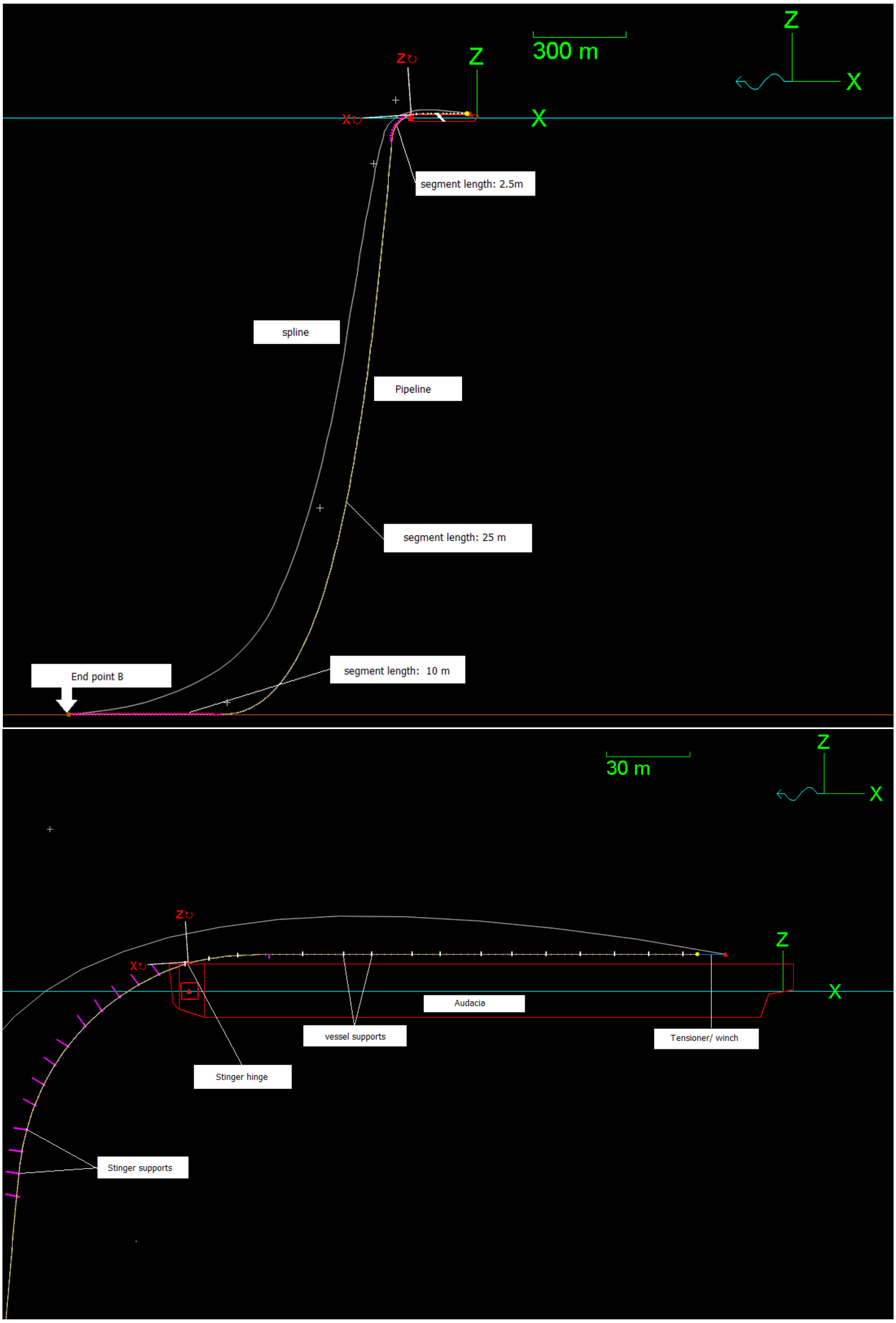

Figure 3.2: OrcaFlex model of pipeline installation in deep water.

- **Line:** A line object represents the pipeline. The line is discretised by numerous straight massless segments connected to each other by nodes. The nodes contain properties such as mass, weight, buoyancy of the half segment length on their both sides. The segments contain the axial, torsional and bending properties of the line, modelled as axial, torsional and rotational spring-dampers respectively (Figure 3.3). The minimum segment length was selected as 2.5 m. The total length of the pipeline is 2822.580 m with the one end (End A) being connected to the vessel and the other end (End B) connected to the seabed. The values of the inner and outer pipe diameter are given to the line.

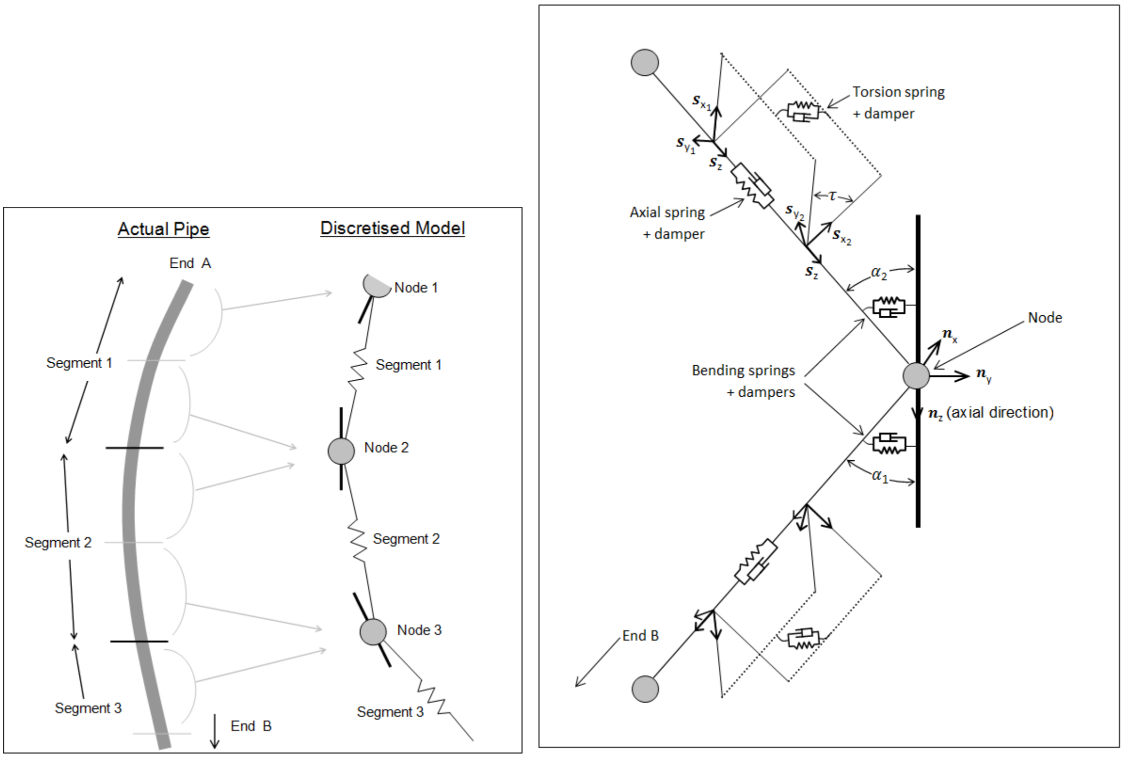

Figure 3.3: Line theory in OrcaFlex. Detail drawing of the structural properties. Axial, torsional and bending stiffness are modelled as axial, torsional and rotational spring-dampers [22].

The pipe has an isotropic, non-linear, hysteretic bending stiffness. Isotropic means that the "x" and "y" bending stiffness have the same value. The bending moment- curvature curve is non-linear, therefore the bending stiffness is defined as variable data. OrcaFlex uses the "plasticity wizard" to form a table of bending moment against curvature, by using linear interpolation. The term "hysteretic" means that if the curvature increases beyond the yielding point and then decreases, the bending moment does not follow the same moment-curvature path, but decreases linearly in a hysteretic path.

- **Winch:** The primary purpose of the winch is to pay-in and -out pipeline while the vessel moves. In addition, in this model the winch represents the tensioner. The axial stiffness of the winch is set to 10^5 kN. It has a specified length of 20 meters and it is connected to the End A of the pipeline.

- **Stinger hinge:** The stinger is connected to the vessel by a hinge. In reality, the hinge can be rotated by 0.1 degrees accuracy. There is an option to define imposed motion for the stinger hinge in OrcaFlex.

- **Spline:** The spline solution is a method to calculate statics in the model. The spline curve is defined by the user and predetermines the position of the line. This position is not the equilibrium position, it is just an initial approximation. This method, puts the line into a position that, as far as possible, follows the spline curve [22]. Afterwards during full statics the true equilibrium position is calculated.

- **Vessel:** The vessel is modeled as rigid body. It has six degrees of freedom; 3 translations (surge, sway, heave) and 3 rotations (roll, pitch, yaw). There is the option to define imposed motion for the vessel.

- **Seabed:** The seabed is modelled as linear elastic springs in the normal and tangential direction with respect to the seabed plane. The linear soil stiffness in both directions was assumed as $100kN/m/m^2$ and the soil friction coefficient was 0.5.

3.2 Bend moment - curvature curve in OrcaFlex 10.3d

Residual curvature in the pipeline can be assessed from the bend moment - curvature diagram obtained from OrcaFlex. The calculation of the non linear curve in OrcaFlex is followed by a set of assumptions. When a uniform and homogenous pipe is to be modelled, OrcaFlex uses the “plasticity wizard” in order to form a table of bend moment against curvature by using linear interpolation [22]. That is to say, bending stiffness is defined as variable data. Three significant parameters compose the creation of the curve: the Ramberg-Osgood relationship, the stress diameters and the direct tensile strain [22]. The Ramberg- Osgood equation [27] is a non linear stress-strain relation for steel under uniaxial stress as shown in the formula 3.1 below.

$$\epsilon = \frac{\sigma}{E} + K * \left(\frac{\sigma}{\sigma_y}\right)^n, \; for \; \sigma \geq 0 \tag{3.1}$$

Where,

ϵ -total uniaxial strain

σ -uniaxial stress

σ_y -yield stress

E -Young’s modulus

K -material constant

n -material constant, exponent characterising the degree of hardening of the curve

For the selected steel type X65 the parameters K, n have values 0.0028 and 25.888 respectively, according to API Specification 5L. The yield stress is 448 MPa and the Young’s modulus 207 GPa. Hence, the stress – strain curve obtained from Orcaflex is shown in Figure 3.4.

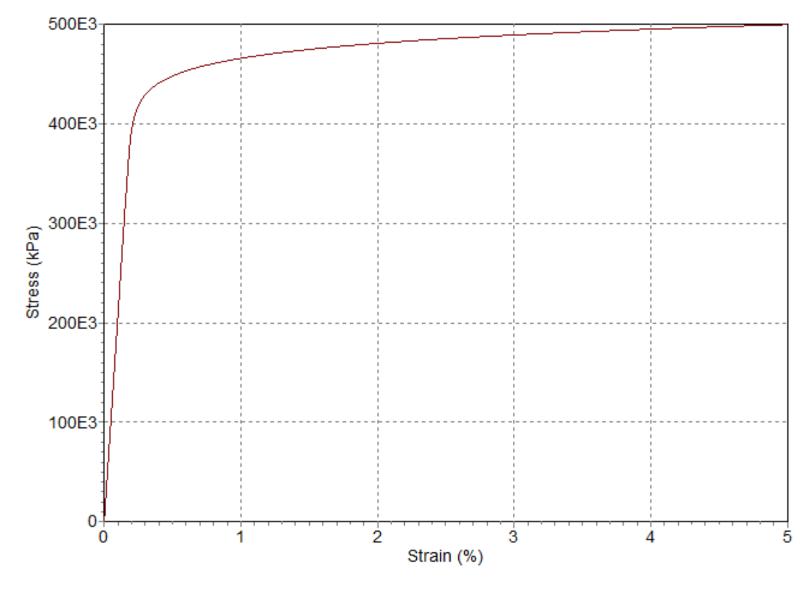

Figure 3.4: Stress- strain curve for X65 steel type pipe with outer diameter 0.457 m and yield stress 448 MPa.

The stress diameters are the inside and outside diameters of the load-bearing cylinder [22]. A uniform diameter profile is considered in this study, hence the stress diameters are taken to be the same as the pipe inner and outer diameter.

Lastly, based on the OrcaFlex documentation [22], the plasticity wizard calculates bend moment curvature relationship by integrating the stress profile across the pipe cross section. This calculation requires a direct tensile strain to be specified – this data item serves that purpose. After performing test calculations it was concluded that the direct tensile strain results in slightly smaller bending moment (around 1%) on the bend moment- curvature diagram. This impact is considered insignificant in this study, for this reason the initial bend moment- curvature diagram is used. The calculation of the bend moment- curvature stops when a maximum value of curvature is reached. More specifically, the maximum value of the calculated strain is $\epsilon_{max} = max(0.05, 5\epsilon_{\sigma_y})$. Therefore the maximum curvature is obtained by equation 3.2 [22] and the final non-linear bend moment- curvature curve is illustrated in Figure 3.5.

$$\kappa_{max} = \frac{\epsilon_{max}}{r_o} \tag{3.2}$$

Where,

r_o -the radius of the outer fibre $(D_o/2)$

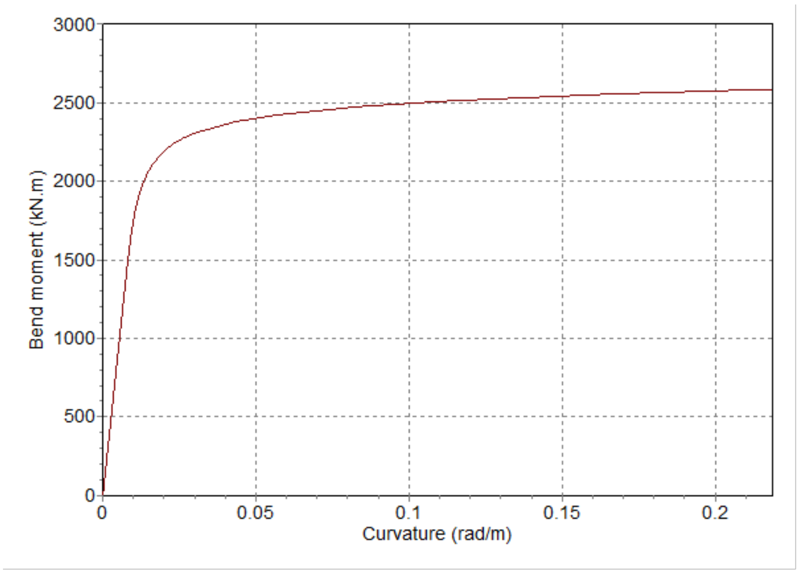

Figure 3.5: Bend moment- curvature curve for X65 steel type pipe with outer diameter 0.457m.

OrcaFlex gives the opportunity to the user to decide whether the non-linear bend stiffness will be elastic or hysteretic. If the bend stiffness is assumed as elastic, the magnitude of bend moment is entirely determined by the current curvature magnitude, as shown in the aforementioned Figure 3.5. In case of hysteretic bend stiffness, the bend moment depends on the history of curvature applied as well as on the current curvature. The hysteretic bend moment - curvature curve is illustrated in Figure 3.6.

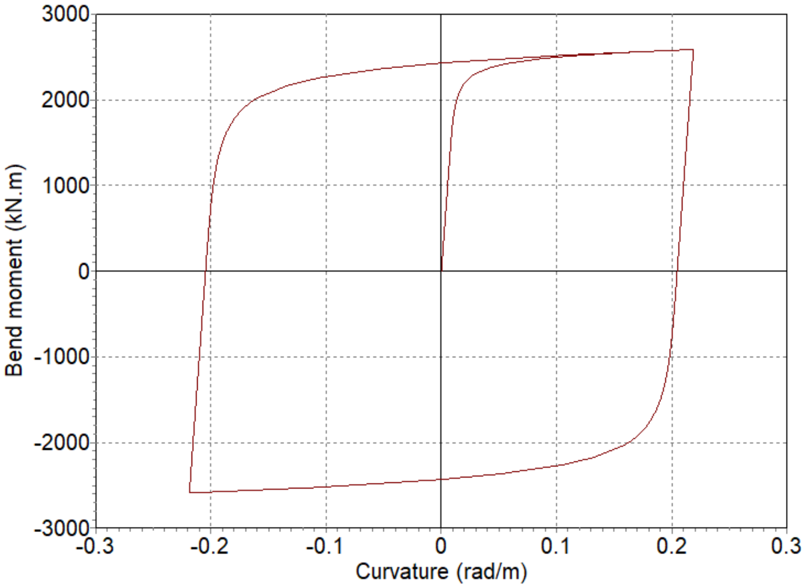

Figure 3.6: Hysteretic bend moment- curvature curve for X65 steel type pipe with outer diameter 0.457m.

Since the aim is to capture the plastic deformation of the pipeline due to an extra inclination of the stinger, and the potential changes of these deformations due to dynamic loads, it is selected to model the bend stiffness as nonlinear and hysteretic[1].

3.3 Methodology

The assessment of the suitable stinger angle involves several steps that need to be followed until the requirements are met, namely the creation of a local residual curvature. A schematic representation of the methodology can be seen in Figure 3.7. According to literature [15], the desirable residual curvature is referred in the form of residual strains. The target residual curvature shape results from 0.2- 0.25 % residual strains in a stress free condition. The 0.2% residual strain in an 18" pipe, is translated to 115 m radius of residual curvature. In other words, the residual curvature should be 0.00875 [rad/m]. The achievement of such a curvature depends on the pipe diameter, wall thickness, the stinger radius as well as the water depth. For this reason, an initial set of parameters was assumed, as already indicated in Table 3.1.

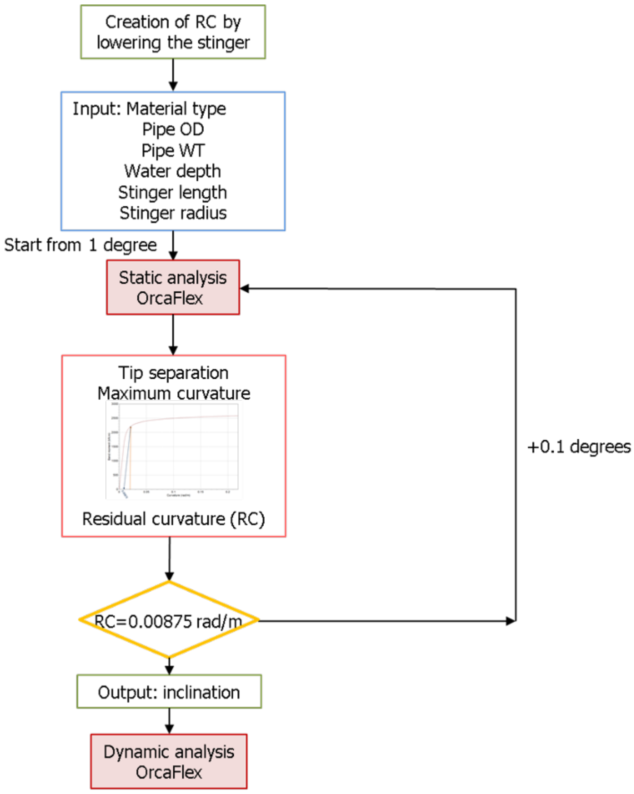

Figure 3.7: Schematic representation of the methodology followed to assess the required stinger inclination.

The steps for the assessment of the suitable stinger angle are:

- Select an initial stinger inclination. The stinger of Audacia is supported by cables which can be lowered and raised on demand. The cables can be set with 0.1 degrees accuracy. The creation of a local residual curvature section is possible by lowering the stinger few degrees with respect to the required angle, depending on the case, during normal installation. Since the goal is to create the residual curvature by causing the least impact on pipeline installation procedure, namely the effects on the pipe integrity and the pull time, 1 degree inclination of the stinger was selected as a starting case.
- Perform static analysis. Before obtaining any results, it is necessary to first implement the tip separation check. It is vital to ensure that the pipeline is not in contact with the final roller box of the stinger in order to ensure the structural integrity of the pipeline and the stinger. This can be achieved by calculating the tip clearance which has a minimum allowable value of 30 cm. OrcaFlex provides the value of support lift out distance, meaning the distance between the centerline of the rollerboxes and the center of the pipe, Figure 3.8. Thus, the actual tip clearance was calculated as shown in Table 3.2.

[1]Comparison has been made between the results from static analyses, when defining nonlinear elastic and nonlinear hysteretic bend stiffness. The outcomes can be found in Appendix A.

Table 3.2: Tip separation check for normal stinger inclination. The clearance between the pipe and the stinger tip is 0.89 m, therefore there is no risk of clash event.

Pipe OD	0.457	[m]
Anti corrosion coating	0.003	[m]
Concrete weight coating	0	[m]
0.5 OOD pipe	0.229	[m]
Bottom of pipe to bottom of surface support	0.035	[m]
OD support	0.5	[m]
Cos30 degrees angle of V-support	0.289	[m]
Clearance to 0.0m tip separation	0.553	[m]
RB-S13-1 Support 2 lift out for all supported lines	1.45	[m]
Tip separation	**0.89**	**[m]**

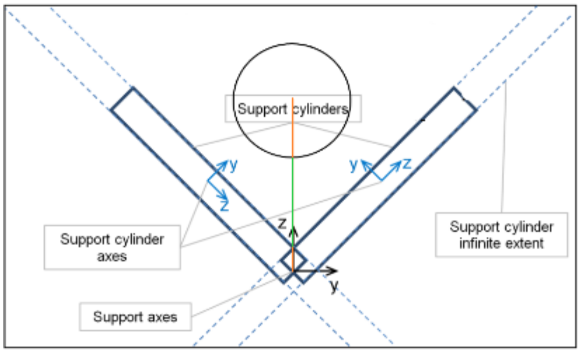

Figure 3.8: Support lift out distance (orange line), actual tip separation (green line).

- Obtain the results of the magnitude and the location of the maximum curvature and the corresponding bending moment. With the use of these data, the residual curvature and the residual strain are calculated by the formulas 3.4, 3.3 given below. The assessment of the residual curvature is based on the bend moment curvature diagram. It can be visualised by drawing a line in the diagram starting from the point which corresponds to the said maximum curvature, having a slope equal to the slope of the elastic region (linear unloading), Figure 3.9. The procedure is repeated for different values of stinger additional inclination, until the residual strain of 0.2% is reached.

$$\kappa_{res} = \kappa_{max} - \frac{M_{\kappa_{max}}}{EI} \tag{3.3}$$

$$\epsilon_{res} = \kappa_{res} * \frac{D}{2} \quad [33] \tag{3.4}$$

Where,

ϵ_{res} -residual strain

ϵ_{max} -maximum bending strain obtained from static analysis

$M_{\kappa_{max}}$ -bend moment at the location of the maximum curvature

κ_{res} -residual curvature

- Once a suitable stinger angle is defined, based on the static analysis, proceed to dynamic analysis. Determine whether the dynamic loads have an impact on the created residual curvature.

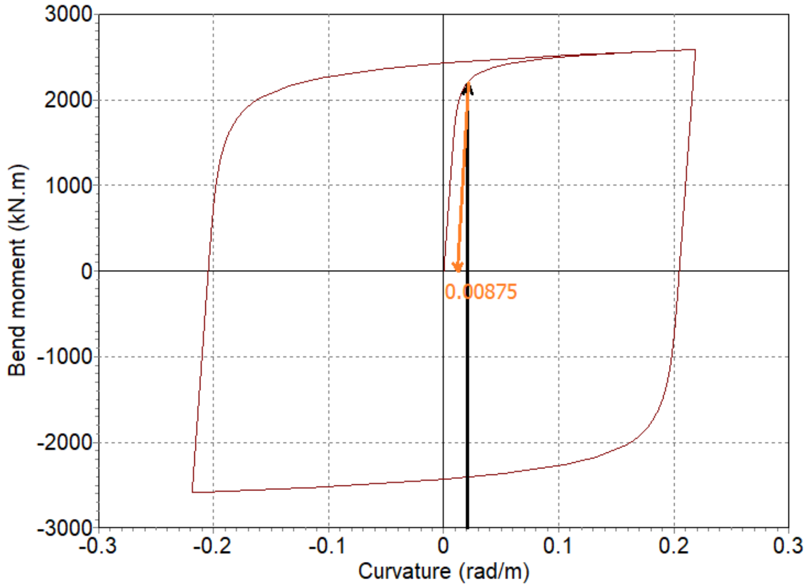

Figure 3.9: The desirable 0.00875 [rad/m] residual curvature obtained from a 0.02 [rad/m] maximum curvature.

3.4 Results

3.4.1 Static analysis

Based on the methodology described above, for an 18 inch pipe (wall thickness 28.5 mm) in 1925 m water depth, multiple stinger angles were tested by performing static analysis, starting from the magnitude of 1 degree. An iteration of the steps followed until the requirements were met, meaning the creation of 0.2% residual strain. The results after changing the stinger angle as well as the results obtained from normal installation are presented in Table 3.3.

0^o **case- Normal installation**

The maximum curvature, created in the pipeline due to the normal stinger configuration, is 0.01 rad/m. This curvature corresponds to 0.33% maximum bending strain. The location of maximum bending is at 246.31 m arc length, see Figure 3.10. It can be seen, that a residual curvature is created due to the plastic strains. However, this residual curvature is smaller than what the residual curvature method requires. The bending strains induced in the pipeline above the stinger can be seen in Figure 3.11.

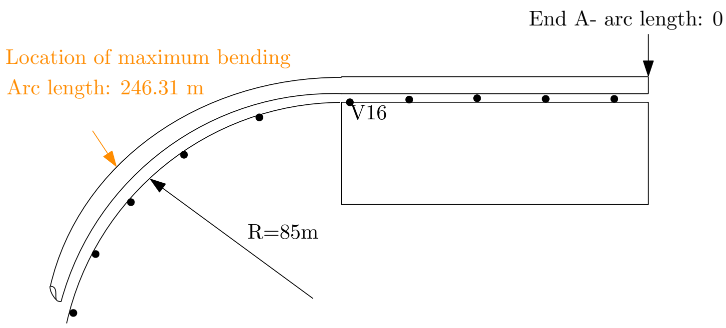

Figure 3.10: The location of maximum bending moment is at 246.31 meters from the beginning of the pipeline, during a normal installation.

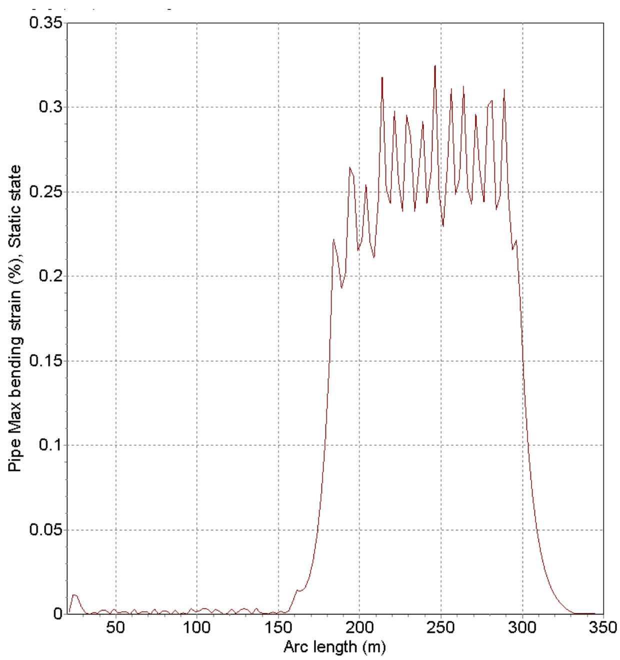

Figure 3.11: Bending strain diagram along the pipeline on the stinger. The location of maximum bending strain is at 246.31 meters from the beginning of the pipeline, during a normal installation.

1.9^o **case- Installation with residual curvature**

From the static analysis yields that a sufficient additional angle is 1.9 degrees. In this case the maximum bending is accumulated in the pipeline part which leaves the vessel and goes above the stinger (Figure 3.12), having bending moment of the magnitude of 2208 kNm according to OrcaFlex 10.3d. This bending moment is 8% larger than the maximum bending moment in the pipe due to 0 degrees stinger inclination. In addition, the maximum bending strain is increased by 45% resulting in a 0.0089 rad/m residual curvature. The plot of the bending strains along the pipeline on the stinger is depicted in Figure 3.13. From the strain distribution in the pipe cross section, it can be seen that the upper part of the pipe is under plastic extension and the lower part, in contact with the rollers, is under plastic compression, Figure 3.14.

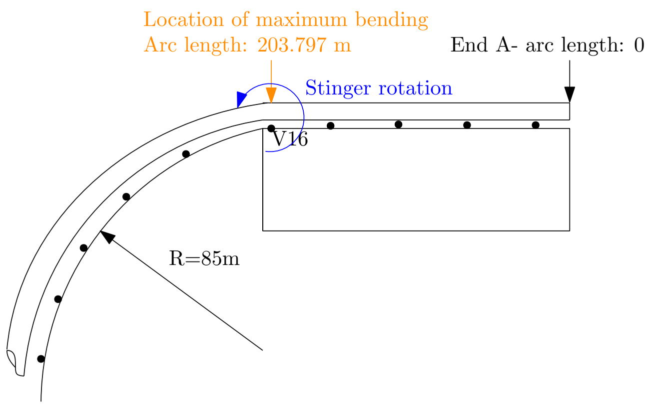

Figure 3.12: Schematic representation of the rotation of the stinger.The critical location where the maximum bending moment is concentrated is at 203.797 meters from the beginning of the pipeline. The node at the 203.797 meters is the critical node.

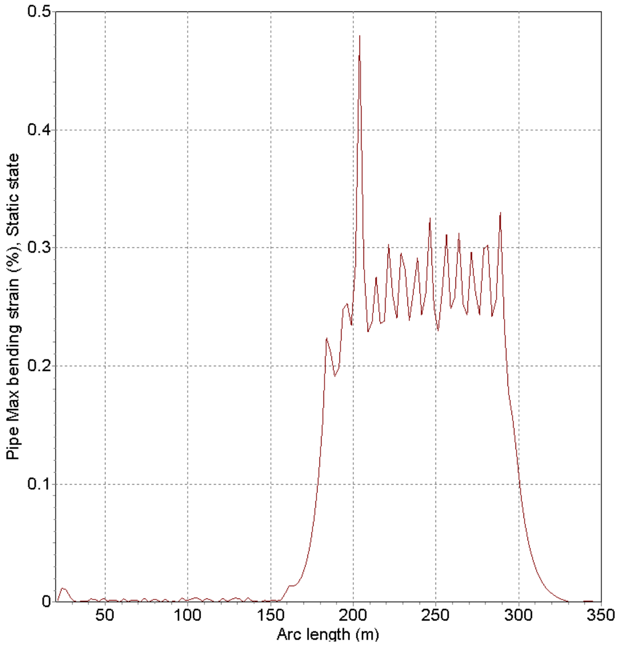

Figure 3.13: Bending moment diagram along the pipeline on the stinger. The location of maximum bending moment is at 203.797 meters from the beginning of the pipeline, during an installation with inclined stinger.

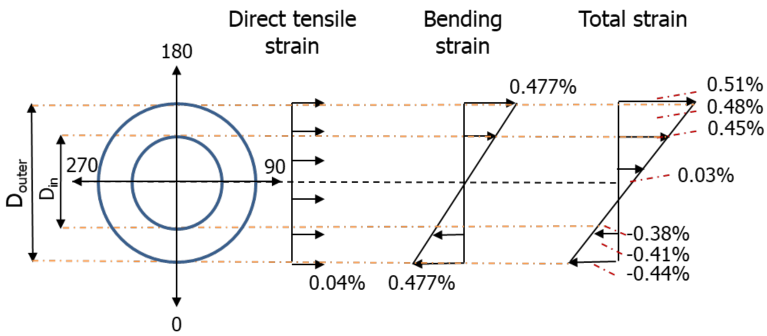

Figure 3.14: Strain distribution over the pipe cross section. The angles indicate the frame of reference for the strain calculation in OrcaFlex. Upper part of pipe under plastic extension and lower part under plastic compression. (Case of 1.9 degrees inclination).

$2.0^o - 2.1^o$ case- Installation with residual curvature

The cases of 2.0 and 2.1 degrees stinger inclination were examined too. Based on the static analyses, it can be seen that the maximum residual curvature was 0.009 rad/m and 0.01 rad/m respectively. Such curvatures correspond to 0.22% and 0.23% residual strains. The location of maximum bending is the same as in the case of 1.9 degrees stinger inclination. From these analyses, it can be concluded that the desirable residual curvature as defined by Geir Endal (0.2- 0.25% residual strain), is created when the stinger rotates by 2.0- 2.1 degrees too. The detailed results from the case of 2.0% inclination can be seen in Table 3.3.

Table 3.3: Static analysis results obtained for normal pipelaying, for 1.9 degrees and 2 degrees inclination.

Inclination	**0 deg**		
	OrcaFlex		Check
Tip clearance	0.89	[m]	Safe
Support reaction force	0	[kN]	Safe
Top tension	2995	[kN]	
Max curvature	0.01	[rad/m]	
Min radius of curvature	70.3	[m]	
Bending moment	2035.07	[kNm]	
Max bending strain	0.33	[%]	Plastic region
Residual strain (ϵ_{max})	0.07	[%]	
Residual curvature (ϵ_{res})	0.0031	[rad/m]	

Inclination	**1.9 deg**			**2 deg**		
	OrcaFlex		Check	OrcaFlex		Check
Tip clearance	1.27	[m]	Safe	1.29	[m]	Safe
Support reaction force	0	[kN]	Safe	0	[kN]	Safe
Top tension	2995	[kN]		2995	[kN]	
Max curvature	0.020	[rad/m]		0.021	[rad/m]	
Min radius of curvature	47.68	[m]		46.33	[m]	
Bending moment	2208.01	[kNm]		2217.56	[kNm]	
Max bending strain	0.48	[%]	Plastic region	0.49	[%]	Plastic region
Residual strain (ϵ_{max})	**0.20**	[%]	✓	**0.22**	[%]	✓
Residual curvature (ϵ_{res})	**0.0089**	[rad/m]	✓	**0.0095**	[rad/m]	✓

3.4.2 Dynamic analysis

Dynamic analysis was performed to examine the impact of dynamic loads (environmental loads, vessel motions) on the creation of the residual curvature, as well as the dynamic behavior of the curvature per se.

It is known that during installation the magnitude of the tension induced by the tensioners can fluctuate. This variation is a result of not only the vessel motions and the environmental loads, but a result of whether the vessel pays out pipeline or not, as well. Monitoring of the tensioner in Audacia reveals that this variation has a magnitude of ±15%. Therefore, a relevant upper and lower bound is set for the tension, before running the dynamic analysis.

The cases of 1.9- 2.0 and 2.1 degrees stinger inclination were all tested. The simulation time was 3 hours (10800s). As environmental loads, waves are imported in the model and more specifically, the maximum sea state in which the vessel Audacia can operate. That is, the sea state with significant wave height (Hs) 3m, wave period (Tz) 7s and 110 degrees wave direction. The residual curvature occurs in the pipeline section located above the last vessel support (V16). The magnitude of the residual curvature was calculated based on the material behaviour during dynamic analysis. The response during dynamics can be seen in the bend moment - curvature diagram (Figure 2.15, 2.16). The results for the case of 1.9 degrees inclination are shown in the Table 2.4 while for 2 degrees in Table 2.5. These results from dynamic analyses are fitted in the initial bend moment- curvature curve, as shown in Figure 3.17. It can be seen that the response starts aligned with the defined bend moment- curvature data and moves away from it as the pipeline moves through the first few curvature cycles. It then settles into a more steady state oscillation that broadly follows a linear bend moment- curvature response. This linear response has a gradient that is equal to the initial linear gradient of the defined bend moment- curvature data, but offset to higher values.

1.9^o **case- Installation with residual curvature**
During dynamic analysis it can be seen that the residual curvature, created in the pipe section above V16, was 0.01 rad/m. In this location, bending is driving the strain response[2]. This curvature corresponds to 0.23% residual strain, which is within the allowable values of 0.2- 0.25%. It can be deducted that, although the residual curvature from the dynamic analysis is larger than that from the static analysis (0.0089 rad/m), it is still an acceptable curvature based on the literature [6].

$2.0^o - 2.1^o$ **case- Installation with residual curvature**

[2]Bending dominates. Details can be found in Appendix B.

The results from the dynamic analyses of the cases of 2.0 and 2.1 degrees are interesting too. For the 2.0 degrees case, it can be seen that the residual curvature is 0.011 rad/m, translated to 0.25 % plastic strains. The maximum allowable value (0.25%) for the plastic strains is reached. Therefore, based the dynamic calculations, the maximum allowable stinger inclination for the case study in this thesis, is 2.0 degrees. Indeed, the 2.1 degrees case, creates a larger residual curvature (smaller radius of curvature) which can be described in terms of strains as 0.26% residual strain. Such a value exceeds the range of allowable plastic strains (0.2-0.25%).

Conclusion

The residual curvature created in the pipe section above the last vessel support due to additional stinger inclination, can be assessed either from static or dynamic analyses. Although the results from the dynamic analyses are more accurate, the static analyses give a good approximation too. The difference in the results from the two analyses is 11% to 14%. In addition, the creation of residual curvature is sensitive to the changes in the stinger inclination. Based on the dynamic analyses, it can be concluded that for the case examined in this thesis, a suitable stinger inclination is 1.9 to 2.0 degrees. Larger inclination results in unacceptable plastic strains in the pipe cross section. Therefore, it is important that the lowering of the stinger is done in a controlled manner, so that the design angle is not exceeded.

Note

If one works with nonlinear elastic material behaviour and wants to approximate the residual curvature in section above the last vessel support, it is recommended to:

- Reduce by half the segment length in the overbend area.
- Obtain the maximum curvature that appears in the node of interest during dynamics and the corresponding bend moment.
- Do the calculations of the hypothetical linear unloading (equation 3.3), to get a good approximation of the residual curvature.

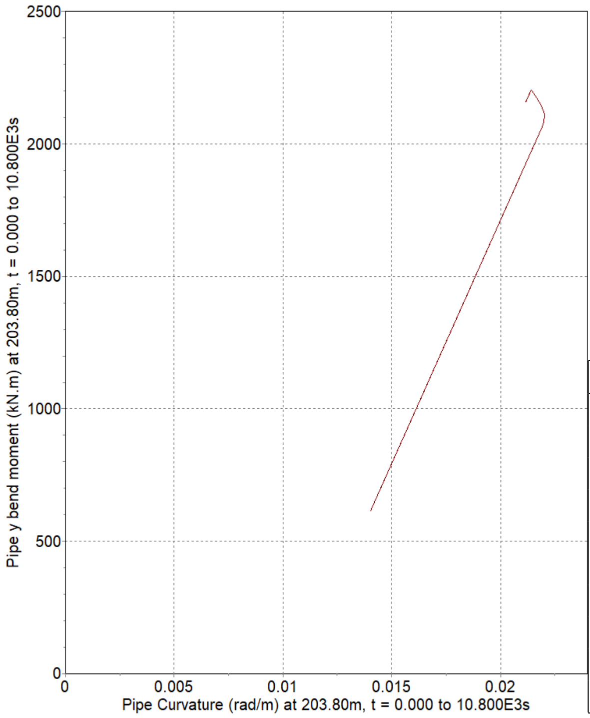

Figure 3.15: Bend moment- curvature response of the section above V16 during dynamics. 1.9 degrees stinger inclination.

Angle	**1.9**	**deg**	
	OrcaFlex		Check
Min tip clearance	0.55	[m]	Safe
Support reaction force	0	[kN]	Safe
Max top tension	3446.29	[kN]	
Max curvature	0.02	[rad/m]	
Min radius of curvature	45.43	[m]	
Max bending moment	2106.21	[kNm]	
Max bending strain	0.49	[%]	Plastic region
Residual strain (ϵ_{max})	**0.23**	[%]	✓
Residual curvature (ϵ_{res})	**0.01**	[rad/m]	✓

Table 3.4: Dynamic analysis: Calculation of residual curvature in the pipeline section above V16, for 1.9 degrees stinger inclination.

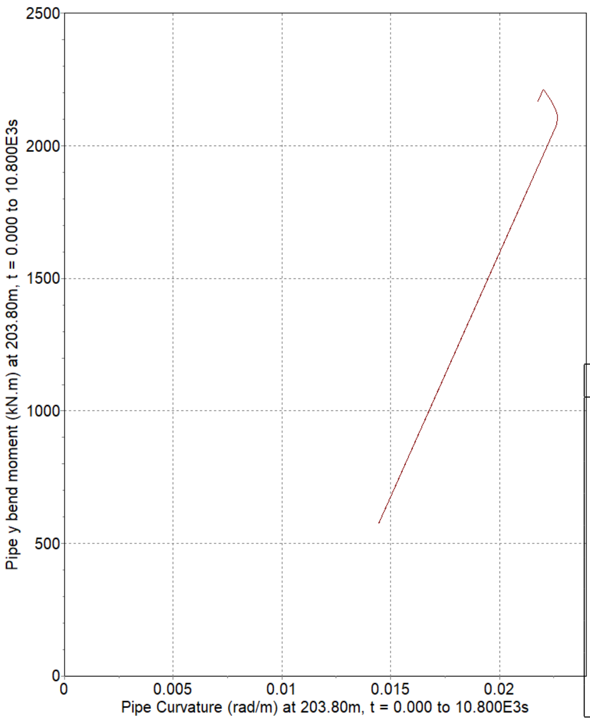

Figure 3.16: Bend moment- curvature response of the section above V16 during dynamics. 2.0 degrees stinger inclination.

Angle	**2.0**	**deg**	
	OrcaFlex		Check
Min tip clearance	0.56	[m]	Safe
Support reaction force	0	[kN]	Safe
Max top tension	3446.32	[kN]	
Max curvature	0.022	[rad/m]	
Min radius of curvature	44.38	[m]	
Max bending moment	2145.51	[kNm]	
Max bending strain	0.52	[%]	Plastic region
Residual strain (ϵ_{max})	**0.25**	[%]	✓
Residual curvature (ϵ_{res})	**0.011**	[rad/m]	✓

Table 3.5: Dynamic analysis: Calculation of residual curvature in the pipeline section above V16, for 2.0 degrees stinger inclination.

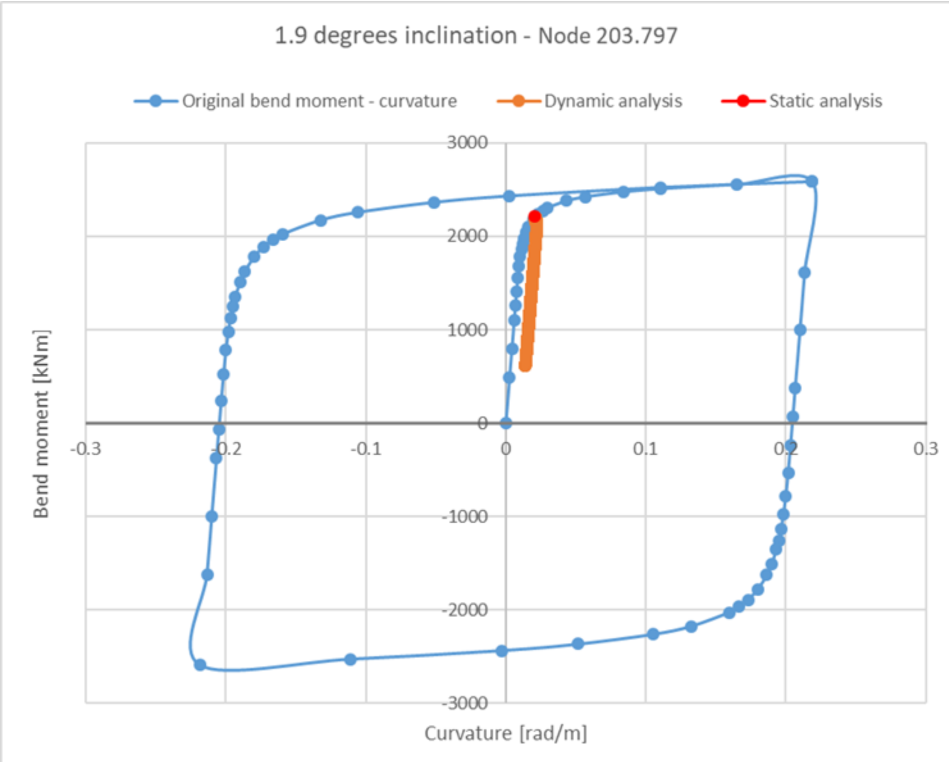

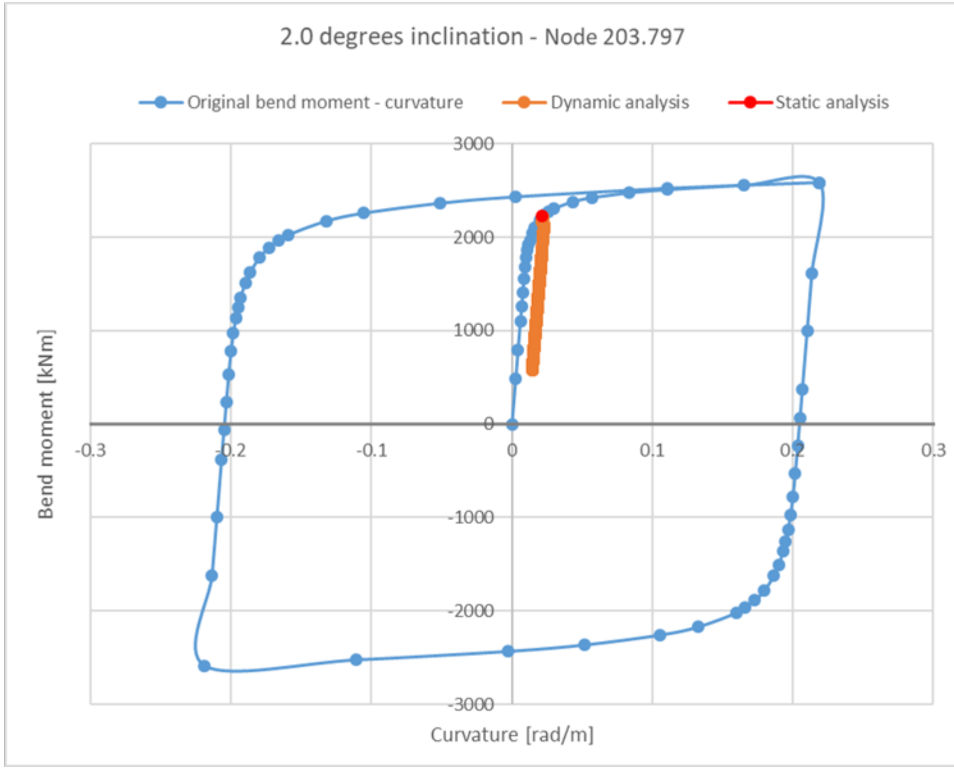

Figure 3.17: Results of bend moment and curvature at the node of interest (203.797) obtained from dynamic analysis for both cases of 1.9 and 2.0 degrees inclination, fitted in the initial bend moment- curvature curve.

Chapter 4

Pipeline integrity

After assessing the necessary stinger inclination which introduces residual curvature in the pipeline, it is important to assure the structural integrity of the said curved section. In this chapter all the fundamental checks will be performed in accordance with the DNV-GL standards and guidelines. Namely, the effects of the reversed stinger rotation will be investigated, as well as the changes in the bending moment capacity and in the cross sectional configuration (residual ovality). In addition, the unity check of local buckling will be performed, followed by a fatigue analysis during installation with inclined stinger. The assessment of the potential growth of weld defects due to the higher strains in the overbend, is not present in this research study. However, based on literature, no increase of the size of the welding defects is expected to happen [25].

4.1 Effects of stinger rotation

Not only investigating the scenario of lowering the stinger is significant, but the one of raising the stinger is important as well. The question here is, what happens to the pipeline when the stinger rotates from the inclined position to its normal configuration. The critical point that is mostly affected by this change in the stinger angle, is the section located above the stinger hinge. Thus, the strains created in the critical point due to the change of the stinger configuration, are evaluated in this subsection. Figure 4.1 represents the discussed issue.

In order to model the aforementioned scenario, OrcaFlex 10.3d was used. The stinger will be raised when the desired length of the pipeline with residual curvature is reached. Therefore, the pipe section that is above the last vessel support (V16), is the last section which experience residual deformation. It is vital, this residual curvature to be modelled. In OrcaFlex it is not possible to change the stinger configuration during a single static analysis. For this reason, "pre-bend" command was used to represent the residual curvature. More specifically, this command bends the pipeline at a location and magnitude specified by the user. In the case of 1.9 degrees stinger angle, a residual curvature of 0.0089 rad/m was created. Therefore, pre-bend of the same magnitude was applied in a pipeline section 48.8 meters long. The pre-bend starts from the stinger hinge until 48.8 meters of its length are covered in order to represent a 48.8 meters long curved pipeline, Figure 4.2.

Static and dynamic analysis was performed for the curved pipeline under normal installation conditions, meaning zero stinger inclination. The resulted moment and strain developed in the pipe section located above the stinger hinge are illustrated in Table 4.1. The results obtained from the installation of straight pipeline are included. It is evident that the pipe section with residual curvature experiences lower strains than the straight pipeline, above the stinger hinge. These are elastic strains. Therefore, the pipeline integrity is not in risk when the stinger configuration changes. The difference between the two cases can be explained when looking at the Figure 4.3. When a straight pipe passes from the stinger it bends because it follows the stinger's configuration. On the other hand, an already bent pipe, having a curvature of smaller radius than the radius of the stinger, will tend to straighten when passing above the stinger. As a conclusion, the reverse rotation of the stinger to its initial position does not influence the created residual curvature, the pipe is bent only elastically on the stinger.

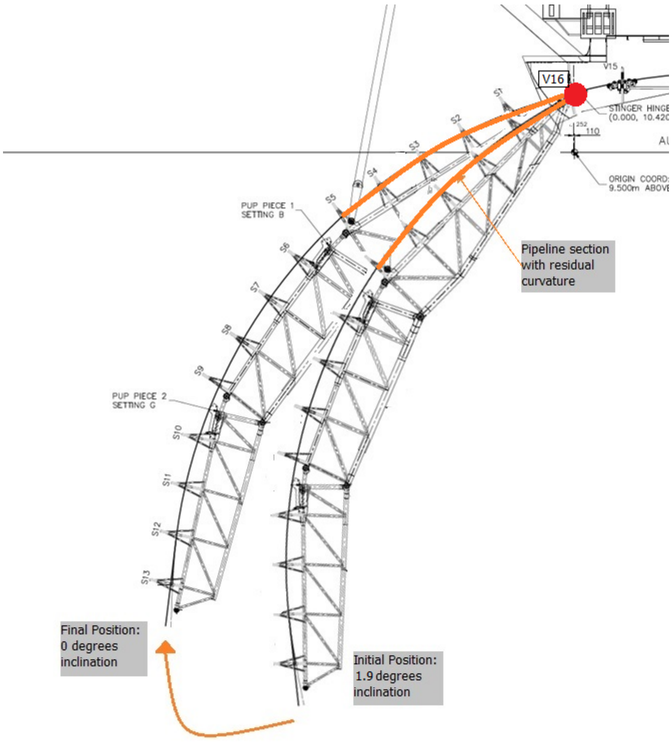

Figure 4.1: Representation of the stinger rotation from the inclined to the normal configuration, and an illustration of the pipeline section which experienced residual strains.

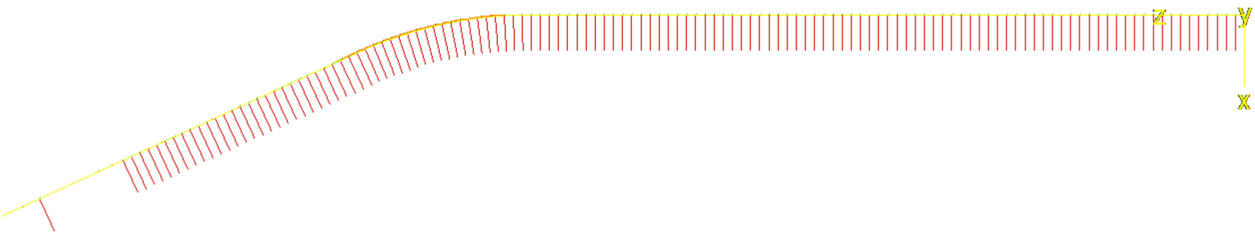

Figure 4.2: Pre-bent pipeline. Curved configuration starts at the location of the stinger hinge and ends after 48.8 meters.

Table 4.1: Effects on the pipeline with residual curvature due to the rising of the stinger from the inclined position to the normal one. Bending moment and bending strain developed in the pipe located above the stinger hinge. Static and dynamic analysis.

0 degrees			
	Static	Dynamic	
Pre-bend curvature	0.0089		[rad/m]
Axis	y		
Section length	48.8		[m]
Bending moment	1184.28	1514.28	[kNm]
Max bending strain	0.15	0.19	[%]
Normal Installation without Pre-bend			
Bending moment	1863.04	1878.22	[kNm]
Max bending strain	0.25	0.27	[%]

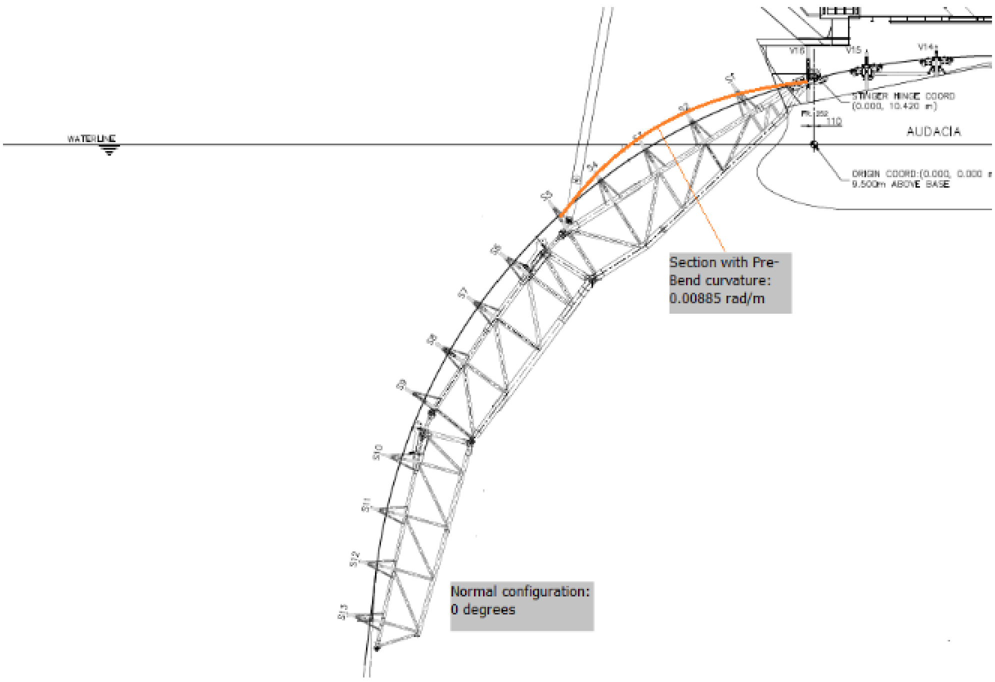

Figure 4.3: Pre-bended pipeline. Curved configuration starts at the location of the stinger hinge and ends after 48.8 meters. When the stinger returns to zero inclination, less bending is induced at the section above the last vessel support, hence there is not any detrimental impact on the configuration of the created residual curvature. Note that the lifted residual curvature illustrated in the figure is unrealistic. It helps the understanding of the different radius of curvature between the pre-bent section and the stinger. In reality the pipeline is fully in contact with the supports of the stinger due to the applied tension and self weight.

4.2 Reduction in bending moment capacity

The decrease in the pipe bending moment capacity due to the inclination of the stinger is calculated in this subsection based on the steps provided in the "Guideline for Installation of Rigid pipelines - Limit state criteria (JIP)" [18]. In general, a decrease results from the plastic strains created due to the combination of bending moment and axial force acting in the pipe. Consequently, the combined loading condition and the geometry of the stinger provokes significant deformations to the pipe. Therefore, a reduction in the moment capacity is expected to also occur during normal installation in deep waters, at the location of maximum bending on the stinger. The amount of reduction due to normal installation and installation with inclined stinger, is compared in this subsection.

Firstly, the initial bending moment capacity of the pipe was calculated. That is, the moment capacity which corresponds to the design compressive strain resistance, ϵ_{RD} of the pipe. DNVGL-ST-F101 [9] provides formulas for the design compressive strain resistance, Formula 4.1. From the relation $\epsilon = k * (D/2)$, the corresponding curvature (κ_{RD}) was obtained. The initial bending moment capacity ($M(\epsilon_{RD})$) was approximated from the moment-curvature diagram.

The calculation of the reduced bending moment capacity was fully based on the moment- curvature diagram. The relation 4.2 provides the calculation of the residual strains ($\epsilon_{s,res}$) resulting from the maximum bending moment on the stinger. When the stinger is inclined, the maximum bending moment (M_s) is concentrated in the point of the pipe that is above V16. Hence, this is the weakest point with the maximum strain on the stinger (ϵ_s). Consequently, the reduced bending strain capacity was estimated from the Formula 4.3. For the corresponding reduced curvature, the reduced bending capacity was obtained from the moment curvature graph, see Figure 4.4. This new bending capacity is the capacity that the pipe section with residual curvature will have when it reaches the seabed.

Finally, the reduced bending moment was subtracted from the initial one. The reduction in capacity ($\Delta M_{p,res}$) should be compared with the design bending moment capacity ($\overline{M_k}$) provided by the DNV-ST-F101 standards, Formula 4.5, which includes a modification of the plastic moment capacity to account for the lateral point load from the rollerboxes. The results are illustrated in Table 4.2.

$$\epsilon_{RD} = \frac{\epsilon_c(p_{min} - p_e)}{\gamma_{SC,DC}} = \frac{\tilde{\epsilon} * \alpha_p * \alpha_{mat}}{\gamma_{SC,DC}} \tag{4.1}$$

Where,

ϵ_{RD} -design bending strain capacity

$\tilde{\epsilon} = \left(\frac{t}{D} - 0.01\right) * \left(\frac{0.85}{\alpha_h}\right)^{1.5} * \alpha_{gw}$

- $\alpha_h = \left(\frac{R_{t,o.5}}{R_m}\right)_{max} = 0.93$

- $\alpha_{gw} = 1.0$, girth weld factor for D/t$\geq$ 20

$\alpha_p = 1 + \frac{20}{3} * \left(\frac{p_{min} - p_e}{p_b^(t)}\right)^2 = 1.0$ -for zero pressure

$\alpha_{mat} = 1.0$ -material factor for $\tilde{\epsilon} * \alpha_p \geq 0.025$

$\gamma_{SC,DC} = 2.0$ -safety class resistance factor for low safety class and Displacement Controlled conditions (DC)

$$\epsilon_{s,res} = \epsilon_s - \frac{M_s}{EI} * \frac{D}{2} \tag{4.2}$$

$$\epsilon_{reduced} = \epsilon_{RD} - \gamma_F * \epsilon_{s,res} \tag{4.3}$$

Where,

ϵ_s -maximum bending strain on the stinger

M_s -maximum bending moment on the stinger

$\epsilon_{s,res}$ -residual bending strain

$\gamma_F = 1.2$ -load effect factor for the functional load to cover the system effect

$$\Delta M_{p,res} = M(\epsilon_{RD}) - M(\epsilon_{RD} - \gamma_F * \epsilon_{s,res}) \tag{4.4}$$

Where,
$M(\epsilon_{RD})$ -the initial bending moment
$M(\epsilon_{RD} - \gamma_F * \epsilon_{s,res})$ -the reduced bending moment

$$\overline{M_k} = \alpha_c * \alpha_{pm} * M_p \tag{4.5}$$

Where,
$M_p = f_y * (D-t)^2 * t$ -the plastic bending moment capacity
$\alpha_c = (1-\beta) + \beta * \frac{f_u}{f_y}$ -the flow stress parameter
$\alpha_{pm} = 1 - \frac{D/t_2}{130} * \frac{R}{R_y}$ -the plastic moment reduction factor accounting for point load

- $R_y = 3.9 * f_y * t_2^2 = 1419.16[kN]$
- R -reaction force from the rollerboxes (V16), $R_{V16} = 488.6kN$ for the case of 1.9 degrees.
- Applies for $R/R_y < 0.5$

$\beta = \frac{60 - D/t_2}{90}$ -factor of combined loading
$t_2 = t$ -prior to operation (negligible corrosion)
f_y -SMYS, for ambient temperature (no de-rating)

Table 4.2: Reduction in bending moment capacity (ΔM) of the pipe due to its plastic bending on the stinger. Cases of zero and 1.9 degrees inclination.

Stinger inclination	1.9	0	[deg]
Diameter,D	0.457		[m]
Thickness,t	0.0285		[m]
β	0.488		
f_u	530		[MPa]
f_y	448		[MPa]
α_c	1.09		
M_p	2346.55		[kNm]
α_{pm}	0.96	0.98	
$\overline{M}_k$	2449.07	2495.74	[kNm]
ϵ_{RD}	2.29		[%]
κ_{RD}	0.100		[rad/m]
M_s	2208.01	2035.07	[kNm]
ϵ_s	0.48	0.33	[%]
$\epsilon_{s,res}$	0.20	0.07	[%]
$\epsilon_{reduced}$	2.0	2.20	[%]
$\kappa_{reduced}$	0.089	0.0096	[rad/m]
$M(\epsilon_{RD})$	2496.8	2496.8	[kNm]
$M_{reduced}$	2483.21	2492.05	[kNm]
ΔM	**13.59**	**4.76**	[kNm]

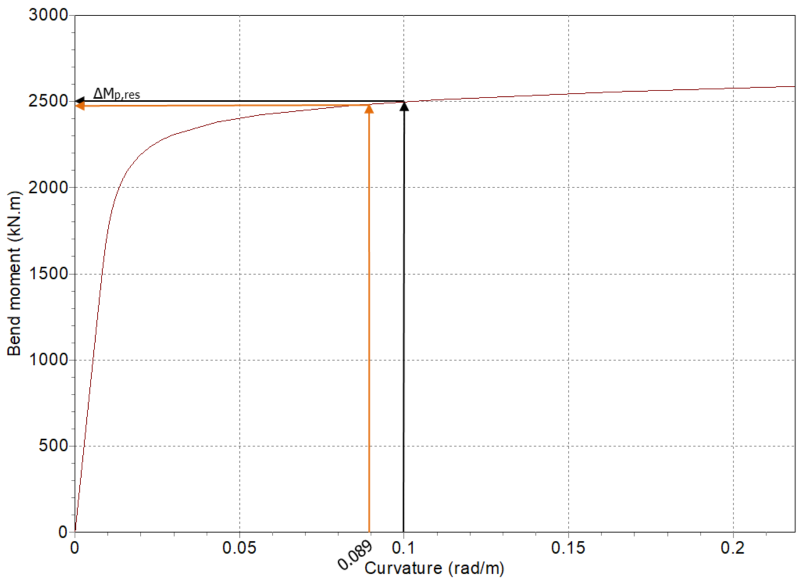

Figure 4.4: Illustration of the reduction in bending moment capacity (ΔM) corresponding to the reduced bending strain of the magnitude of 2.0% (0.089 reduced curvature).

Table 4.3: Reduction of bending moment capacity when the stinger angle is 0, 1.9 and 2 degrees.

Angle	0		1.9		2.0	
	Static	Dynamic	Static	Dynamic	Static	Dynamic
$\Delta M[kNm]$	4.76	6.39	13.59	16.26	14.44	16.93

The design bending moment capacity, $\overline{M_k}$ was calculated 2449 kNm, based on the DNV-ST-F101 standards [9]. This capacity includes the effect from lateral point loads from the V16 support. Hence, the 13.59 kNm reduction constitutes 0.55% of the design capacity. A reduction in the pipe's bending moment capacity is also observed during normal installation. In this case the reduction is less significant. Similarly, when considering the dynamic loading, the reduction during normal installation is 6.4 kNm while for an installation with inclined stinger, it is 16.3 kNm. Consequently, it can be stated that among comparison between normal installation and installation with increased stinger inclination, the bending moment capacity of the pipe when it is laid on the seabed will be reduced. The difference is larger when the stinger is lowered. And after calculating the new bending moment capacity for the case of 2 degrees inclination, it is understood that the higher the inclination, the larger the reduction in the capacity. However the magnitude of the reduction is not significant.

4.3 Local buckling

One of the main concerns when allowing for higher strains in the pipe, is the risk of local buckling. For this reason, the local buckling check in the overbend was conducted in accordance with the Installation JIP [18] and the DNVGL design standards [9]. The accompanying conditions are the following:

- The pipelines are straight in stress-free condition
- Deep water (no concrete coating)
- $15 \leq D/t \leq 60$
- Internal/ external pressure is not considered (bare pipeline at the overbend)

The local buckling check was conducted analytically and compared with the corresponding check performed in OrcaFlex software. The environmental loads are not taken into account when performing static analysis. Therefore, in the analytical calculation only the functional loads were present. In contrast, OrcaFlex includes environmental loads in static analysis, namely the current and the wind loads but not the wave loads. These loads were assumed to be zero, in order to achieve agreement between the two approaches.

The functional loads are the maximum bending moment (M_F) and the corresponding axial tension (S_F). In this way, the local buckling check for load-controlled conditions refers to the pipe cross section with the maximum bending moment. That is the section located above the stinger hinge. Similarly, the displacement-controlled conditions criterion refers to the maximum compressive strain (ϵ_{SD}). It is calculated by subtracting the direct tensile strain from the maximum bending strain.

When determining the value of the load effect factor for functional loading (γ_F), different scenarios must be distinguished, as described in the DNV design standards [9]. The first case is the so called system effects, where many pipe sections are subjected to an invariant loading condition. Secondly is the case of local check. The local check is applied when there is single joint failure. In the guidance it is stated that only system effects should be checked for installation. An example is the installation by reel, during which the whole pipe undergoes the same deformation over time. The case examined in this document involves the creation of an additional deformation in predetermined sections of the pipeline. This deformation is created locally in the area above the stinger hinge (V16). Hence, if we "freeze" the time, it can be seen that only a single cross section of the pipe is exposed to a unique maximum bending moment, indicating that system effects cannot be used. Therefore, although for normal installation procedure DNVGL standards propose system effects, in the specific case of creating local residual curvature, local check should be considered in the local buckling criterion.

The local buckling check differs when Load Controlled (LC) conditions or Displacement Controlled (DC) conditions occur. As already mentioned, the maximum strains appear at a supported location. Therefore, the displacement controlled (DC) criterion is applicable. However, if interested, the calculations for LC conditions can be found in the Appendix D.

4.3.1 Displacement Controlled Conditions

Pipe members subjected to longitudinal compressive strain (bending moment and axial force), lateral force due to support and have external pressure equal to the internal, should satisfy the following criterion [9]:

$$\left[\frac{\epsilon_{SD}}{\frac{\epsilon_c(t_2,0)}{\gamma_{SC,DC}}}\right]^{0.8} \leq 1.0 \tag{4.6}$$

where,
$\epsilon_{Sd} = \epsilon_F * \gamma_F * \gamma_c + \epsilon_E * \gamma_E + \epsilon_I * \gamma_F * \gamma_c + \epsilon_A * \gamma_A * \gamma_c$, the design compressive strain

- For static analysis, only ϵ_F (maximum compressive strain) is considered
  $\epsilon_F = \epsilon_{max\ bending} - \epsilon_{tensile}$

- For dynamic analysis, ϵ_E is the compressive strain due to the environmental loads and is defined as shown in the equation 4.9, where:
  $\epsilon(t)$, is the compressive strain calculated from dynamic analysis
  ϵ_F, the compressive strain obtained from the static analysis

- $\gamma_F = 1.1$ for local check

- $\gamma_c = 1.0$ for Displacement Controlled conditions, S-lay installation

$\epsilon_c(t_2, 0) = (\tilde{\epsilon} * \alpha_p * \alpha_{mat}) * (1 - \sqrt{\frac{\frac{D}{t_2}}{80} * \frac{R}{R_y}})$, accounts for lateral force (also, see equation 4.1)
$\gamma_{SC,DC} = 2.0$, safety class resistance factor for low safety class (Table 5-2 [26])

Static analysis results

As already discussed, the event of local buckling was examined for the pipe section located above the V16 vessel support. The cases of the two proposed stinger angles (1.9 and 2.0 degrees) were examined, Table 4.4. In both cases the criterion is satisfied and there is an agreement between the results from the analytical calculations and OrcaFlex.

Table 4.4: Local buckling check in the pipe section above V16, for displacement controlled conditions, when the stinger inclination is 1.9 degrees and 2.0 degrees. Static analysis.

Displacement Controlled conditions				
1.9 degrees			**2.0 degrees**	
$\epsilon_{\text{maxbending}}$	0.48	%	0.49	%
ϵ_{t}	0.04	%	0.04	%
ϵ_{F} compressive strain	0.44	%	0.46	%
ϵ_{Sd}	0.49	%	0.50	%
ϵ_{RD}	2.29	%	2.29	%
Local buckling check	**0.29**	**Satisfied**	**0.30**	**Satisfied**
OrcaFlex result	**0.29**	**Satisfied**	**0.30**	**Satisfied**

Dynamic analysis results

Local buckling criterion was examined after the dynamic analysis as well. In this case the effects from the environmental loads are present. It is assumed that the time needed for the system to buckle is much smaller than the characteristic period of the dynamic motion. The steps followed and the criteria were the same as presented in the previous subsection with the only difference being the presence of M_E, S_E, ϵ_E, in the calculation of the design loads and strains. The functional loads must be separated from the environmental loads. According to DNVGL-ST-F201 [10] the combined load can be treated as a linear superposition of the environmental load and the functional load. OrcaFlex uses the static state of the model as the functional load case. The same approach was followed in the analytical calculation of the local buckling check. Hence, the environmental loads were obtained from:

$$M_E(t) = M(t) - M_F \tag{4.7}$$

$$S_E(t) = S(t) - S_F \tag{4.8}$$

$$\epsilon_E(t) = \epsilon(t) - \epsilon_F \tag{4.9}$$

The values of the bending moment, the axial tension and the compressive strain obtained from the dynamic analysis, were the maximum ones, in order to examine the worst case. The formula of the unity check assumes that these loads are applied slowly and continuously in the pipe. Based on this evidence, there is a conservative nature in the results based on the dynamic analysis.

The results for Displacement Controlled (DC) conditions are shown in Table 4.5. The criterion was again satisfied, for both stinger angles.

Table 4.5: Local buckling check in the pipe section above the stinger hinge, for displacement controlled condition, when the stinger inclination is 1.9 degrees and 2.0 degrees. Dynamic analysis.

Displacement Controlled conditions				
1.9 degrees			**2.0 degrees**	
γ_E	1.3		1.3	
$\epsilon_{\text{maxbending}}(t)$	0.49	%	0.52	%
$\epsilon_{\text{t}}(t)$	0.04	%	0.04	%
compressive strain,$\epsilon(t)$	0.45	%	0.47	%
ϵ_F	0.44	%	0.46	%
ϵ_E	0.005	%	0.016	%
ϵ_{Sd}	0.49	%	0.52	%
ϵ_{RD}	2.29	%	2.29	%
Local buckling check	**0.29**	**Satisfied**	**0.31**	**Satisfied**
OrcaFlex result	**0.29**	**Satisfied**	**0.31**	**Satisfied**

4.4 Cross section ovality

The increased strains which appear in the pipeline when rotating the stinger may increase the pipe cross section ovality. Ovalisation is the deviation of the line pipe perimeter from the circle [9]. As described by Murphey and Langner [35], when a pipe is bent beyond the proportional limit, plastic deformation of the material begins and based on the magnitude of the strain, the plastic deformation can increase and create a residual curvature. A further increase in bending strain can cause ovalization of the pipe cross section. Correspondingly, the slope of the stress - strain curve tends to zero [35]. At the same time, the simultaneous action of tension in the pipe can increase the ovalization drastically [20], Figure 4.5.

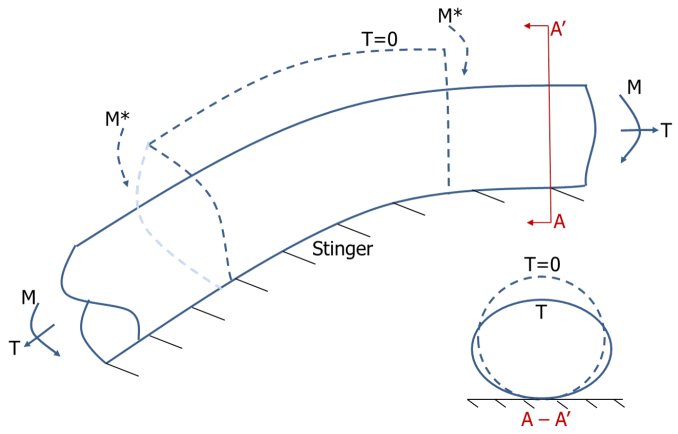

Figure 4.5: Enhancement of the cross sectional ovalization due to the presence of tension.

Since the residual ovality of the cross section influence the collapse resistance (resistance to external pressure) of the pipeline in the sagbend [20], it is crucial to investigate whether there is a significant increase in the residual ovality during the installation phase. Based on the analytical equations provided by Torselletti et al [34] the residual ovality was calculated as shown in the equations 4.10, 4.11 in which the effect of both bending and local reaction from the roller is included. These formulas are based purely on finite element analysis and not in physical tests.

The node in which residual ovality is more likely to occur is where the maximum bending strains are concentrated. As already discussed, this is the location where the pipeline passes above the last vessel support (V16). For the calculation of the induced ovality, the inputs used are the applied local strain and the reaction force from the support. The strain is calculated based on the maximum tensile and minimum compressive strain as $\epsilon_b = (\epsilon_{max} - \epsilon_{min})/2$, where the respective strains are obtained from the analysis in OrcaFlex. The support reaction force is obtained from the analysis as well and it corresponds to the total force of the whole support structure as if it was a flat support and not a V-shaped, as presented in Figure 4.6. The initial ovality (from fabrication) was assumed to be 1% [34] in order to examine an extreme case. However, in reality the pipelines are normally fabricated with an ovality less than 1%. The ovality was assessed for static conditions.

$$f_{Applied} = f_{fab} + k_\delta * \frac{2 * \delta_{EI,R}}{D} + \left[\alpha * \left(1 + \frac{D}{\beta * t}\right) + \frac{R}{R_Y * k_R}\right] * \left(2 * \epsilon_b * \frac{D}{t}\right)^2 \tag{4.10}$$

$$f_{Residual} = (f_{Applied} - f_{fab}) * \left(\frac{\epsilon_b}{\epsilon_c}\right) + f_{fab} \tag{4.11}$$

Where,

$\delta_{EI,R} = 1.203 * \frac{R}{t*E} * \left(\frac{D}{2*t}\right)^{1.22}$ -the elastic dent [34]

$R_Y = 3.9 * f_y * t^2$ -as already introduced in the local buckling check

R -the reaction force in the rollers in contact with the pipe

ϵ_b -the applied local (residual) strain for the case of 1.9 degrees inclination due to the combined effect of bending and tension.

$\alpha = 0.03$

$\beta = 120$

$k_\delta = 1 + \frac{(D-0.06)}{2}$

$k_R = \frac{D/t}{14}$

$\epsilon_c = \epsilon_{c,OS-F101} * \left(1 - \sqrt{\overline{\alpha_R} * \frac{R}{R_y}}\right)$ -is the critical strain

$\overline{\alpha_R} = \frac{D/t}{80}$

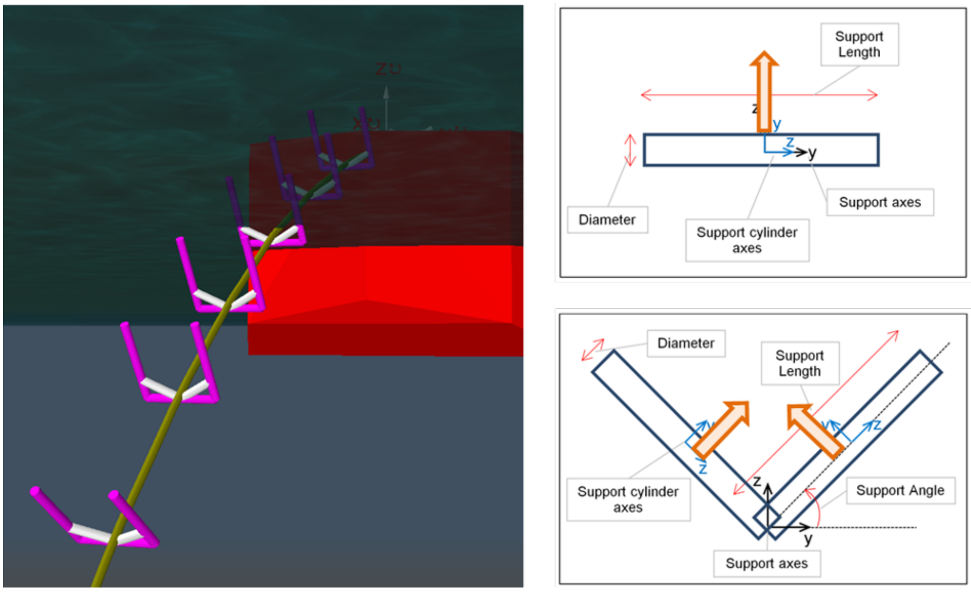

Figure 4.6: Total support reaction force, as calculated in OrcaFlex.

Table 4.6: Residual ovality of the pipe section (above V16) under the effect of bending and support reaction force, for static conditions.

k_{δ}	0.929	-
k_R	1.146	-
$\overline{\alpha_R}$	0.2	-
$\delta_{EI,R}$	1.26	mm
R_Y	1419.16	kN
R_{static}	488.6	kN
$\epsilon_{b,(static)}$	0.48	%
$\epsilon_{c,OS-F101}$	4.57	%
ϵ_c	3.37	%
$f_{Applied}$	2.3	%
$f_{Residual}$	1.19	%

The residual flattening due to bending and point loads, combined with the out-of-roundness tolerance from fabrication of the pipe, should not exceed a certain magnitude. In principle, the possibility of having local buckling and collapse at the sagbend region, is the factor that determines the limiting value for residual ovality in the overbend. More specifically, the residual ovality should be such that the collapse pressure of the pipe in the sagbend is not significantly decreased, so that the unity check for local buckling in the sagbend is satisfied. From the assessment (Table 4.6) of the residual ovality (1.19%), the collapse pressure can be calculated from the formula 4.12 provided in the DNV standards [9] and afterwards the local buckling check for load controlled conditions in the sagbend can be performed (4.13). It is calculated that for a pipe section which has the residual ovality created on the stinger, the unity check of local buckling is satisfied to a great extend ($0.33 < 1.0$). After some test calculations it is revealed that buckling in the sagbend can only occur when the residual ovality is enormously high, around 9%. This is explained by the fact that during S-lay installation in deep water there is high tension in the pipeline to ensure controlled bending in the overbend, therefore the bending in the sagbend is significantly decreased. "In deep water, the sagbend region is not critical from the point of view of allowable strain" [25]. Hence, for the case of S-lay installation the governing limit for residual ovality is the one reported in the DNV standards [9], namely 3%.

$$(p_c(t) - p_{el}(t)) * (p_c(t)^2 - p_p(t)^2) = p_c(t) * p_{el}(t) * p_p(t) * f_{residual} * \frac{D}{t} \tag{4.12}$$

$$\left[\gamma_m * \gamma_{SC,LB} * \frac{M_{Sd}}{M_k} + \left(\gamma_m * \gamma_{SC,LB} * \frac{S_{Sd(p_i)}}{\alpha_c * S_p(t_2)}\right)^2\right]^2 + \left[\gamma_m * \gamma_{SC,LB} * \frac{p_e - p_{min}}{p_c(t_2)}\right]^2 \leq 1 \tag{4.13}$$

Where,
p_c -characteristic collapse pressure (resistance to external over pressure)
$p_{el}(t) = \frac{2*E*\left(\frac{t}{D}\right)^3}{1-\nu^2}$
$p_p(t) = f_y * \alpha_{fab} * \frac{2*t}{D}$
$\alpha_{fab} = 1.0$ -fabrication factor for seamless pipe
p_{min} -the minimum internal pressure that can be sustained. Taken as zero for installation of empty pipeline.

In conclusion, the increased bending of the pipe above the last vessel support when rotating the stinger by 1.9 degrees, creates a 1.23% residual ovality. This ovality is within the allowable limit of 3%.

4.5 Fatigue analysis

This section concerns the impact of the stinger inclination on the pipe integrity in terms of fatigue. A pipeline is exposed to damage caused by the installation stresses due to the laying process [2]. Generally, a structural detail can resist a limited number of cycles of a certain stress range. For this reason the structures are designed such that they can withstand the damage during their lifetime. The fatigue damage during the proposed installation method will be compared with the fatigue from the common installation in order to distinguish the differences.

Fatigue depends on two parameters: the stress ranges and the number of cycles of each stress range. Fatigue damage is defined as the number of applied load cycles divided by the corresponding number of cycles to failure at a constant stress range, known as Miner's sum (Formula 4.15) [35], [38]. At the installation phase, one parameter that influence the fatigue of the pipeline is the stationary time or pull time. During a pull time the pipeline is kept stationary in order for the welds to be completed. A pipe section will remain stationary at one location until another pipeline pull is made. During this stationary time, most fatigue will happen at the part of the pipeline that is positioned at the worst node location. Therefore, the fatigue in this location during a pull time must be calculated as well as the total accumulated fatigue damage of a pipe section while it is being lowered in the water.

4.5.1 Methodology

Welds are in general the most critical sections in what concerns fatigue [9]. It will be assessed whether there is an unacceptable fatigue damage of the welded joints when the stinger is rotated by 1.9 degrees. According to the DNV standards, the design fatigue lifetime of the pipe can be split between the different phases of installation, as laid and operation. During installation normally 10% of the total fatigue damage can be consumed (this utilization factor can change after agreement with the pipeline operator). Therefore, the maximum allowable fatigue damage (limit) during installation is 10/DFF, where DFF is the design fatigue factor presented in the DNV code. For medium safety class, DFF=6, hence the maximum fatigue damage that corresponds to installation is 1.67%. If the fatigue damage at the worst node is less than the limit of 1.67%, the remaining fatigue damage can be used to assess the allowable stationary time in case a weld repair is required. The calculation of the maximum allowable stationary time will not be presented in this thesis, since the main focus is on pipe integrity matters.

According to the standards, if the $\epsilon_{l,nom} > 0.4\%$, the linear damage hypothesis (4.15) can be used and fracture assessment is required. The maximum allowable amount of cycles N at a certain stress level for pipeline girth welds, can be determined based on a specified fatigue curve[2]. This so-called S-N curve can be expressed in the following form:

$$log_{10}N = log_{10}K - m * log_{10}\sigma_R \tag{4.14}$$

where,
N -the maximum allowed amount of cycles [-]
σ_R -stress range [MPa]
K, m -curve fitting constants

$$\Omega = \sum \frac{n_i}{N(\Delta\epsilon_i)} \tag{4.15}$$

where,
Ω -Miner's sum
n -the number of cycles for a particular stress range [-]
$N(\Delta\epsilon_i)$ -the maximum allowed number of cycles of the particular stress range [-]

The coefficients describing the S-N curve are based on a weld classification system. According to DNV-RP-C203 specifications, S-N curve in air (corresponding F curve shown in Figure 4.7) can be used for a non-flooded pipe during installation. It is assumed that the field coating is good enough to ensure that the field joint is not exposed to any sea-water. The terms $log_{10}K$ and $-m$ of such a curve receive the values 11.699 and -3.00 respectively. The corresponding S-N curve obtained from OrcaFlex is illustrated in Figure 4.8.

The fatigue damage of the pipe due to the environmental loads was calculated in OrcaFlex. The results refer to the outer fibre of the pipe cross section (radial position selected as "outer"). In addition, OrcaFlex calculates the fatigue damage of points along the pipe's circumference, defined by the selected number of angles. For example, a sufficient number of angles is 8, Figure 4.9.

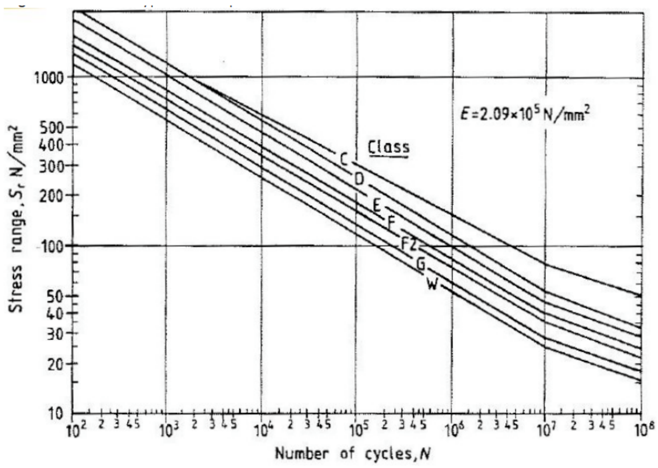

Figure 4.7: Example of S-N curves for different conditions [2].

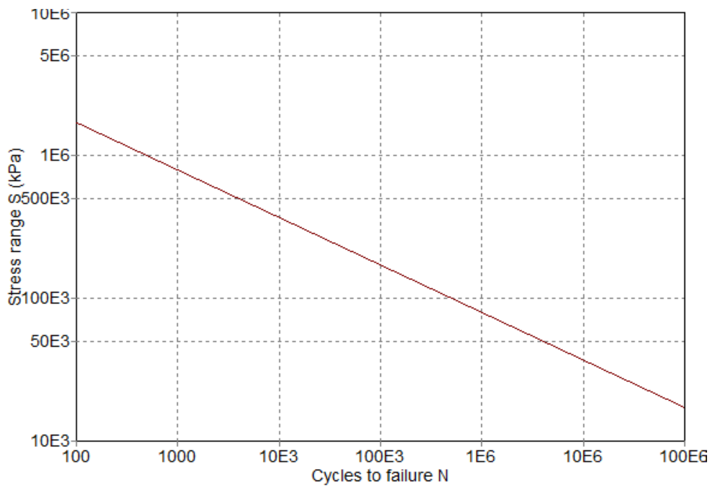

Figure 4.8: The S-N curve obtained from OrcaFlex for $log_{10}K$ and $-m$, 11.699 and -3.00 respectively.

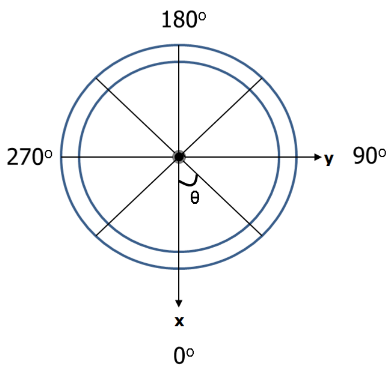

Figure 4.9: Fatigue calculation at 8 different locations of the pipe's circumference.

4.5.2 Results

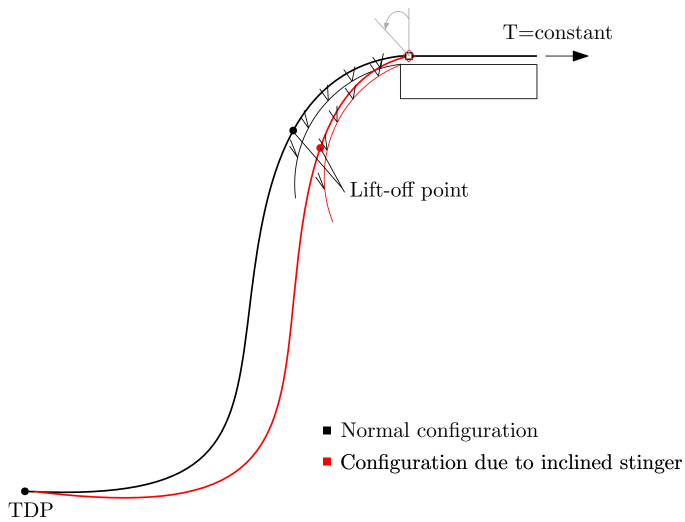

Figure 4.10: Pipeline configuration during normal installation and installation with inclined stinger. The tension is kept constant.

Two fatigue analyses were conducted in OrcaFlex. One analysis refers to the fatigue damage during normal installation and the other calculates the fatigue damage when the stinger is inclined. In the model of the inclined stinger, the tension is kept constant (Figure 4.10) based on the dynamic analysis performed in Chapter 3. The damage per node along the length of the pipeline during a pull time for both cases, is depicted in Figure 4.11. The pull time is assumed as 15 minutes. The critical node, the node with the larger fatigue damage, is the one at 298.82 m, as shown in Table 4.7. This node is located close to the lift-off point but refers to a supported location in the static configuration. The fatigue damage per pull time at the critical location is 0.0006 during normal installation and 0.00055 during installation with inclined stinger.

Table 4.7: Fatigue analyses results for normal installation and installation with inclined stinger.

Angle	0	1.9
Critical node	298.8214	298.8214
Fatigue damage per pull time	0.0006	0.00055
Total accumulated fatigue	0.00467	0.00526

The minor difference in the fatigue damage at this particular location can be explained when observing the stress range diagrams. The time history of the tensile stress in the critical node is the same for both cases. However, there is a notable difference at the bending stress ranges. The bending stress time history for both cases can be seen in Figure 4.12. The corresponding histograms are presented in the same figure as well. It can be seen that at the arc length of 298.82 m, there are more high bending stress range amplitudes during normal installation, while when the stinger is inclined, there are more low bending stress range amplitudes. This reduction in the fatigue damage of the critical node when we lower the stinger is due to geometrical reasons. By rotating the stinger hinge the lift-off angle increases and we drive the pipeline to exit the stinger in a more straight configuration (bending fluctuations are smaller). In addition, it can be seen in the Figure 4.11, that the rapid increase of fatigue is shifted towards the nodes before the critical node, resulting in a reduction of the maximum (peak) fatigue damage. This is also attributed to the same geometrical reason.

Regarding the total accumulated fatigue damage, it is the summation of the damage per pull time of all nodes from the stinger until the touchdown point. It can be seen in Table 4.7 that the total fatigue damage during normal installation is less than when installing pipeline via an inclined stinger. That is due to the higher fatigue damage caused at the nodes at the beginning of the stinger (from 203.797 m until 220 m, as shown in Figure 4.11). In this location, the bending stress range amplitudes are significantly increased compared to normal installation. When the stinger inclination increases, the departure angle of the pipeline increases too, resulting in increased bending fluctuations. Regarding the actual magnitude of the fatigue damage, one should be aware of the modelling limitations that exist. These limitations, which are explained later on, make the results of fatigue calculations in OrcaFlex conservative. Finally, the accumulated fatigue damage from any case is less than the maximum allowable damage of 0.0167, meaning that the remaining fatigue life can be consumed in case of an urgent stop of the installation.

The calculated fatigue damage refers to the case when the stinger is always in the inclined position. Such calculations serve the assessment of whether or not the stinger is allowed to stay lowered in case of an urgent weld repair. However, in normal conditions, during the proposed installation method, the stinger is kept in the inclined position only for four to six consecutive pulls, depending on the length of the residual curvature that is to be achieved. Afterwards, the stinger will be rotated back to its normal position. Hence, at the beginning of the installation a pipe section on the stinger will be exposed to the fatigue damage caused due to inclined stinger and afterwards to the damage due to normal configuration. One may think that these changes must be taken into consideration when calculating the accumulated fatigue damage during the proposed installation method. However, this step can be neglected, because as seen in Figure 4.11, the fatigue damage of the suspended pipeline is approximately the same for both installation methods.

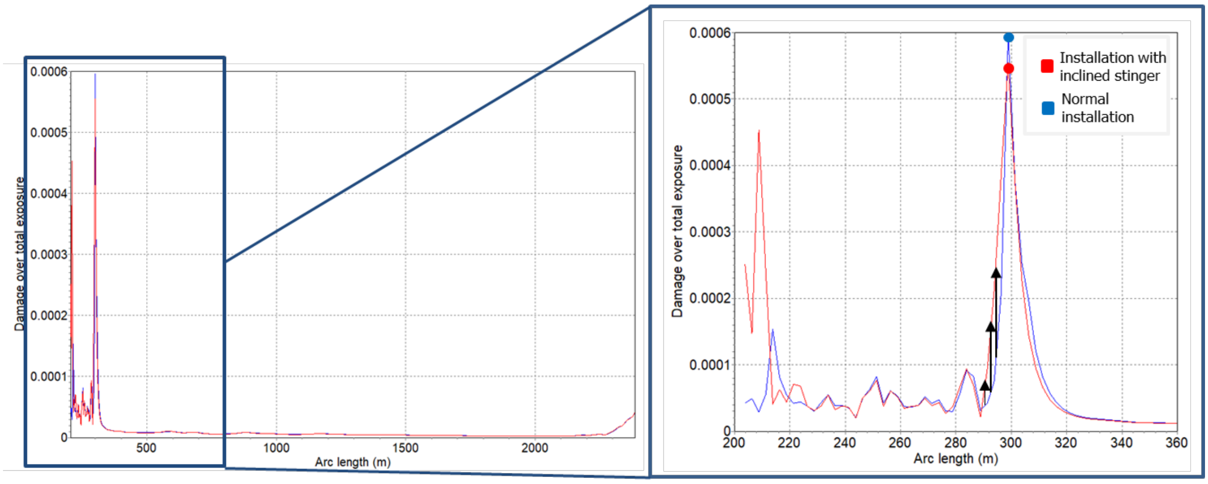

Figure 4.11: Comparative diagram of the fatigue damage of the nodes along the length of the pipeline for the cases of normal installation and installation with inclined stinger.

Note

When doing fatigue analysis in OrcaFlex, one should be aware of the modelling limitations that exist.

- Incorrect stress results: It is not possible to capture a non-linear stress response. The stress response will always be assumed to be linear and elastic. The tensile stress will always be linearly proportional to the wall tension and the bending stress will always be linearly proportional to the bending moment. This means that for the nodes loaded in the plastic region (as the node at the stinger hinge when using inclined stinger) the bending stresses as calculated in OrcaFlex are not correct (larger). For more information, see Appendix E.
- Stress range amplitude: In order to be able to capture realistic bending stress range amplitudes in OrcaFlex, one should be aware that hysteresis has to be taken into account in the model. If hysteresis

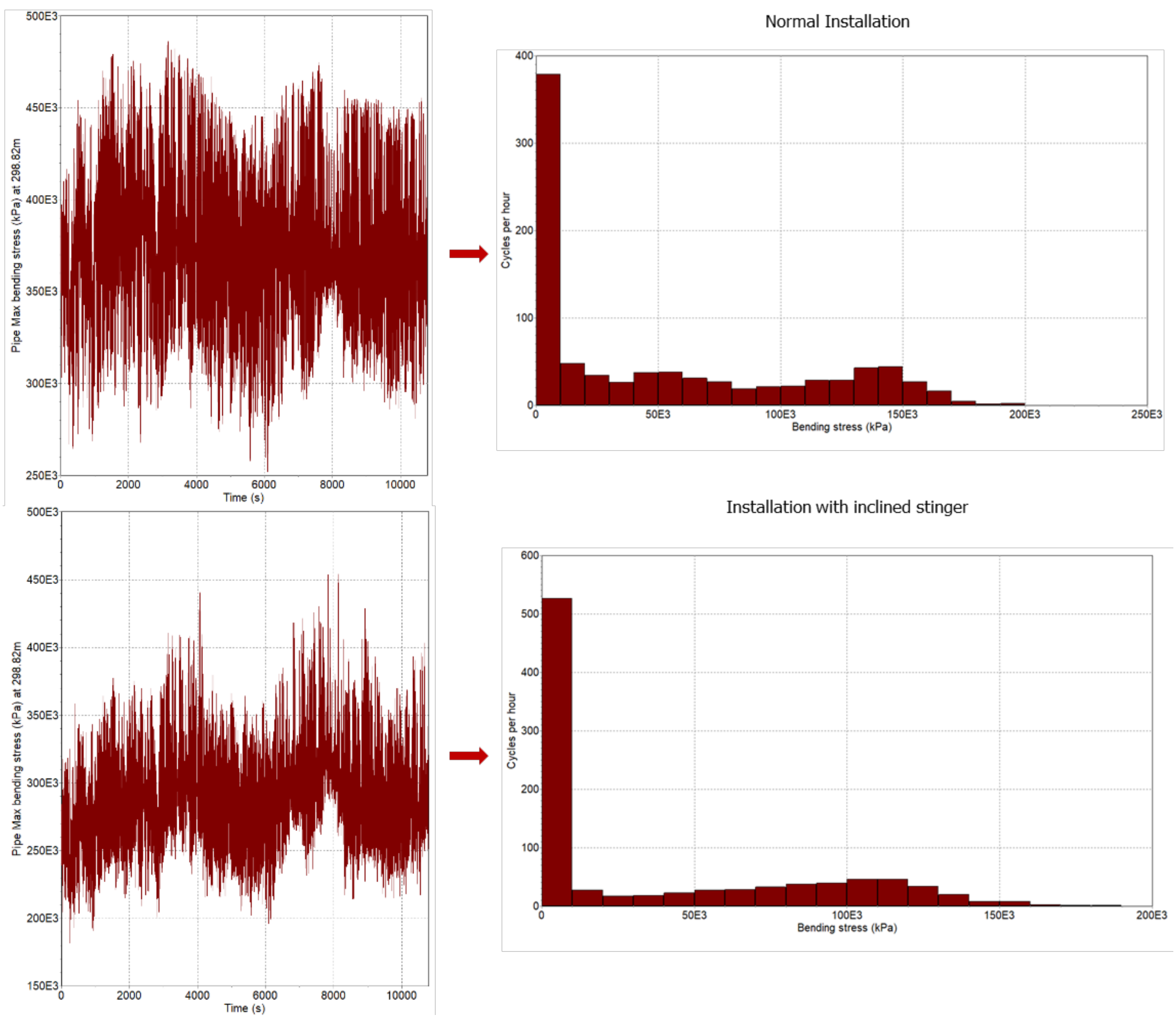

Figure 4.12: For both installation methods: time history of the bending stress in the critical node (298.8214 m) and the corresponding histograms.

is not considered in the model, then OrcaFlex assumes an elastic material behaviour. This means that even if the material is loaded in the plastic region (and the yielding point is exceeded), in case of unloading the stresses will follow the same nonlinear path. This would lead to an underestimation of the stress range amplitude and of course to a non realistic material behaviour. Normally, the stresses follow the linear relaxation path once an already yielded material is unloaded. This behaviour is captured in OrcaFlex only when bending hysteresis is enabled. Therefore, although the magnitude of the stresses per se is larger, as explained above, the magnitude of the range amplitude, when hysteresis is activated, is realistic.

- Weakness of tensioner model: The tensioner is represented by a winch which pays-in and out pipeline, to keep the tension within a deadband. This results into a significant forward and backward pipe movement during dynamics. In addition, if the tension tends to go beyond the upper limit (T_{max}) more than that it tends to go below the lower limit (T_{min}), then the winch will pay-out more than pay-in and vice versa. Hence, it is possible that the winch will never reach its original length and the nodes of the pipeline will shift to different locations. This means that the fatigue damage of the nodes will be calculated according to their new positions every time in the simulation. This movement of the nodes is unrealistic especially in deep water installations. In deep waters, the pipeline is hardly moving while in shallow waters the pipe movement is larger than what the tensioner model can do.

> This movement of the nodes is the primary reason that unusual results are observed in the fatigue analysis in OrcaFlex. First of all, in principle the maximum fatigue damage during installation is observed at the lift-off point. The lift-off point (the point in which the pipeline is not supported by the stinger anymore) experiences the biggest bending fluctuations due to the movement of the suspended pipeline. However, due to this forward and backward pipeline movement, the lift-off is not constant. This is the reason why the maximum fatigue damage appears in the node before the lift-off point.
>
> Similarly, the big increase of the fatigue damage in the node located at the stinger hinge is explained. The node repeatedly travels from the vessel to the stinger and vice versa. Therefore, it goes from a straight shape to a fully bent shape. When the stinger is inclined, the node travels from a straight configuration to an even more bent situation. This reason explains why the fatigue damage skyrockets for the case of inclined stinger. In deep water installations, usually the pipe hardly moves on the stinger. Therefore, such a high fatigue damage is expected to drop but still remain larger than the fatigue damage during normal installation.

To verify the expectations regarding the impact of the stinger inclination on the fatigue damage of the pipeline, a post processing tool was used where the large pipeline movement due to the tensioner is avoided. Details can be found in Appendix F. As expected, the increase of the pipeline departure angle results in an increase of the fatigue damage of the pipeline located at the beginning of the stinger. In addition, the maximum fatigue damage occurs at the lift-off point and for larger stinger inclinations, it was calculated that the fatigue damage of the lift-off point increases. This comes in contrast with the initial claim that the pipeline leaves the stinger in a more straight configuration resulting into smaller bending fluctuations. At this point a disclaimer is added; due to the time limitation of the project we are unable to investigate further on the fatigue damage of the lift-off point. However, it is evident that during installation with inclined stinger, the critical points are both the lift-off point and the point at the stinger hinge.

As a conclusion, the fatigue damage calculations in OrcaFlex are not reliable enough due to the aforementioned modelling limitations. However, comparison can still be made without taking into account the actual value of fatigue damage. For the particular case examined here, the stinger inclination would result in a small difference in the total fatigue damage in the pipeline. Based on this evidence, it is recommended that for each project, fatigue analysis is done for both pipeline configurations (due to normal and inclined stinger) and calculation of the maximum allowable stationary time is done based on the project specific critical configuration.

Chapter 5

Pipeline rotation analyses

Observations of pipelay operations indicate the onset of pipeline rotation about the pipe longitudinal centerline during installation in deep waters. The need of gaining insight into the behaviour of pipeline rotation has resulted in extensive research, reviewed in Chapter 2.4.3. The complexity of this research topic results from the impact of various parameters involved. One of the governing parameters is the plastic bending history or the residual curvature in the pipeline. In addition, according to researchers the most preferred scenario for triggering buckling, is 90 degrees rotation. That implies that the residual curvature is at the same plane as the seabed [26]. If the residual curvature rotates by 180 degrees, meaning that its ”crown” has a downward orientation, then the in-place behavior in buckling is still acceptable [7]. However, larger angles of rotation may lead to high stress/strain in the pipeline. Hence, it is important to investigate the impact of the residual curvature on the rotational behaviour of the pipeline.

5.1 Model description

Since this research study involves plastic deformation of the pipeline, it is already known that rotation will be initiated during installation. This rotation affects the on-seabed pipeline configuration, which will determine the response to buckling during operation. 3-D numerical analyses were conducted in OrcaFlex software to assess the impact of the residual curvature on the pipeline rotation and the as-laid configuration. The following conditions define the model:

- Feeding line: To be able to examine whether rotation is initiated due to plastic deformation of the pipeline on the stinger, a pipeline cross section must move from the vessel through the stinger to the sagbend area and finally land on the seabed. To represent this pay-out process in OrcaFlex, a new line element, the ”feeding line” is introduced in the model. Feeding line can be considered as a flexible hose being unwound from a rotating drum [22] (Figure 5.1). The one end of the feeding line is connected to the vessel and the other to the main pipeline. Therefore, as time progresses the drum unwinds the hose at a constant rate, so that the main pipeline is being lowered in the water. The pay-out rate was set to 0.5 m/s. This value was selected such that the analyses can be successfully completed in a relatively small total simulation time. The feeding line has the same diameter, thickness and material type as the main pipeline. The bending, axial and torsional stiffnesses are linear and elastic.
- To correctly model the pay-out process, a forward vessel motion must be included. The speed of motion is assumed equal with the pay-out rate, hence 0.5 m/s.
- The End A of the main pipeline, connected to the feeding line, has infinite bending and torsional stiffness to ensure that the two lines are rigidly connected. The End B of the main pipeline, anchored on the seabed, has infinite bending and torsional stiffness too.
- The orientation angles of the end points and connection points of the main pipeline and the feeding line are the same, so that twist is not induced due to deviations.
- The End B of the main pipeline is anchored on the seabed, 300 meters away from the touchdown point. It was investigated whether this boundary condition has an impact on the angle of pipeline rotation. Details can be found in Appendix G.
- Both lines have uniform wall thickness, therefore the possibility of creating instability in the model due to variable wall thickness is vanished.

- Both lines have a torsional stiffness GI_T calculated based on the following relations

$$G = \frac{E}{2 * (1 + v)} \tag{5.1}$$

$$I_T = \pi * \frac{(OD^4 - ID^4)}{32} \tag{5.2}$$

where,

G	-Shear modulus
I	-Torsional moment of inertia
E	-Young's modulus [MPa]
v	-poisson's ratio (0.3)
OD	-outer diameter [m]
ID	-inner diameter [m]

- Coupling between tension and torque is not taken into account, meaning that axial strains cannot induce torque.
- Bending and torsion coupling is fully modelled in OrcaFlex. This generally means that some bend moments present in one part of the line can become torque elsewhere in the line. The coupling of the two moments occurs particularly in three situations:
  1. The line has a pre-bend in one plane and is bent out of that plane.
  2. The line has hysteretic bend stiffness and the line is bent in one plane and then bent again in a different plane of bending.
  3. The line has non-isotropic bend stiffness.

  Here, the line has isotropic bend stiffness, therefore only the first two situations, described above, refer to the models used in this section.
- The model is not perfectly symmetrical, so that a small out of plane bending is induced in the catenary area.
- The disturbance due to the environmental loads is not taken into account, therefore the wave height, the current and wind velocity is set to zero.
- The seabed is flat with zero slope. It is modelled as an elastic seabed, meaning that it behaves as a simple elastic spring in directions normal and tangential to the seabed plane [22]. This gives a seabed normal resistance that is proportional to the penetration, and a seabed lateral resistance that is proportional to the lateral displacement of the contact point [22]. The linear soil stiffness for both directions was assumed as $100kN/m/m^2$. The soil friction coefficient is 0.5.
- The tension is maintained constant during pay-out. Ergo, the curvature of the sagbend area is constant too.

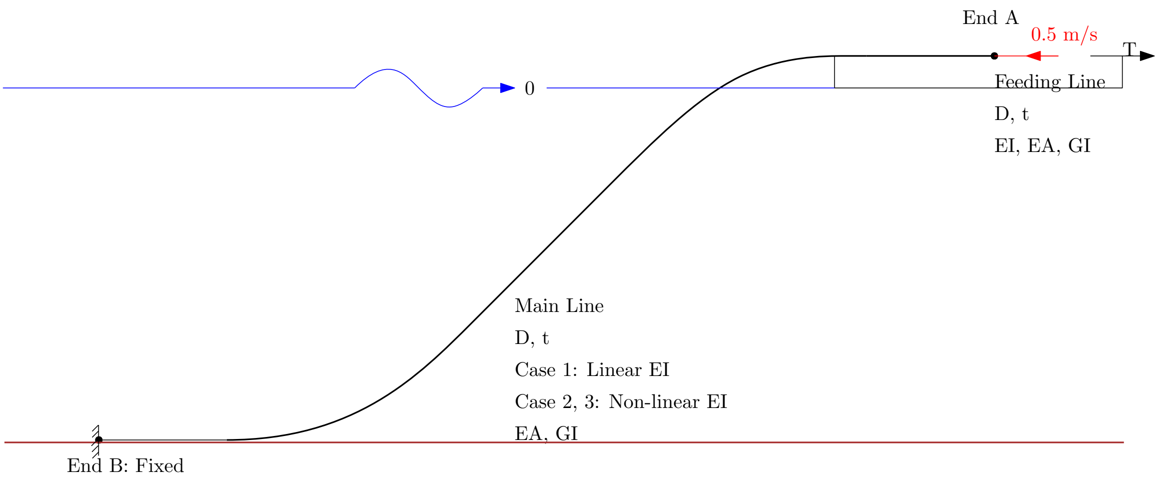

Figure 5.1: Schematic representation of the position of the main pipeline and the feeding line at the start of the simulation. Environmental conditions and line properties are presented as well.

5.2 Analyses and results

A comparative study was conducted for three different cases:

- Case 1- Limit case- Elastic material: The bending stiffness of the material is linear and elastic. The stinger inclination is the one decided for a normal installation (zero additional inclination). Hence this case describes a normal pipeline installation where the material is bent only elastically.

- Case 2- Elastoplastic material- Normal installation: The bending stiffness of the material is non-linear and hysteretic, to represent the case where the pipeline is plastically deformed during normal installation in deep water.

- Case 3- Elastoplastic material - Residual Curvature: The bending stiffness of the material is non-linear and hysteretic. The stinger inclination is the one designed for a normal installation. A pre-bent section is included in the main pipeline having a curvature of 0.0089 rad/m. This value equals the residual curvature that we create in this research when lowering the stinger by 1.9 degrees (as shown in Chapter 3). In this way we represent the installation of the pipeline with a local residual curvature.

Dynamic analyses were conducted for all the three different models. Feeding line is paid-out only during dynamic simulations. The following subsections present the results of rotational behaviour and as-laid configuration of the pipeline on the seabed.

The focus is on the rotation of the pipe section which initially is on the stinger (Figure 5.2). During the dynamic analysis this section leaves the stinger and the analysis is completed once the section is laid on the seabed. Hence, at the presentation of the results, reference will be made to nodes of this pipe section. Hereby some important nodes are introduced (Figure 5.3). The nodes are named after their position, the arc length, meaning the distance from the start of the pipeline (End A).

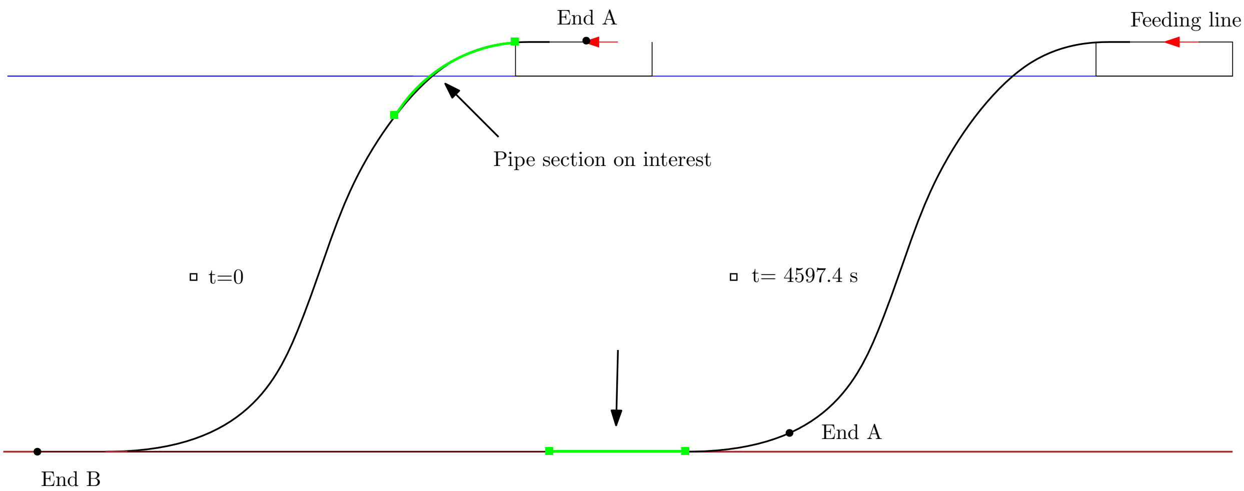

Figure 5.2: Indication of the pipe section of interest. Start of simulation (t=0): Pipe section on the stinger. End of simulation (t=4597.4s): Pipe section laid on the seabed.

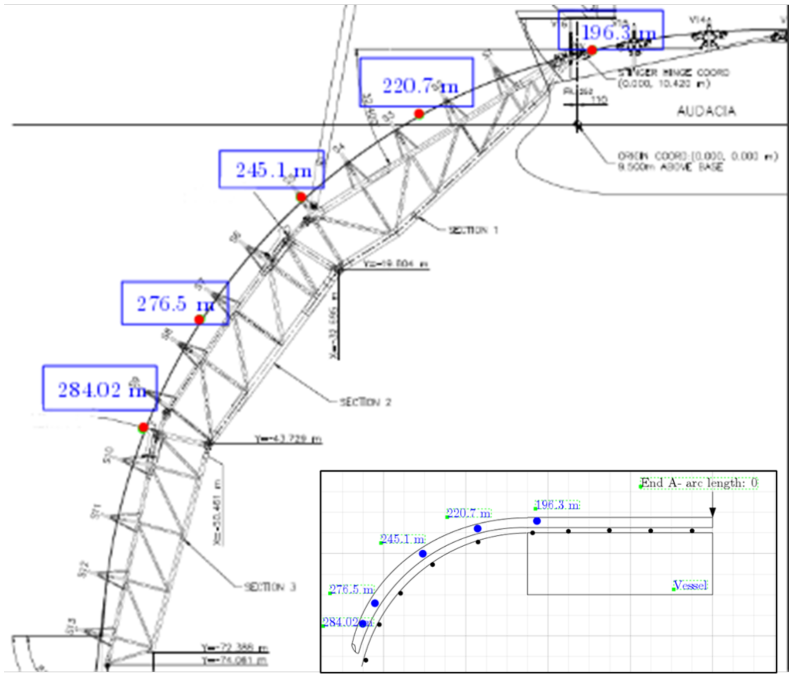

Figure 5.3: Nodes at the arc length of 196.3 m, 220.7 m, 245.1 m are the start, mid-point and end of the imposed pre-bent section. The node at 276.5 m is the node with the maximum bending strain due to the stinger radius and the node at 284.02 m is the last node under plastic strains in the overbend.

Case 1- Limit case: Elastic material

When using linear bending stiffness, the pipeline rotation is infinitesimal. The pipeline elastically bends in the overbend area, it is pulled straight in the water and finally it bends (again elastically) in the opposite direction in the sagbend (Figure 5.4). The detailed plots of bending moment and strain time history of the outer fibre of a node can be found in Appendix G. At the end of the simulation the main pipeline is laid on the seabed. The lateral deflections of the position of the pipeline on the seabed from a straight line are infinitesimal, something that was also expected due to the elastic material.

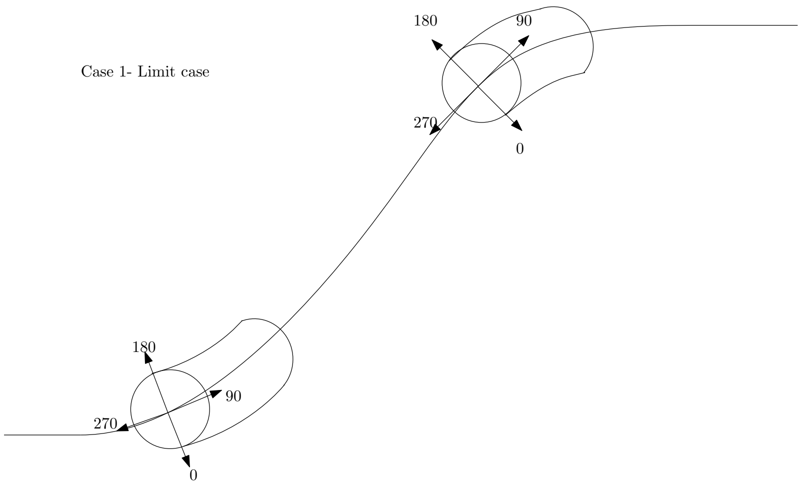

Figure 5.4: Case 1- Limit case: Illustration of pipeline orientation during installation. 0 degrees refer to the bottom of the cross section and correspondingly the 180 degrees to the top of the cross section.

As a conclusion, no noteworthy rotation is triggered when the pipeline is loaded in the elastic region[1] or

[1]A supplemental case was tested to assess whether there is any limitation (such as disabling of bend moment- torsion coupling) due to the modelling of elastic material. A new model was created where the material was elastoplastic and its yielding point was not exceeded during the dynamic analysis. The results were identical with Case 1.

when the material is defined as linear and elastic. This comes to an agreement with previous research where pipeline rotation was observed only when plastic strains were induced in the pipe cross section. However, the modelling of this case was very useful to ensure that there is not any other excitation, except from the out of plane bending, which can create instability in the model.

Case 2: Elastoplastic material- Normal installation

After creating the stable model of case 1, we can incorporate non linear bending stiffness. During installation in deep water, the pipe is loaded beyond the yielding point due to the stinger's radius of curvature. Hence, this case examines the initiation of rotation during a typical installation procedure in deep water. To take into account plastic strains in OrcaFlex, the bending stiffness of the pipeline is specified as non-linear and hysteretic, as already introduced in Figure 3.6 of Chapter 3.

As already revealed from the literature review, pipeline rotates when is plastically deformed [14]. The maximum bending strain developed in the pipeline from the stinger is 0.36 [%] (plastic area). The tension gradually decreases from the overbend to the sagbend. As a result, the residual curvature takes shape as it travels to the sagbend. Rotation starts when the plastically deformed nodes travel from the overbend to the sagbend. More specifically, a progressive twist appears when these nodes reach the area of reverse bending (at t= 3729 s). A schematic representation of the rotation of the section of interest is illustrated in Figure 5.5. "Gamma" angle in OrcaFlex is the angle between the node axis and the global axis. The rotation profile of the node at 284.02 m is the one illustrated in Figure 5.6. The rotation of all nodes in the section of interest follows the same trend. Just before reaching the touchdown point, the section of interest has its maximum rotation, Figure 5.7. The node which appears to have the maximum angle (131.3 deg) is at 196.3 m. When the section reaches the touchdown point and few seconds later is laid on the seabed, it rotates in the opposite direction. This happens because the residual curvature wants to rest on the seabed. The final and reduced rotation angles along the main pipeline laid on the seabed are shown in Figure 5.8.

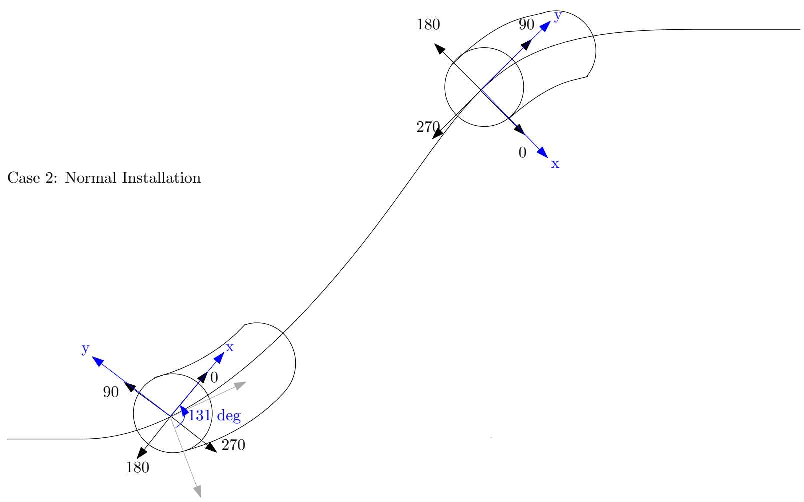

Figure 5.5: Case 2- Elastoplastic material- Normal installation: Illustration of pipeline orientation during installation. 0 degrees refer to the bottom of the cross section and correspondingly the 180 degrees to the top of the cross section.

The detailed plots of bending moment and strain time history of the outer fibre of the node at 198.8 m can be found in Appendix G.

The final on-seabed configuration of the main pipeline is the one depicted in Figure 5.9. As seen, there is a small curvature on the seabed which results from the 0.36[%] plastic strains in the overbend. The maximum curvature on the seabed is 0.002 [rad/m] (Figure 5.10). The maximum lateral deflection from the straight line is 0.9 meters approximately. The nonlinear lateral deflection belongs to the nodes which experienced plastic strains on the stinger. The pipeline is fully in contact with the seabed.

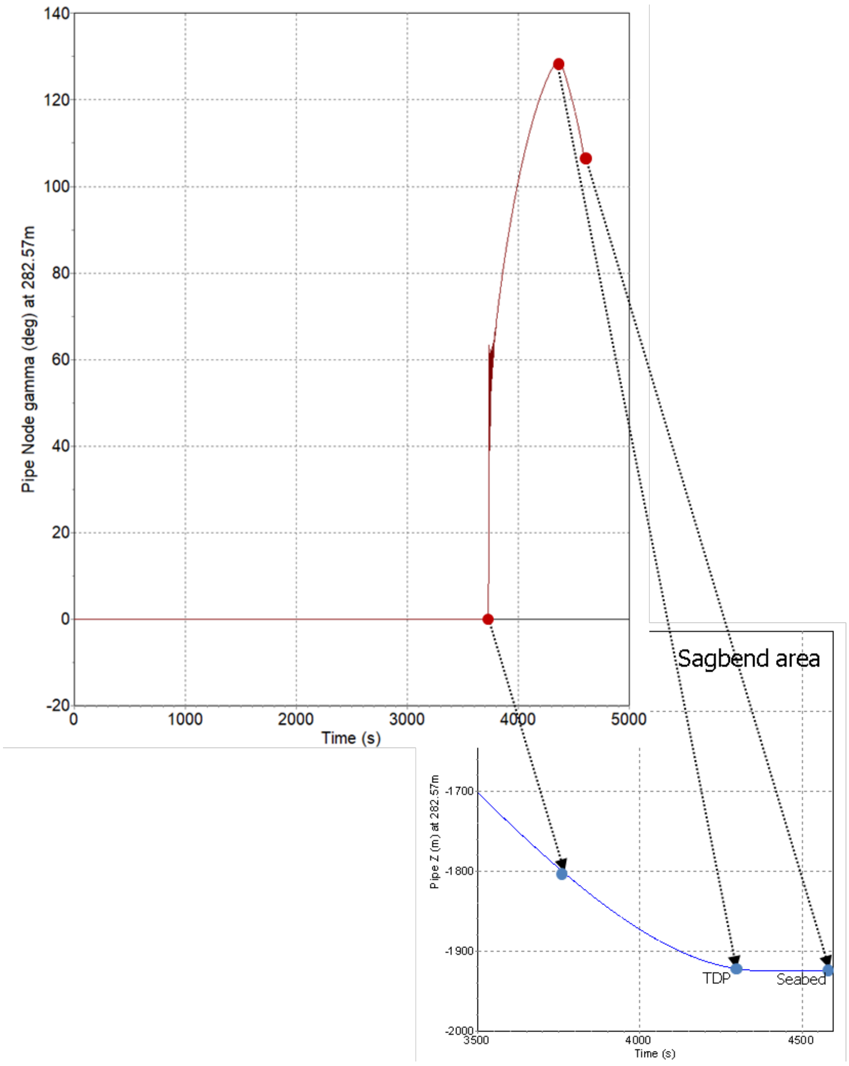

Figure 5.6: Case 2- Elastoplastic material- Normal installation: Rotation profile over time for node at 284.02 m during normal installation. Angle increases when the node passes from the sagbend area, gets its maximum value at the touchdown point and decreases when the node is in contact with the seabed.

In summary, for the case examined in this thesis, the pipeline is loaded beyond the yielding point on the stinger. When the pipeline exits the stinger and reaches the sagbend, it starts rotating until it finally lands on the seabed. The maximum total twist angle is 131.3 degrees while the final angle, when the pipe section is laid on the seabed, is 109.65 degrees. The maximum lateral deflection of the pipeline on the seabed is 0.9 meters. Finally the maximum in- place curvature is 0.002 [rad/m].

Note

It can be seen from the rotation along the pipeline length (Figure 5.8), that the angles gradually decrease to zero. This happens due to the certain boundary condition; End B is fixed. There is a high possibility that this boundary condition has an impact on the allowable rotation in the pipeline. To investigate if this is true, extra models are created where the End B is placed 1300 and 3300 meters far from the touchdown point. Details can be found in Appendix G.

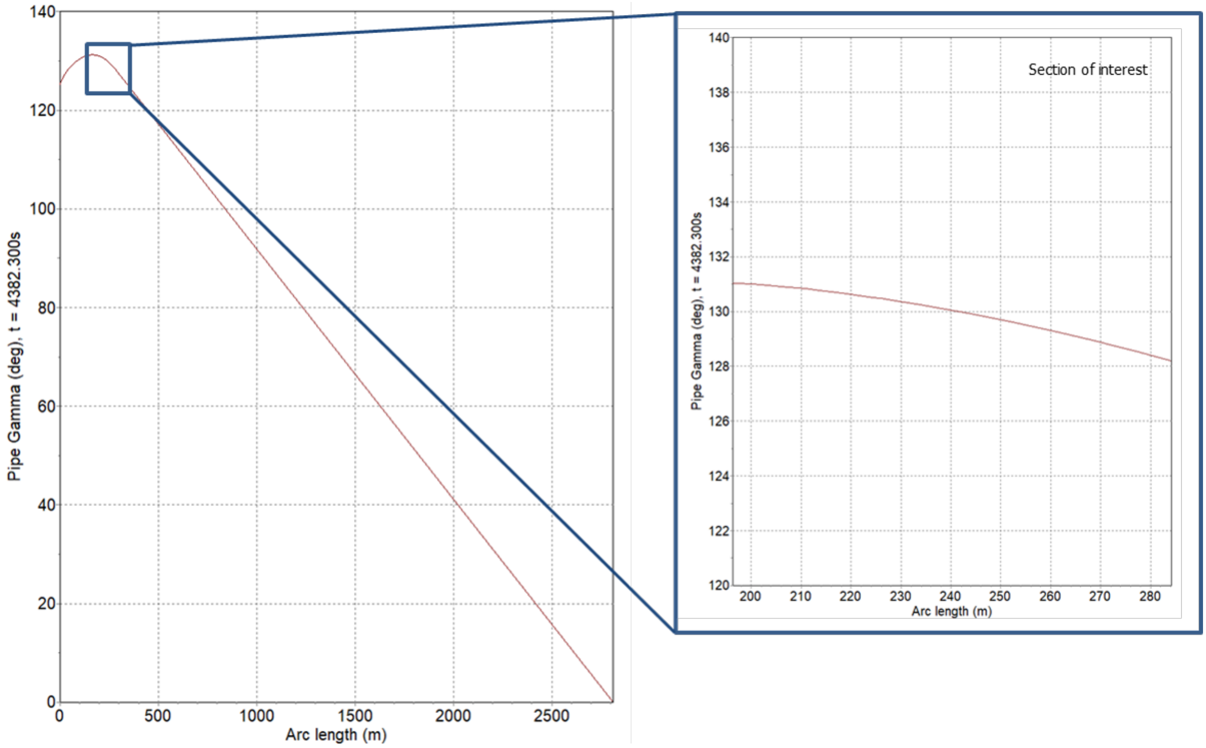

Figure 5.7: Case 2- Elastoplastic material- Normal installation: Maximum rotation angles of the nodes along the length of the pipeline just before the section of interest reaches the touchdown point. The angles of the nodes in the section of interest can be seen in the enlarged plot. Normal installation.

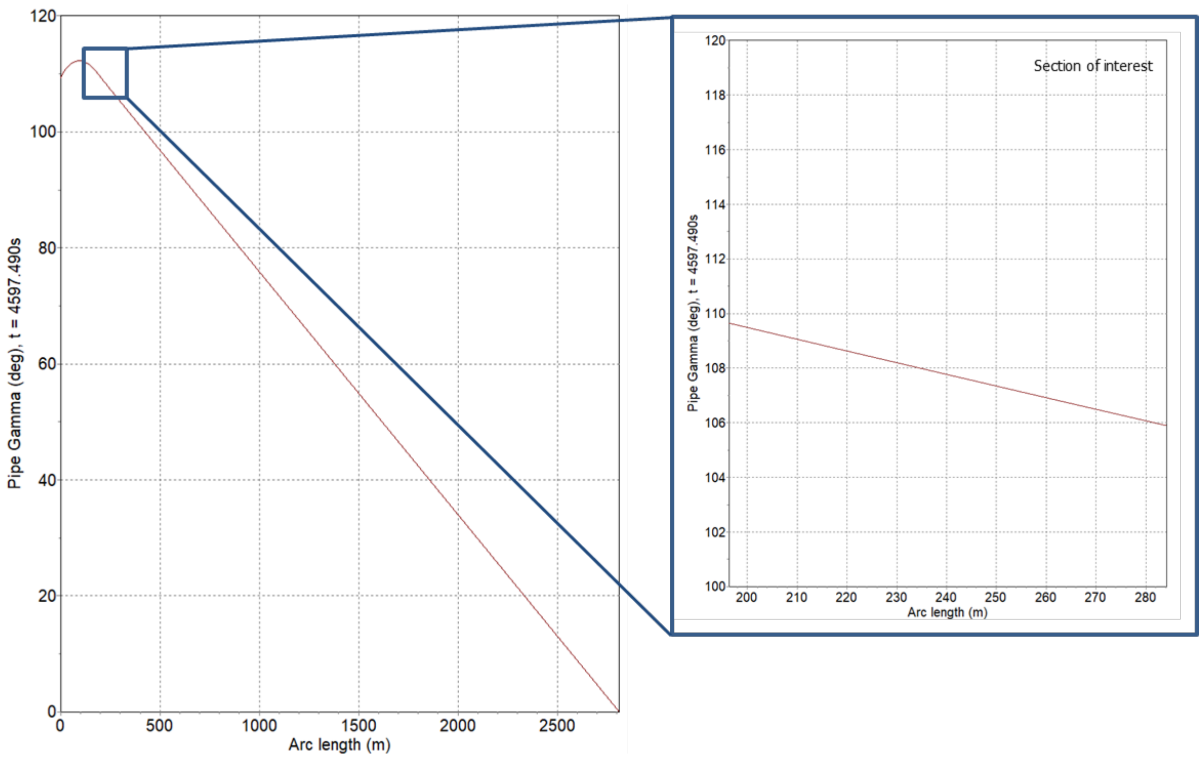

Figure 5.8: Case 2- Elastoplastic material- Normal installation: The final rotation angles of the nodes along the length of the pipeline at the end of the simulation. The angles of the nodes in the section of interest can be seen in the enlarged plot. Normal installation.

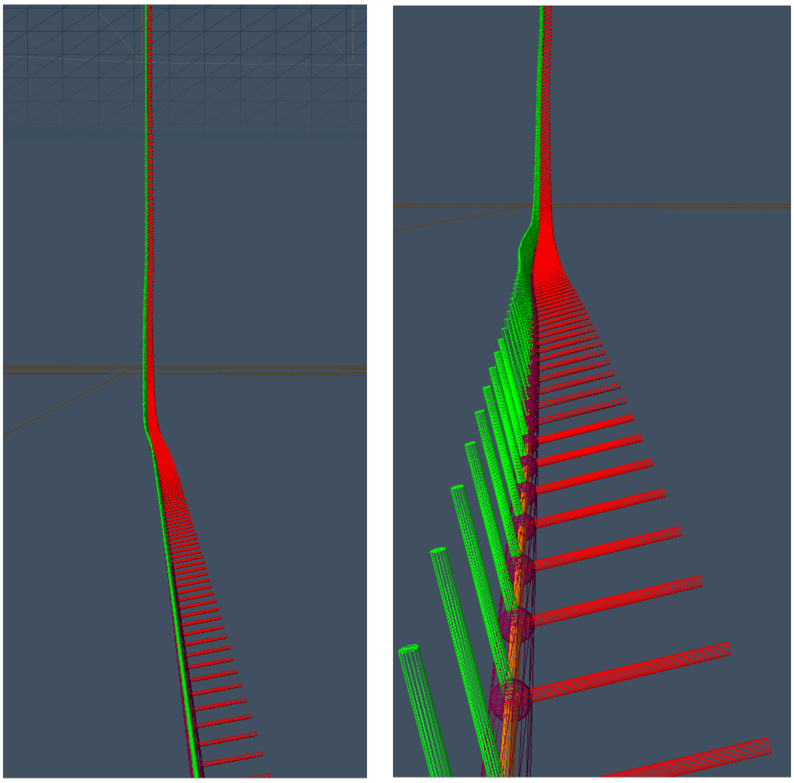

Figure 5.9: Case 2- Elastoplastic material- Normal installation: The pipeline configuration on the seabed after normal installation.

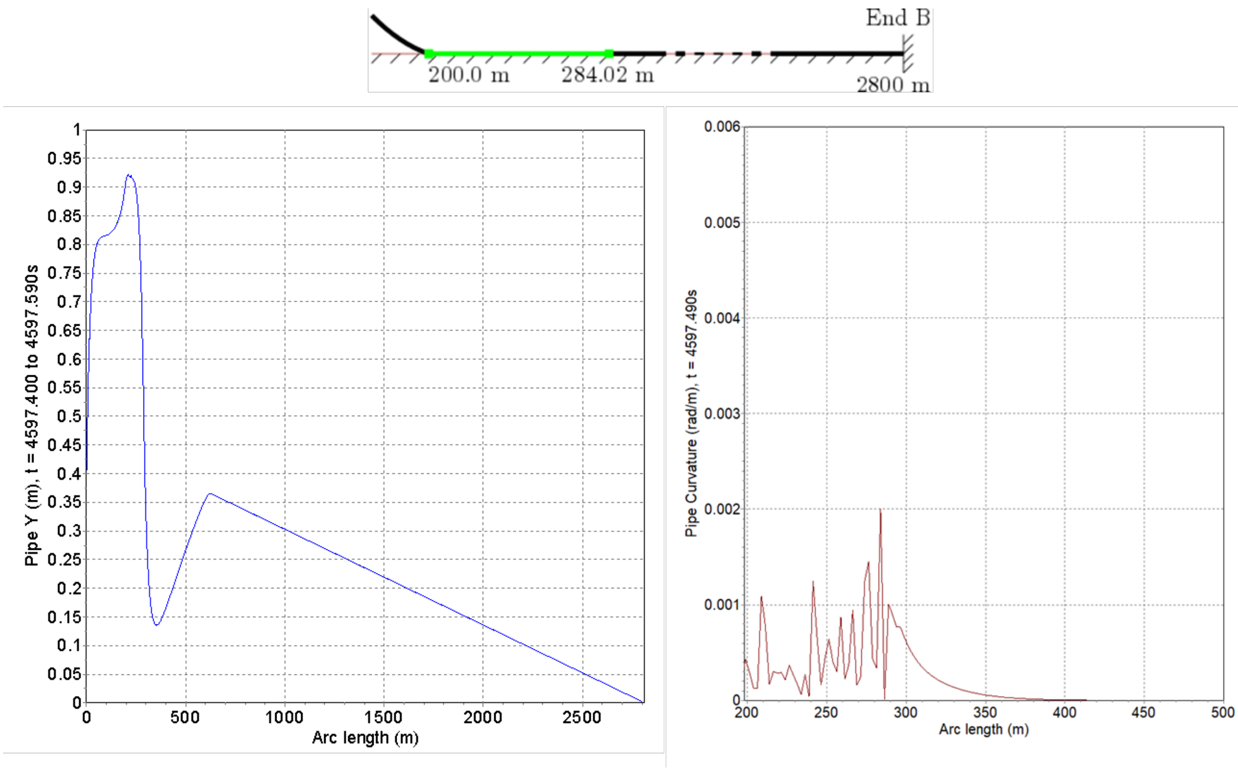

Figure 5.10: Case 2- Elastoplastic material- Normal installation. Left: Lateral deflection of the pipeline from a straight line at the end of the dynamic simulation. Pipeline laid on the seabed having a "curved" shape with maximum deflection from the anchored end point of 0.9 meters approximately. Right: The curvature of the section of interest on the seabed. Maximum curvature of 0.002 [rad/m].

Case 3: Elastoplastic material- Residual curvature

The third case represents the installation of the pipeline with additional residual curvature. Chapter 3 concludes that for an 18 inches pipeline installed in deep water, an 1.9 degrees extra inclination of the stinger results in extra bending of the pipeline on the stinger hinge. As already discussed, the goal is to create 48.8 meters long sections which will have this residual curvature. Hence, case 3 is designed to investigate the effect of the extra curved pipe section on the rotation of the pipeline in deep waters.

It was highlighted earlier that the residual curvature is introduced in OrcaFlex by the pre-bent command. A pre-bent pipe section is placed at the beginning of the stinger having the value of 0.0089 [rad/m]. The stinger inclination is the same as for normal installation (therefore the same as case 1 and case 2). In this way the model represents the stage in which the extra bent pipeline section is already created and the installation process continues without the extra stinger inclination any more.

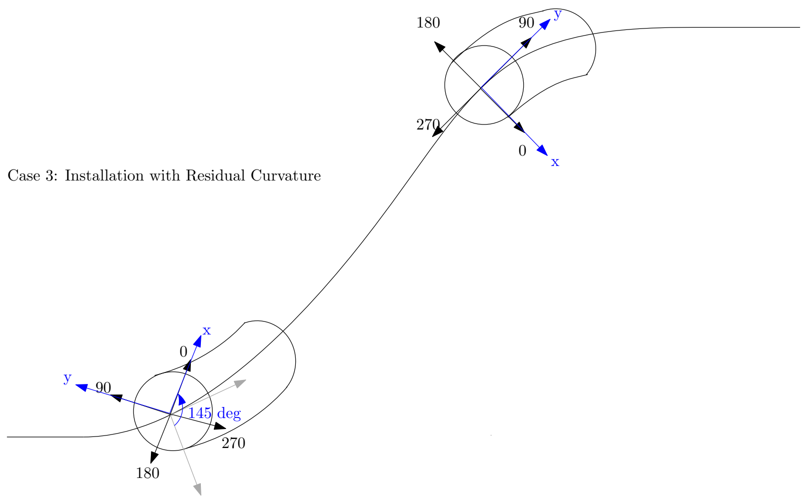

Figure 5.11: Case 3- Elastoplastic material- Residual curvature: Illustration of pipeline orientation during installation. 0 degrees refer to the bottom of the cross section and correspondingly the 180 degrees to the top of the cross section.

The dynamic analysis is completed when all the nodes from the overbend reach the seabed. The pipeline rotation starts earlier than the rotation in case 2 (t= 3510 s). A schematic representation of the rotation of the section of interest is illustrated in Figure 5.11. The rotation profiles of the nodes follow the same trend as in case 2. The maximum rotation, again, appears just before the section of interest reaches the touchdown point. These maximum angles are presented in Figure 5.12. It can be noticed that the maximum pipeline rotation (145.17 degrees) is larger when installing pipeline with an extra bent section (residual curvature). Afterwards, the pipe section rotates in the opposite direction until it rests on the seabed. The final reduced angles can be seen in Figure 5.13. The final angles in this case (104.75 degrees) are smaller than that in Case 2. This means that, again, the rotation in the opposite direction is larger. Thus, the angle between the orientation of the node axis at the beginning and end of the simulation, is reduced.

Figure 5.14 illustrates how the residual curvature lands on the seabed. Figure 5.15 depicts the on-seabed pipeline position in Y direction. It can be seen that the nodes of the residual curvature have a maximum lateral deflection from the straight line of 1.6 meters. The pipeline is fully in contact with the seabed. The curvature of the initially pre-bent pipe section has reduced to 0.0075 rad/m due to the bottom tension that exists on the seabed. The bottom tension straightens the pre-bent section in the elastic region. However, this curvature is still beneficial for the lateral buckling behaviour during operation [26].

The detailed plots of bending moment and strain time history of the outer fibre of the node at 198.8m can be found in Appendix G.

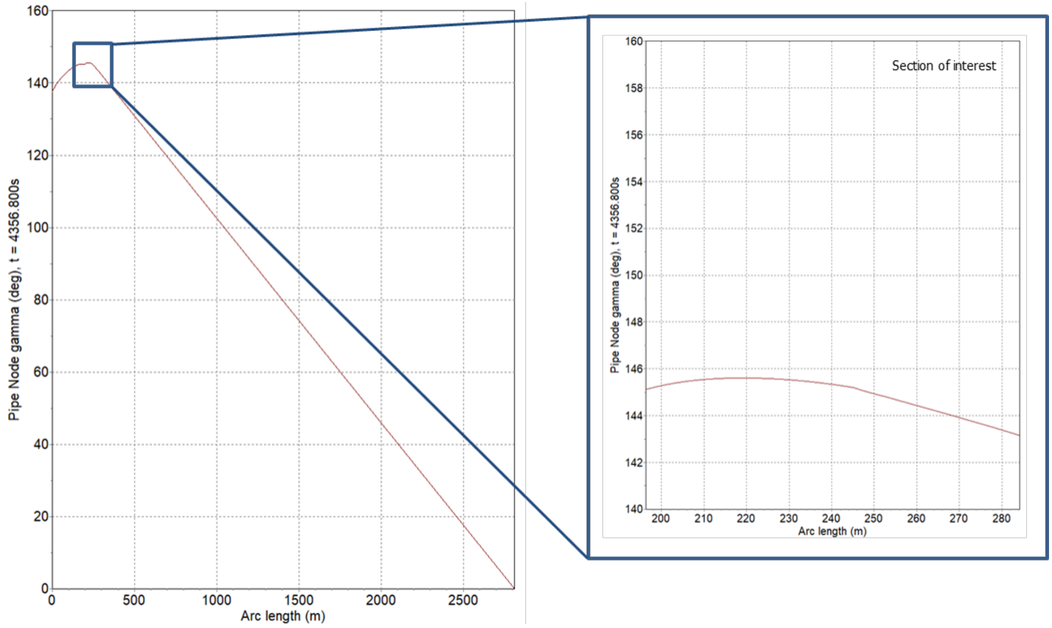

Figure 5.12: Case 3- Elastoplastic material- Residual curvature: Maximum rotation angles of the nodes along the length of the pipeline just before the section of interest reaches the touchdown point. The angles of the nodes in the section of interest can be seen in the enlarged plot. Installation with residual curvature.

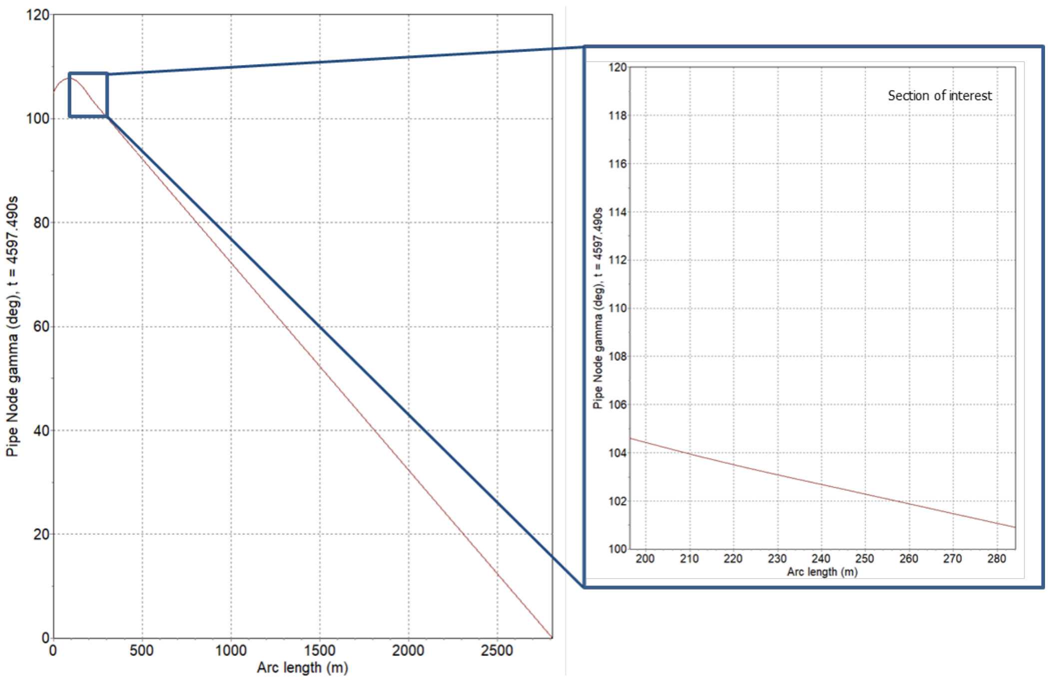

Figure 5.13: Case 3- Elastoplastic material- Residual curvature: The final rotation angles of the nodes along the length of the pipeline at the end of the simulation. The angles of the nodes in the section of interest can be seen in the enlarged plot. Installation with residual curvature.

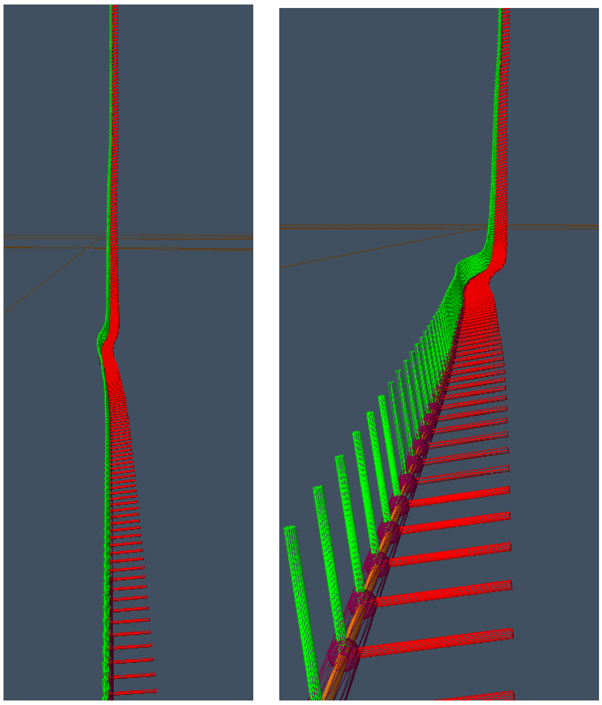

Figure 5.14: Case 3- Elastoplastic material- Residual curvature: The pipeline configuration on the seabed after installation with residual curvature.

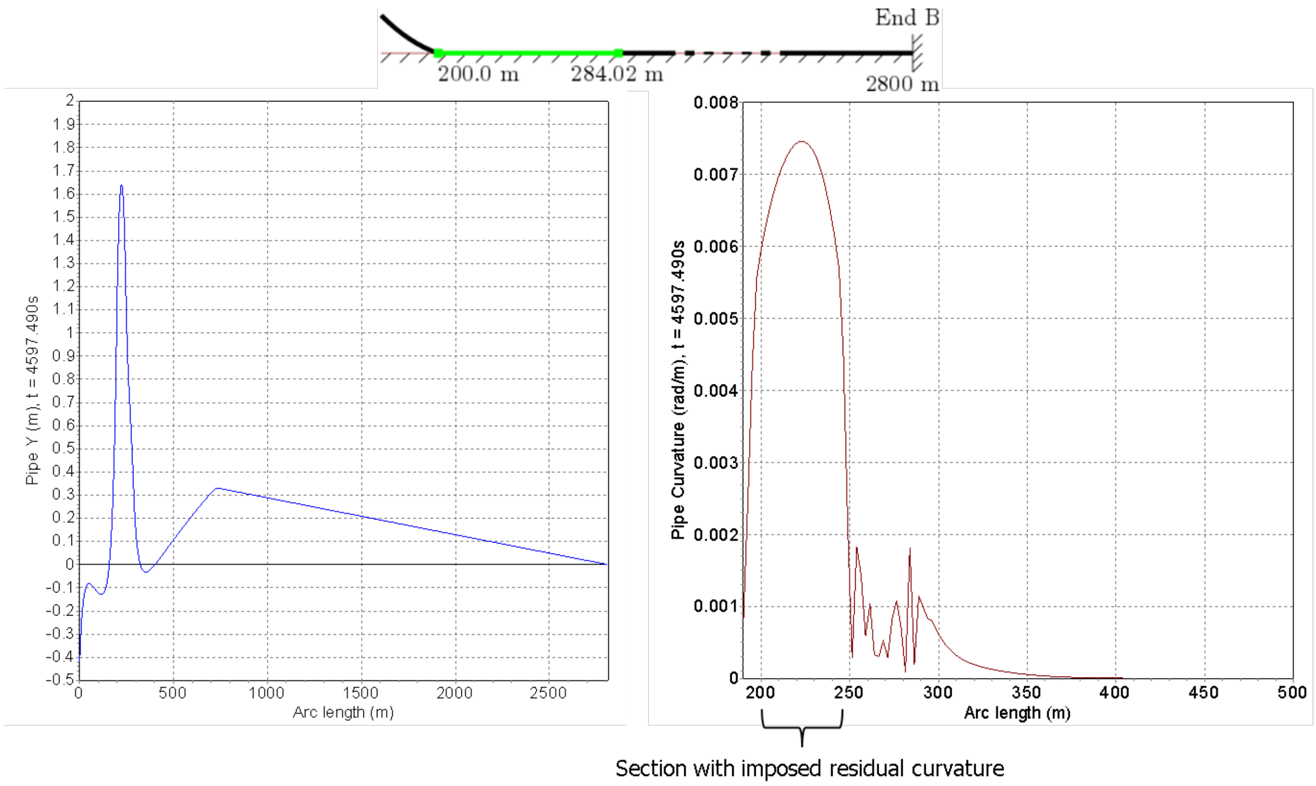

Figure 5.15: Case 3- Elastoplastic material- Residual curvature: Left: Lateral deflection of the pipeline from a straight line at the end of the dynamic simulation. Pipeline laid on the seabed having a "curved" shape with maximum deflection from the anchored end point of 1.6 meters approximately. Right: The curvature of the main pipeline on the seabed. The values between the arc length of 196.3 and 245.1 belong to the pre-bent pipe section. Maximum curvature of 0.0075 [rad/m].

To conclude, when an extra residual curvature is created in the pipeline, an increase in the rotation should be expected. Also, the magnitude of the curvature is reduced due to the impact of the bottom tension. However, the residual curvature will not be influenced, because the tension straightens the pipe only in the elastic region.

Summary

A summary of the results from the three examined cases is presented in Table 5.1. Comparative study was conducted to assess the impact of the residual curvature on the behaviour of the pipeline before landing on the seabed. It can be concluded that the presence of residual curvature leads to an increase in the pipeline twist angle.

Table 5.1: Summary of results from rotational analyses.

	Maximum twist angle [deg]	Maximum Y-position [m]	Maximum on-seabed curvature [rad/m]
Case 1- Limit case	≈ 0	≈ 0	0
Case 2- Normal installation	131.3	0.9	0.002
Case 3- Installation with Residual curvature	145.2	1.6	0.007

5.3 Auto - model

The model of case 3, described in the previous section, was created to assess the pipeline behaviour when there is a residual curvature in the pipeline. The stinger inclination was zero and a pre-bent pipe section was placed after the stinger hinge. It would be really interesting to create a model in which the overall procedure will be done automatically, avoiding the use of pre-bend command. The first attempt to create such an "auto" model is described in this section.

The "auto"- model refers to a model in which pipeline is being paid-out from the vessel and the stinger hinge rotates automatically during the simulation. An imposed motion is set for the hinge. This imposed motion can be modelled by time history data. Since the goal is to create a 48.8 m long residual curvature, the stinger should remain in the inclined position for the requisite period of time. To define this time period, the vessel speed and the pay-out rate are needed. After many trials it was noticed that the model is sensitive to rapid speed changes. For this reason, a smooth build up of the vessel and pay-out speed is created as shown in Figure 5.16. When the stinger needs to rotate back to its initial position, the vessel movement and pay-out procedure stop and again continue when the stinger finds its position. Note that the vessel speed and pay-out speed as well as their rate of change with time should be identical, so that the S-configuration of the pipeline is not affected. Therefore, based on the defined pay-out speed, the stinger should remain lowered for 97.5 seconds in the simulation. The Figure 5.17 below presents the time history data imported for the stinger hinge. Note that there is a limitation to the number of data that can be given. That is 100.000 values.

There are some significant limitations is this model. Firstly, there are consequences due to the absence of tensioner in the model. In principle, a winch element is used to model the tensioner in OrcaFlex. The winch is connected to the vessel and to the start of the pipeline. However, in the models where pay-out of pipeline occurs, the new "feeding" line "deports" the winch, since the feeding line must now be connected to the start of the pipeline and the vessel. As a consequence, the induced tension can only be controlled by the vessel speed and pay-out speed. It was observed that when the stinger rotated back to its initial position, unacceptable high tension was developed in the pipeline. It is crucial and strongly recommended that one improves the model to avoid the development of such unrealistic tension. Otherwise the model cannot be used for the correct assessment of the magnitude of the created residual curvature.

Secondly, not only the creation of the residual curvature is important but also its behaviour until it lands on the seabed. The travelling of the nodes from the stinger to the seabed cannot be captured in this model, when deep water is used (water depth larger than 1000 m). The time step of the dynamic simulation is 0.01 s. It is selected such that OrcaFlex does not give the error of large time step. Note that variable time step cannot be used when there is line "feeding" in the model. This means that the total simulation time, accounting for the maximum allowable values in the table of the hinge data, should be 100.000/ 0.01= 1000 s. As already shown in Figure 5.16, the maximum speed is 1.5 m/s. Hence, 1.5*1000= 1500 m of pipeline will be paid-out during the whole simulation. This reveals that for ultra deep water, there is not enough time for the nodes to travel from the stinger to the seabed, unless a higher vessel and pay-out speed is used. However, for higher speeds (i.e. maximum speed 2.5 m/s) is was observed that the smooth S-configuration of the sagbend was affected and compressive force was induced in the touchdown point. Hence, there is a sensitivity to high speeds. As a conclusion, the speeds should remain low (max 1.5 m/s) which means that this model is unable to capture the behaviour of the residual curvature on the seabed for ultra deep water projects.

Due to the time limitation for the accomplishment of this master thesis, no further effort could be paid to make this model run properly. As future work it is strongly recommended that the development of high tension is addressed. This optimised model will be very handy if the company wishes to use the local residual curvature method in future projects.

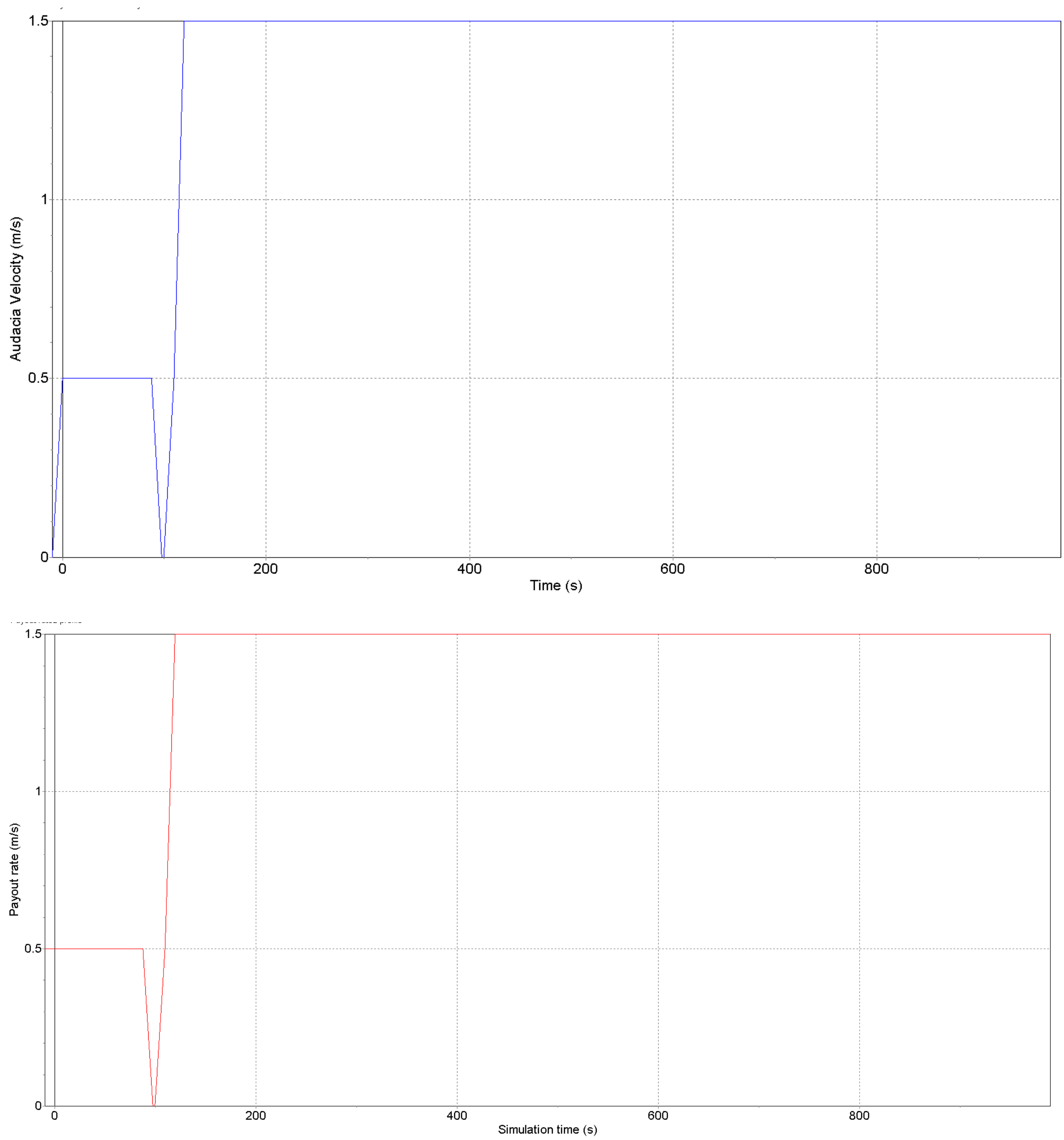

Figure 5.16: Vessel speed and pay-out speed, as defined for the "auto"- model.

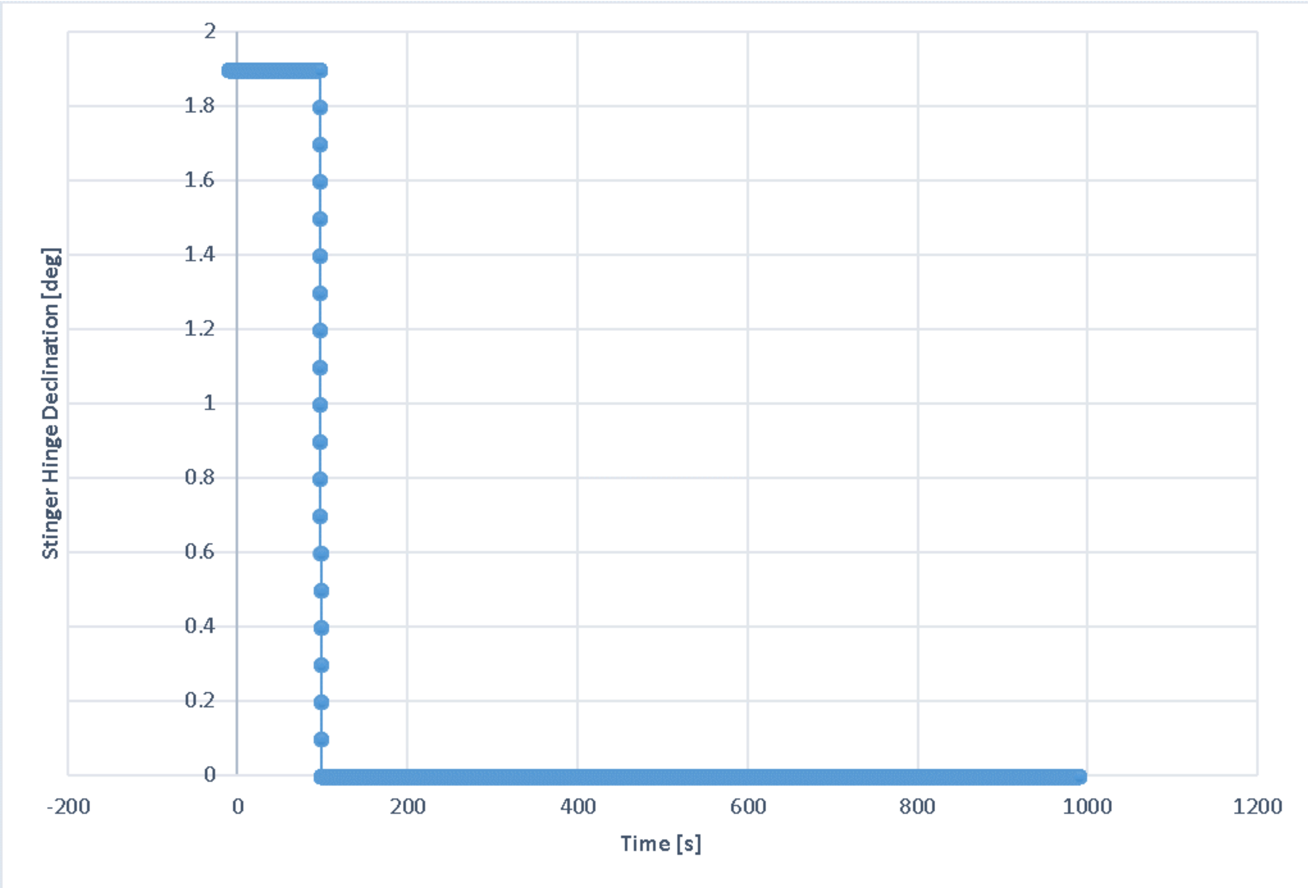

Figure 5.17: Time history data for the stinger hinge rotation.

Chapter 6

Stinger integrity

6.1 Risk of collision

It is of utmost importance to examine whether the curved pipe section collides with the stanchions of the stinger, so that to determine the stinger integrity. The pre-bend command was used in order to represent the residual curvature of the pipeline. The locations where the lateral displacement was checked were at the beginning of the stinger, where the residual curvature is created, and at the end of the stinger, where the residual curvature leaves the stinger. For this reason, two models were created for the two different locations of the residual curvature. Namely, a 0.0089-pre-bend curvature in y-direction was applied at the first and the last 48.8 meters of the stinger, see Figure 6.1. The stinger inclination was set to zero.

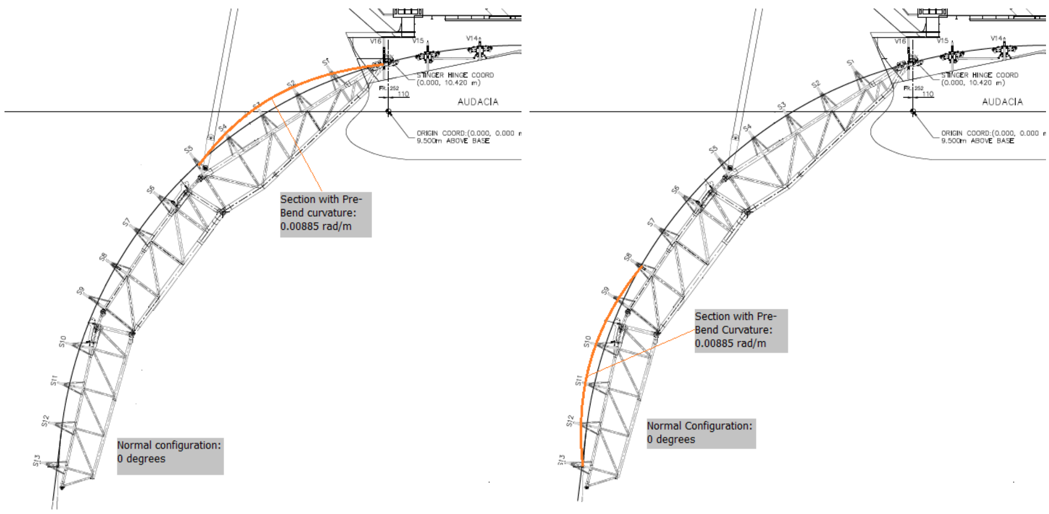

Figure 6.1: Two locations of the residual curvature: at the beginning and at the end of the stinger.

The governing parameter to ensure the stinger integrity is the lateral displacement of the pipe per se. This can be determined easily when performing static analysis, since the vessel is stationary and environmental effects are not present. However, during a dynamic analysis it is important to be able to separate the vessel motions from the pipeline motions in order to have a clear indication of a potential contact. In OrcaFlex, the results of the lateral movement of the pipeline include the movement of the stinger (vessel). The pure pipeline displacement can be obtained when subtracting the stinger movement from the total pipeline movement. To achieve this, two massless 6D buoys with negligible properties were inserted in the model. One buoy was connected to the stinger and the other one to the pipe, but both of them located exactly at the same position in the model (at the middle of the residual curvature). In this way, the buoys had the same movement as the stinger and the middle of the curved section respectively. Hence, the clear pipeline lateral displacement is the difference between the lateral displacement of the two buoys.

The lateral displacement of the pipeline was compared with the horizontal distance between the pipe and the sides of the stinger. The width of the stinger stanchions in Audacia is 4.320 meters. Therefore, the lateral movement of the pipeline must be smaller than 2.16 meters.

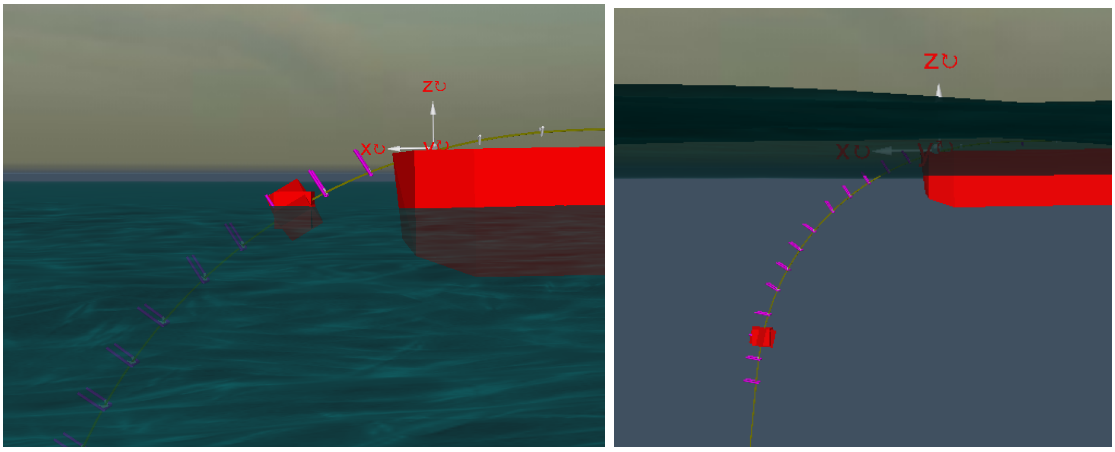

Figure 6.2: Illustration of the buoys' position. Case 1: at the middle of the residual curvature which is located at the beginning of the stinger (top figure). Case 2: at the middle of the residual curvature located at the end of the stinger (bottom figure).

6.1.1 Static analysis

After performing static analysis, it was observed that the maximum displacement when the curvature was located at the beginning and at the end of the stinger, was 0.0001m and 0.0006m respectively. It is smaller than the distance between the pipeline and the sides of the stinger. Therefore, clash event did not occur.

6.1.2 Dynamic analysis

The lateral displacement of the pipeline with residual curvature was examined when the environmental effects are present. As in static analysis, two locations of the curvature were checked: at the first and the last 48.8 meters of the stinger length. After performing dynamic analysis, the maximum displacement for the first case was 0.05 meters while for the second case 0.11 meters, see Figure 6.3. Both displacements are smaller than 2.16 meters.

The lateral displacement of the pre-bent section on the stinger was compared with the movement of a normal (straight) pipeline. It was observed that the both pipelines had exactly the same displacement in y-direction. Therefore, it is concluded that the pipeline installation with residual curvature do not influence the way the pipe moves on the stinger. Needless to say, there is no risk of collision between the pipe and the stanchions of the stinger.

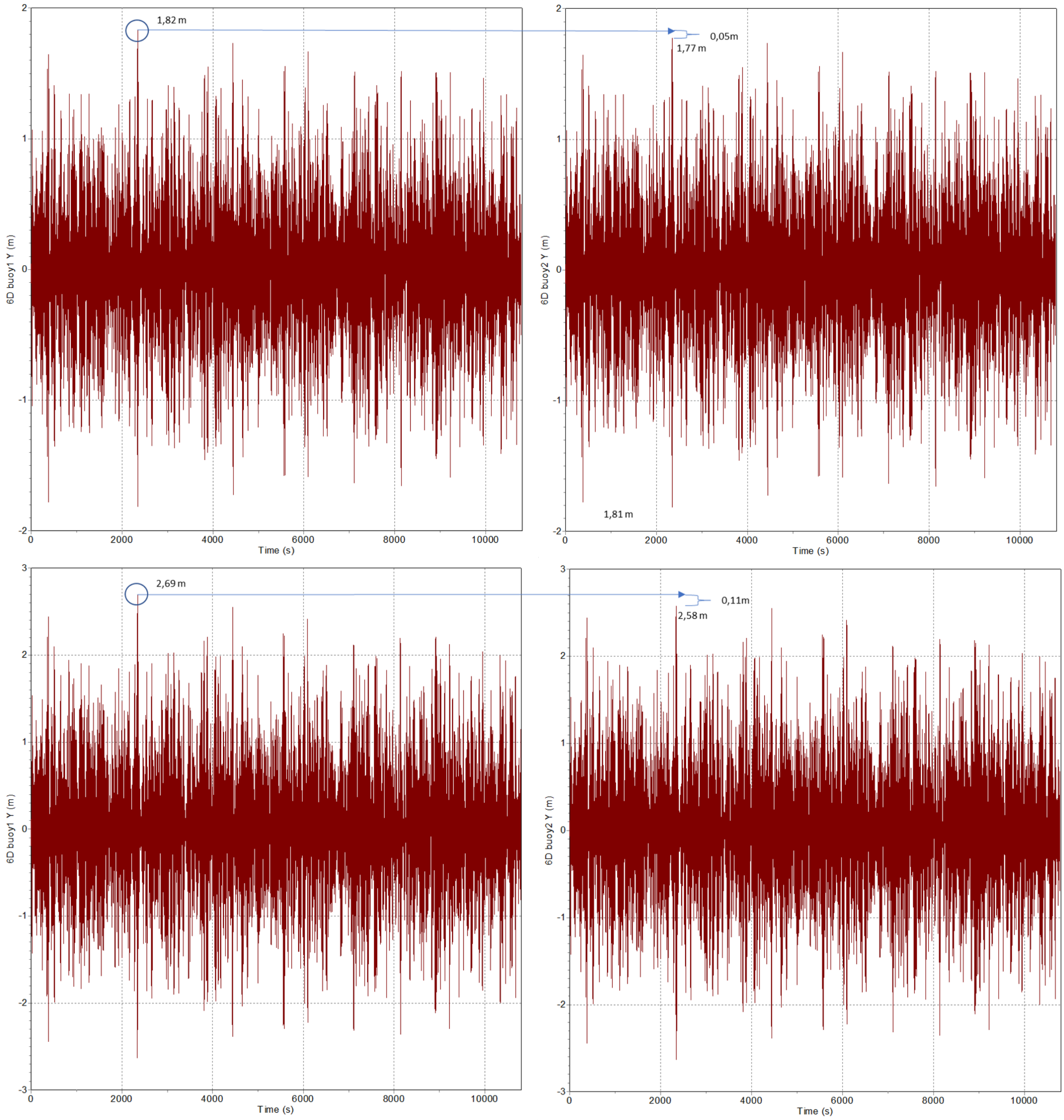

Figure 6.3: Lateral displacement of the two 6D buoys, when the residual curvature is at the beginning of the stinger (top graphs) and at the end of the stinger (bottom graphs). Buoy 1 connected to the pipeline, buoy 2 connected to the stinger. The buoys are located at the middle of the residual curvature in each case.

6.2 Rollerbox integrity

A second important check to ensure that the pipeline can be safely installed through an inclined stinger, is the integrity of the supports. When the stinger is rotated, the departure angle of the pipeline is increased. The weight of the pipeline is distributed unequally between the last vessel support (V16) and the first stinger support (S1): the support of the vessel needs to withstand higher load from the pipeline. This load should not exceed the maximum capacity of the rollerbox (100 tons).

The safety of the rollerbox was checked for both static and dynamic conditions. The reaction force of the support was calculated in OrcaFlex. Both cases of 1.9- and 2.0- degrees stinger inclination were examined and compared with the normal installation. As seen in the Table 6.1 the reaction force of V16 increases as the stinger angle increases. The forces for both cases are smaller than the load capacity, therefore the structure is safe. The capacity of the rollerbox will be exceed only for the extreme inclination of 5 degrees and more.

However, for the particular case examined in this thesis, such inclination will never be proposed. When the stinger rotates by 5 degrees, the bending strain induced in the pipe is 1% (unacceptable). Therefore, it can be concluded that the rollerbox capacity will never be exceeded for the stinger inclinations that ensure the pipeline integrity.

Table 6.1: Maximum support reaction force of V16 obtained from static and dynamic analysis in OrcaFlex for the cases of 0, 1.9, 2.0 degrees stinger inclination.

Angle [deg]	0		1.9		2.0	
	Static	Dynamic	Static	Dynamic	Static	Dynamic
V16 reaction force [kN]	278.76	351.79	488.6	726.08	497.53	734.65
	Safe	Safe	Safe	Safe	Safe	Safe

Chapter 7

Adjustments to installation procedure

The lowering of the stinger is integrated in the pipeline installation procedure in the most convenient way. More specifically, the stinger angle can be changed during the pull time. Based on past projects, the pull time is approximately 5 to 15 minutes and it refers to the time needed for the pipe to change stations in the firing line. During the pull time the vessel is stationary. This duration is enough for lowering or lifting the stinger by 1.9-2.0 degrees. Hence, the changes in stinger inclination do not cause any downtime at the installation.

In addition, the stinger will remain lowered during four consecutive pulls. The firing line in Audacia has a single joint welding station, meaning that 12.2 meters of pipe are welded to the main pipeline, during one pull time and consequently 12.2 meters of pipeline move on the stinger. Keeping in mind that the length of the pipe section with residual curvature should be 40 meters approximately, 40 meters of pipeline need to be pulled out on the inclined stinger. That is to say, after four consecutive pulls, the required configuration of the curvature will be created and the stinger should be raised back to its initial position. The following 1 kilometer of pipeline will be installed normally (82 pulls).

In the pre-engineering phase of the pipeline project the vertical position of the roller boxes is calculated to ensure this smooth transition. These calculations will remain the same during the installation of residual curvature as well. The elevation of the roller boxes should be designed as for a normal installation procedure. Their position will remain the same during the whole installation project.

Consequently, it is evident that the adjustments to the stinger do not add extra time to the installation procedure. Abandonment of the pipeline is not required as well, due to the sufficient cable capacity which can withstand raising the stinger by aforementioned degrees. In addition, it is not required to pull the pipeline more when the stinger is lowered. The residual curvature can be achieved due to the extra bending. Extra tension is not necessary. Therefore, the proposed installation method is independent of changes in the tensioner settings. All these aspects are evidence of the cost effective nature of the said methodology.

Table 7.1: Summary of stinger settings during pipeline installation of 18 inch outer diameter in deep waters.

Pipe OD 18 [in] Water depth 1925 [m]				
Normal pipeline installation			**Pipeline installation with LRC**	
Stinger length	110	[m]	110	[m]
Stinger radius	85	[m]	85	[m]
Stinger inclination	0	[deg]	1.9	[deg]
Pipeline length to install	1000	[m]	48.8	[m]
Tension	T		T	

Chapter 8

Results summary

For the particular case examined in this master thesis, the basic results are listed here.

Table 8.1: Set of input data which constitute the framework of the case examined in the research study.

Pipe OD	18	[in]
Wall thickness	28.5	[mm]
Water depth	1925	[m]
Young's modulus	2.07E+11	[Pa]
Stinger length	110	[m]
Stinger radius	85	[m]
Material	X65	
Yield stress	448	[MPa]
Tensile strength	530	[MPa]

- 1.9 - 2.0 degrees stinger inclination provide the sufficient (0.008-0.01 rad/m) residual curvature in the pipe. This result is based on static and dynamic analysis. The maximum curvature occurs in the pipe section located above the last support of the vessel (V16).
- When dynamic loads (vessel motions, waves) are present, the target plastic strains are still achieved in the pipe, without jeopardising the pipeline integrity.
- After imposing plastic strains in a 48.8 meters long pipe section, the stinger is raised back to its normal position. The created residual curvature is independent of this reverse rotation of the stinger.
- In principle, the creation of plastic strains in the overbend during installation would cause a reduction in the bending moment capacity of the pipe. In the present case, the reduction is small (0.55%- 0.6%.)
- The unity check for local buckling at the location where the maximum plastic strains occur, is satisfied for both static and dynamic calculations. The results of the displacement controlled (DC) conditions criterion were 0.21- 0.32. The results correspond to both cases of 1.9 and 2.0 degrees inclination.
- The residual ovality in the pipe cross section, due to the combined action of bending, tension and point load from the support, is 1.19 %. This value is less than the maximum allowable ovality (3%) mentioned in the DNV standards.
- The total accumulated fatigue damage of the pipeline during normal installation and installation with inclined stinger does not exceeded the maximum allowable fatigue damage (0.0167). There is an impact from the stinger inclination, however due to modelling limitations (tensioner modelled as winch) the results from the fatigue analysis performed in OrcaFlex are not realistic enough and clear conclusions cannot be drawn.
- Analysis of the pipeline behaviour when it moves from the stinger to the seabed, revealed that the pipeline rotates in the sagbend area if it is plastically deformed in the overbend area. In addition, for larger plastic deformation (residual curvature) the rotation is larger too.
- The pipe section with residual curvature does not collide with the sides of the stinger during installation.
- The capacity of the rollerboxes of the last vessel support is not exceeded when lowering the stinger by 1.9- 2.0 degrees. The maximum inclination that the rollerboxes can withstand is 5 degrees, for the case examined in this thesis.

Chapter 9

Conclusions and Recommendations

9.1 Conclusions

The scope of this master thesis was to examine the feasibility of creating a local residual curvature in the pipeline with S-lay installation method. A single case of deep water installation was used, providing a guidance for the steps that need to be made if the local residual curvature is used in future projects. Four research questions were defined at the beginning of this research study. This section brings back these research questions followed by the findings of this project.

How can the local residual curvature method be incorporated in the S-lay installation method?
The creation of residual curvature by lowering the stinger was investigated in this thesis. More specifically, static and dynamic analyses were performed in OrcaFlex software to assess the induced curvature in the pipeline for different stinger inclinations. The calculation of the residual curvature was based on the bend moment curvature diagram. The results from the cases of 1.9, 2.0 and 2.1 degrees inclination indicate that the imposed curvature is sensitive to the stinger angle. Based on this evidence, it can be concluded that the stinger must be lowered in a controlled manner, so that the design-angle is not exceeded.

Which adjustments are required in the procedure of normal pipe laying?
The goal is to create pipe sections with residual curvature at regular intervals. Therefore, the stinger should be lowered only when a curved pipe section is to be created. For the rest of the installation the stinger will remain at its normal inclination. The lowering of the stinger can be done during a pull time. This means that the change in the stinger angle does not cause any delay to the installation procedure.

Which are the effects of such alternations on the pipeline structural integrity?
When lowering the stinger, the part of the pipeline supported by the last vessel support, appears the maximum bending strain. This is the critical location where the pipeline integrity must be ensured. This study presents the calculations of the following integrity checks:

- Reduction in bending moment capacity
- Local buckling
- Residual ovality
- Fatigue damage

For the case studied in this project, it was proven from the aforementioned checks that the pipeline integrity is not in risk. Therefore, based on the project specific results, pipe sections with residual curvature are safely created when lowering the stinger.

Which is the behaviour of the residual curvature while suspended in the catenary area?
A comparative study was conducted, to distinguish the effect that the residual curvature has on the behaviour of the pipeline before landing on the seabed. It was shown that rotation is initiated when there are residual strains in the pipeline. When the section with residual curvature reach the sagbend area, it takes shape due to the reduction in the axial tension, and the out-of-plane bending causes the residual curvature to rotate. The rotation of the created residual curvature section was larger than the rotation of the pipeline during normal installation.

9.2 Recommendations

This study provides a guidance for the implementation of the residual curvature method with S-lay installation procedure. Although the main issues regarding the creation and installation phase of the residual curvature were sufficiently covered, there are some topics that can be further investigated.

- The analyses in this research study are performed in OrcaFlex software. It is recommended to further validate the insights of this study regarding the creation of residual curvature and the pipeline integrity, by performing analyses in a finite element software such as Abaqus.
- In this thesis, nominal pipe properties have been assumed. However, it is highly probable that there are tolerances in the pipe properties. Therefore, a future work would be to ensure that the residual curvature is applied at a pipe section where the pipe properties have been found favorable based on pipeline dimensional and welding inspections.
- The interpretation of the effect of the stinger inclination on the fatigue damage of the lift-off point is lacking and is recommended as future work.
- The accurate prediction of the rotation angle of the pipeline in the sagbend area, requires a more detailed model. The rotation depends on several parameters and each of them have their own effect on the rotation. The soil type is a parameter which is difficult to define in the projects. In addition, the pipe-soil interaction significantly influences the pipeline behaviour during both installation and operation. For this reason it is worth investigating which is the impact of different soil types and friction coefficients on the shape and rotation of the residual curvature.
- Regarding pipeline rotation, one additional factor that is worth investigating is the interaction of two adjacent curved sections, for deep water cases. More precisely, one can investigate if the rotation of one curved section influences the rotation of the following curvatures. Also, if the adjacent curvatures have the same configuration on the seabed.
- This thesis investigated the creation and installation of the residual curvature. The assessment of whether the created curvature meets the initial objective (mitigation of rogue buckles) or not, requires analyses for operational conditions.
- A parametric study is recommended. Iterative calculations for different pipe properties, water depth and stinger radius will give insight about how feasible is to install a pipeline with residual curvature generally. In addition, this sensitivity study will provide the starting point for the design of the suitable stinger angle in future projects.

Bibliography

[1] S. Ali. Greening natural gas delivery – lng versus pipelines, 2014. https://blog.nationalgeographic.org/2014/05/13/greening-natural-gas-delivery-lng-versus-pipelines/ [Accessed: 15/10/2020].

[2] Allseas. Fatigue post processor. user's guide and validation manual., 2004.

[3] Allseas. Pipeline engineering- introduction file, 2015.

[4] D. Berhe. Controlled lateral buckling design of pipelines. Master's thesis, University of Stavanger, Norway, 2014.

[5] J. Chee, A. Walker, and D. White. Controlling lateral buckling of subsea pipeline with sinusoidal shape pre-deformation. *Ocean Engineering*, 151:170–190, 2018.

[6] C. Cooper, R. Aryan, P. Krawczyk, J. Canney, and S. Rabouille. In-place analysis of the edradour production pipeline residual curvature buckle initiator. In *Offshore Pipeline Technology Conference, Amsterdam, Netherlands.(To be presented)*, 2017.

[7] P. Cooper, T. Zhao, and F. Kortekaas. Residual curvature method for lateral buckling of deepwater flowlines. *OPT, March*, 1, 2017.

[8] P. A. Damsleth, Y. Bai, P. Nystrøm, and C. Gustafsson. Deepwater pipeline installation with plastic strain. In *Proc. of OMAE'99*. 1999.

[9] G. DNV. Dnvgl-st-f101, submarine pipeline systems. *Standard (DNV GL)*, 2017.

[10] G. DNV. Dnvgl-st-f201, dynamic risers. *Standard (DNV GL)*, 2019.

[11] P. D. Economic and E. P. Scientific Policies. An assessment of the gas and oil pipelines in europe, an extensive briefing note, 2009. https://www.europarl.europa.eu/RegData/etudes/note/join/2009/416239/IPOL-ITRE_NT(2009)416239_EN.pdf [Accessed: 15/10/2020].

[12] G. Endal. Method for pipelaying from a coil to the sea bed, controlling thermal expansion, June 28 2005. US Patent 6,910,830.

[13] G. Endal and P. R. Nystrom. Benefits of generating pipeline local residual curvature during reel and s-lay installation. In *Offshore Pipeline Technology Conference, Amsterdam, The Netherlands*, 2015.

[14] G. Endal, O. Ness, R. Verley, K. Holthe, and S. Remseth. Behavior of offshore pipelines subjected to residual curvature during laying. Technical report, American Society of Mechanical Engineers, New York, NY (United States), 1995.

[15] G. Endal, S. R. Giske, K. Moen, and S. Sande. Reel-lay method to control global pipeline buckling under operating loads. In *International Conference on Offshore Mechanics and Arctic Engineering*, volume 45479, page V06BT04A005. American Society of Mechanical Engineers, 2014.

[16] M. Gallegillo, X. Qi, G. Ofoha, R. Bhide, N. Messias, and T. Helland. Post-reeled behaviour of pipelines with global buckling mitigation by the residual curvature method. In *International Conference on Offshore Mechanics and Arctic Engineering*, volume 57700, page V05BT04A030. American Society of Mechanical Engineers, 2017.

[17] R. E. Hobbs. In-service buckling of heated pipelines. *Journal of Transportation Engineering*, 110(2): 175–189, 1984.

[18] I. JIP. Guideline for installation of rigid pipelines - limit state criteria, 2015.

[19] E. Karjadi, P. Cooper, H. Smienk, and F. Kortekaas. Benefits and deep water install ability challenges of residual curvature method for lateral buckling mitigation. In *International Conference on Offshore Mechanics and Arctic Engineering*, volume 57700, page V05BT04A016. American Society of Mechanical Engineers, 2017.

[20] S. Kyriakides and E. Corona. *Mechanics of offshore pipelines: volume 1 buckling and collapse*, volume 1. Elsevier, 2007.

[21] W. Liu and A. Liu. Numerical research on the lateral global buckling characteristics of a high temperature and pressure pipeline with two initial imperfections. *PloS one*, 13(3):e0194426, 2018.

[22] O. Manual. Online at http://www. orcina. com/softwareproducts/orcaflex/documentation. *OrcaFlex. pdf*, 2012.

[23] M. l. Martinez and G. Brown. Evolution of pipe properties during reel-lay process: experimental characterisation and finite element modelling. In *International Conference on Offshore Mechanics and Arctic Engineering*, volume 41979, pages 419–429, 2005.

[24] J. O. Oladimeji, C. V. Ossia, and J. U. Okoli. On the structural integrity of s-lay method of pipeline installation. *American Journal of Mechanical Engineering*, 4(4):124–130, 2016.

[25] D. Perinet, I. Frazer, et al. Strain criteria for deepwater pipe laying operations. In *Offshore Technology Conference*. Offshore Technology Conference, 2008.

[26] T. J. Powell, Q. Bai, M. Brunner, S. Searle, et al. Challenges of using residual curvature method in deep water pipelines. In *SNAME 24th Offshore Symposium*. The Society of Naval Architects and Marine Engineers, 2019.

[27] W. Ramberg and W. R. Osgood. Description of stress-strain curves by three parameters. 1943.

[28] T. Renes. Radial stinger flexibility. the influence on roller box loads and strains in the pipeline during deep water pipelay. 2010.

[29] A. Roy, V. Rao, C. Charnaux, P. Ragupathy, and T. Sriskandarajah. Straightener settings for under-straight residual curvature of reel laid pipeline. In *International Conference on Offshore Mechanics and Arctic Engineering*, volume 45479, page V06BT04A046. American Society of Mechanical Engineers, 2014.

[30] X. Song and X. Song. Study of lateral buckling of submarine pipeline. In *2nd International Conference on Electronic & Mechanical Engineering and Information Technology*. Atlantis Press, 2012.

[31] V. Taams. The onset of pipeline twist during reel-lay operations. 2016.

[32] M. Teigen and M. Ibrahim. Investigation of the behaviour of the lateral buckling control method: Reel-lay induced imperfection. In *International Conference on Offshore Mechanics and Arctic Engineering*, volume 56512, page V05AT04A019. American Society of Mechanical Engineers, 2015.

[33] A. Tewolde. Pipelay with residual curvature. Master's thesis, University of Stavanger, Norway, 2017.

[34] E. Torselletti, L. Vitali, E. Levold, and K. J. Mork. Submarine pipeline installation jip: Strength and deformation capacity of pipes passing over the s-lay vessel stinger. In *International Conference on Offshore Mechanics and Arctic Engineering*, volume 47497, pages 227–235, 2006.

[35] U. P. S. under Bending. Collapse and fatigue–murphy, ce, langner, cg. In *Proceedings of the 4th International Conference on Offshore and Arctic Engineering (OMAE 1985)*.

[36] N. J. Vaughan, P. Foss, A. Rødstøl, P. R. Nystrøm, et al. Prediction of pipeline rotation during the installation of residual curvature sections by reel-lay. In *The 28th International Ocean and Polar Engineering Conference*. International Society of Offshore and Polar Engineers, 2018.

[37] D. N. Veritas. Global buckling of submarine pipelines, structural design due to high temperature/high pressure. *RP-F110, Oslo, Norway*, 2007.

[38] D. N. Veritas. Fatigue design of offshore steel structures. *DNV Recommended Practice DNV-RP-C203*, 2010.

[39] H. Vermeulen et al. Theory and practice of installing pipelines by · the pre-snaking method. In *The Fifth International Offshore and Polar Engineering Conference*. International Society of Offshore and Polar Engineers, 1995.

Appendix A

Nonlinear elastic vs nonlinear hysteretic bend stiffness

OrcaFlex gives the opportunity to the user to select between two options when using nonlinear material bending stiffness. That is, the nonlinear elastic and the nonlinear hysteretic option. When selecting hysteretic behaviour, torsion must be included the analysis. On the other hand, the torsion can be disabled when using elastic material. After examining numerous test cases during this master thesis, some differences were observed on the static results obtained from the two options. These differences are presented and explained in this section, so to advice the future users beforehand.

For both cases, exactly the same pipeline and vessel model was used. When looking at the results of the static analysis, it is observed that the magnitude of bending moment in the overbend area (where the pipeline is in contact with the stinger supports) is larger when considering hysteresis. Similarly, the strains are higher too. Figures A.1, A.2.

The increased moments and strains at the nodes of the line object on the stigner, when hysteresis is enabled, can be explained after gaining information from the manual of OrcaFlex. The reason lies in the way OrcaFlex handles the contact between supports and line object. If torsion is enabled, the nodes of the line at the overbend experience shear force and bending moment determined by the support reaction forces. If torsion is disabled, the line object cannot receive moments directly onto its nodes. Instead, the neighboring nodes must receive shear forces. These shear forces are related to the intended moment by the bending stiffness of the line and the magnitude is such that they produce the same effective bend moment.

The results from the two cases can come to a closer agreement if one reduces the segment length at the location of interest. For example, if the segment length is 50% smaller (therefore, $2.5(m)/2 = 1.25(m)$) the difference on the magnitude of the bending moment between the two cases, is significantly reduced. Figures A.3, A.4.

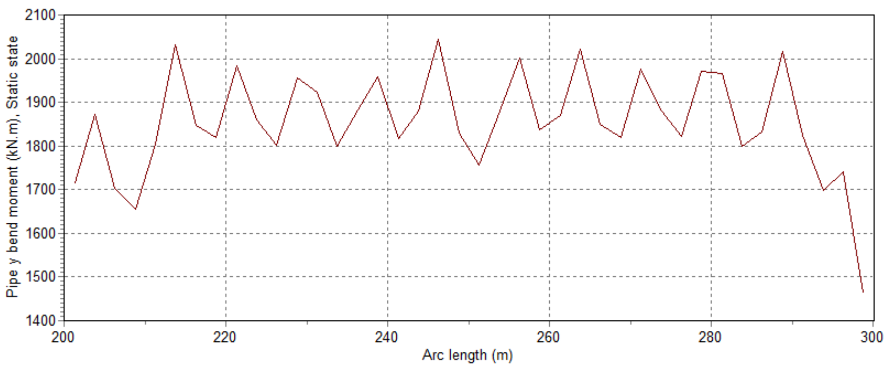

Figure A.1: Nonlinear hysteretic bend stiffness. Torsion enabled. Segment length 2.5 m. Bend moment of the nodes in contact with the stinger supports. Static analysis.

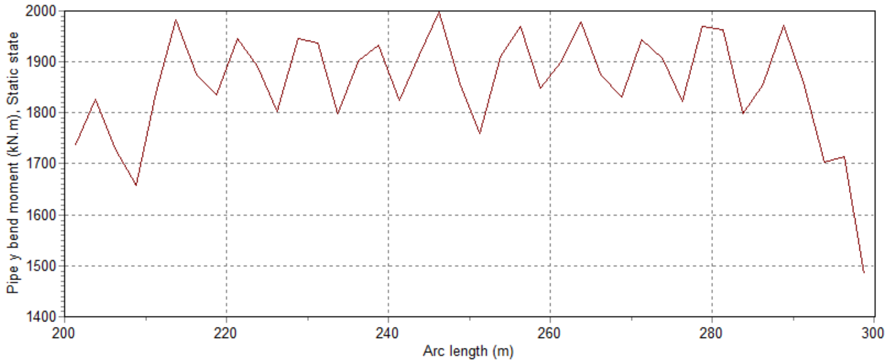

Figure A.2: Nonlinear elastic bend stiffness. Torsion disabled. Segment length 2.5 m. Bend moment of the nodes in contact with the stinger supports. Static analysis.

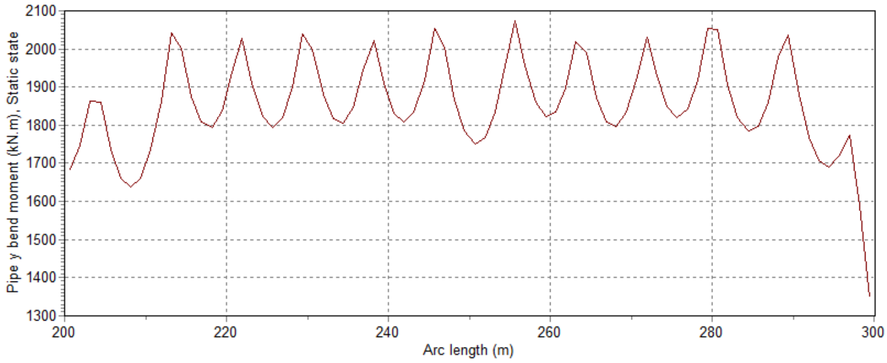

Figure A.3: Nonlinear hysteretic bend stiffness. Torsion enabled. Segment length 1.25 m. Bend moment of the nodes in contact with the stinger supports. Static analysis.

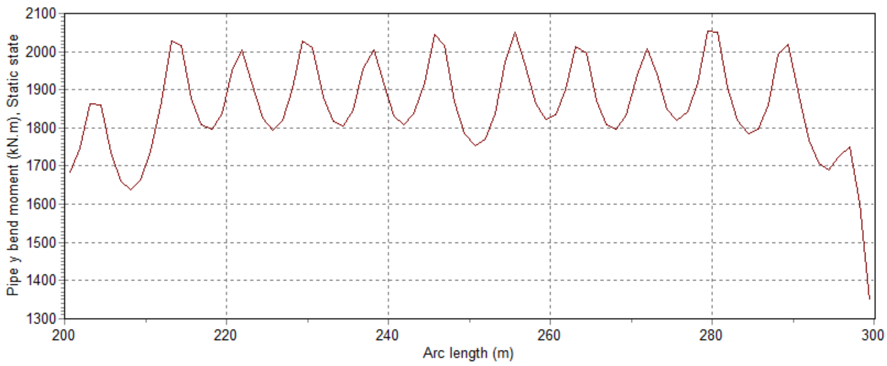

Figure A.4: Nonlinear elastic bend stiffness. Torsion disabled. Segment length 1.25 m. Bend moment of the nodes in contact with the stinger supports. Static analysis.

Appendix B

Bending and strain response

When lowering the stinger, the bending moments above the last vessel support increase. The maximum curvature occurs in this location. Observation of the maximum Von Mises strain time history and the curvature time history, reveals that there is a strong correlation of their variation. This means that bending dominates and there is a minor impact of the direct tensile strain on the strain behaviour. The time history plots of the max Von Mises strain and curvature of the same node (at 203.797 arc length), when the stinger inclination is 1.9 degrees, are illustrated below (Figure B.1).

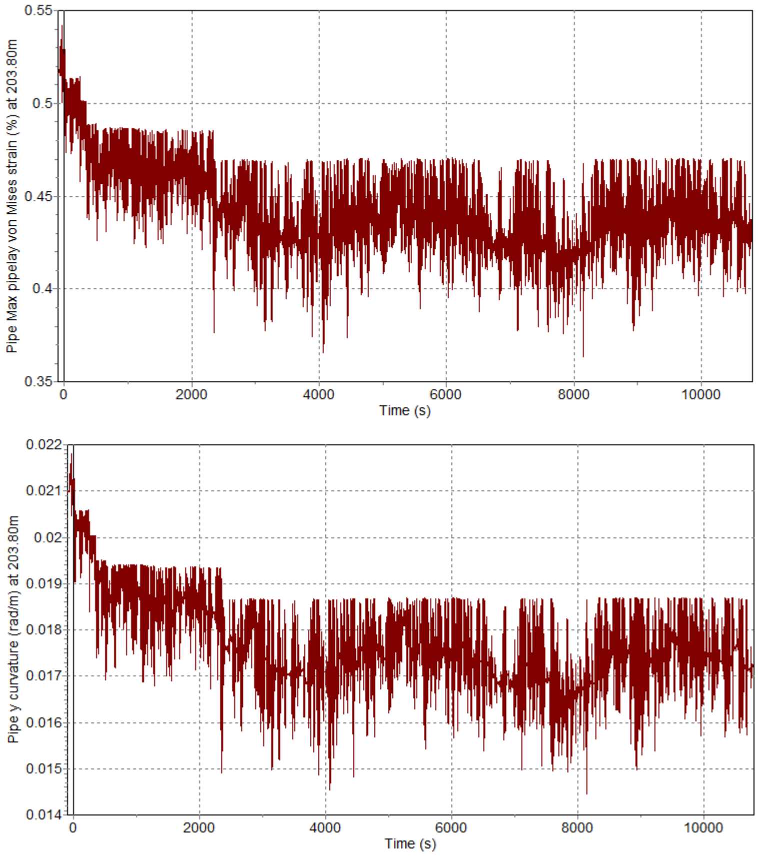

Figure B.1: Strong correlation of the variation of the maximum Von Mises strain (top graph) and curvature (bottom graph) with time. Therefore, bending is driving the strain behaviour.

Appendix C

Model behaviour during dynamic analysis

Build-up stage is the time during which the wave and vessel motions are smoothly ramped up from zero to their full size [24]. The dynamic analysis starts after the build-up stage. One may come across an unusual bend moment - curvature behaviour, as the one in Figure C.1, while the motions of the wave and vessel are harmonic. To overcome this issue, one should look at the duration of the build-up stage. Large duration (100 s in Figure C.1) leads to irregularities. Usually, the duration of the build-up stage must be at least equal to one wave period. Therefore, when reducing the duration to 10 s, the corresponding bend-moment diagram is recognizable (Figure C.2). The results corresponding to the build-up stage are unrealistic and must not be used. Therefore, in order to get a good approximation of the maximum curvature from dynamic analysis, it must be checked that the duration of the build up stage is properly calculated.

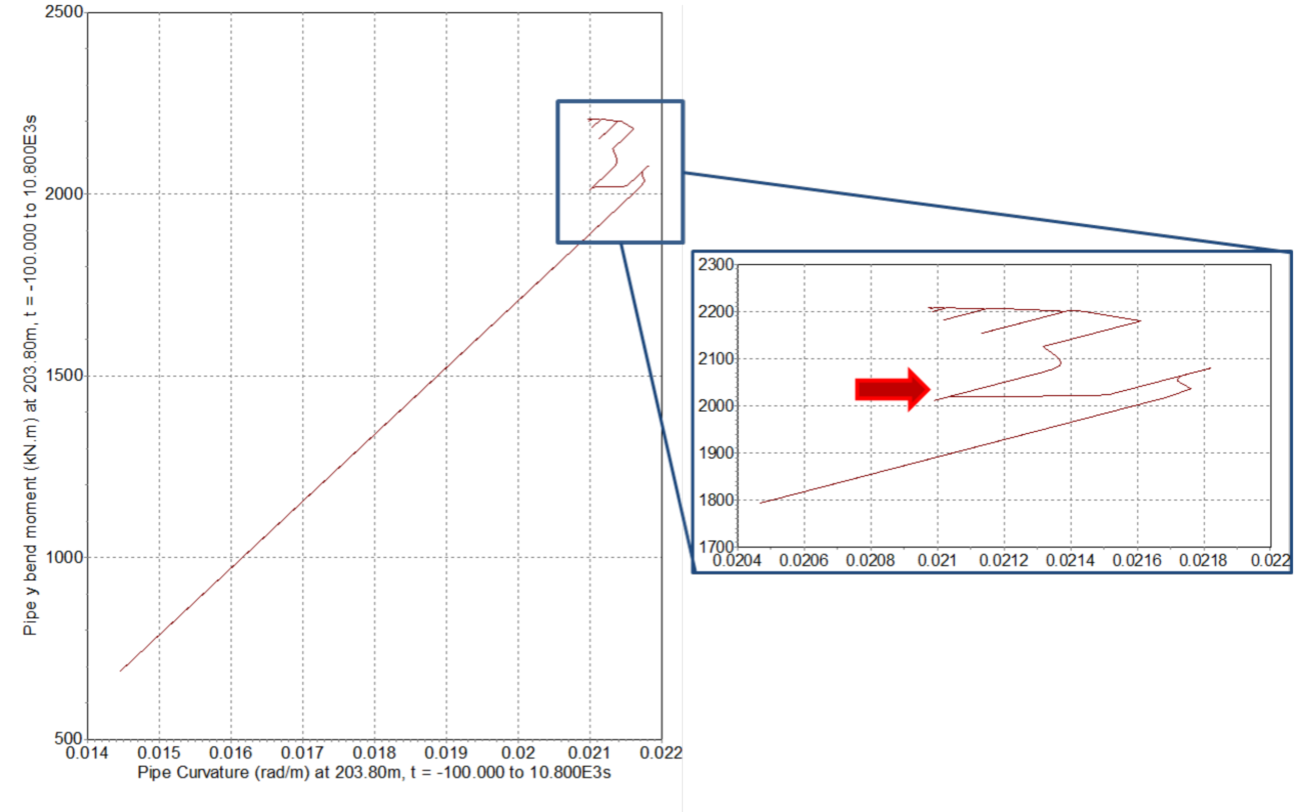

Figure C.1: 100 s duration of build-up stage and unusual bend moment- curvature behaviour.

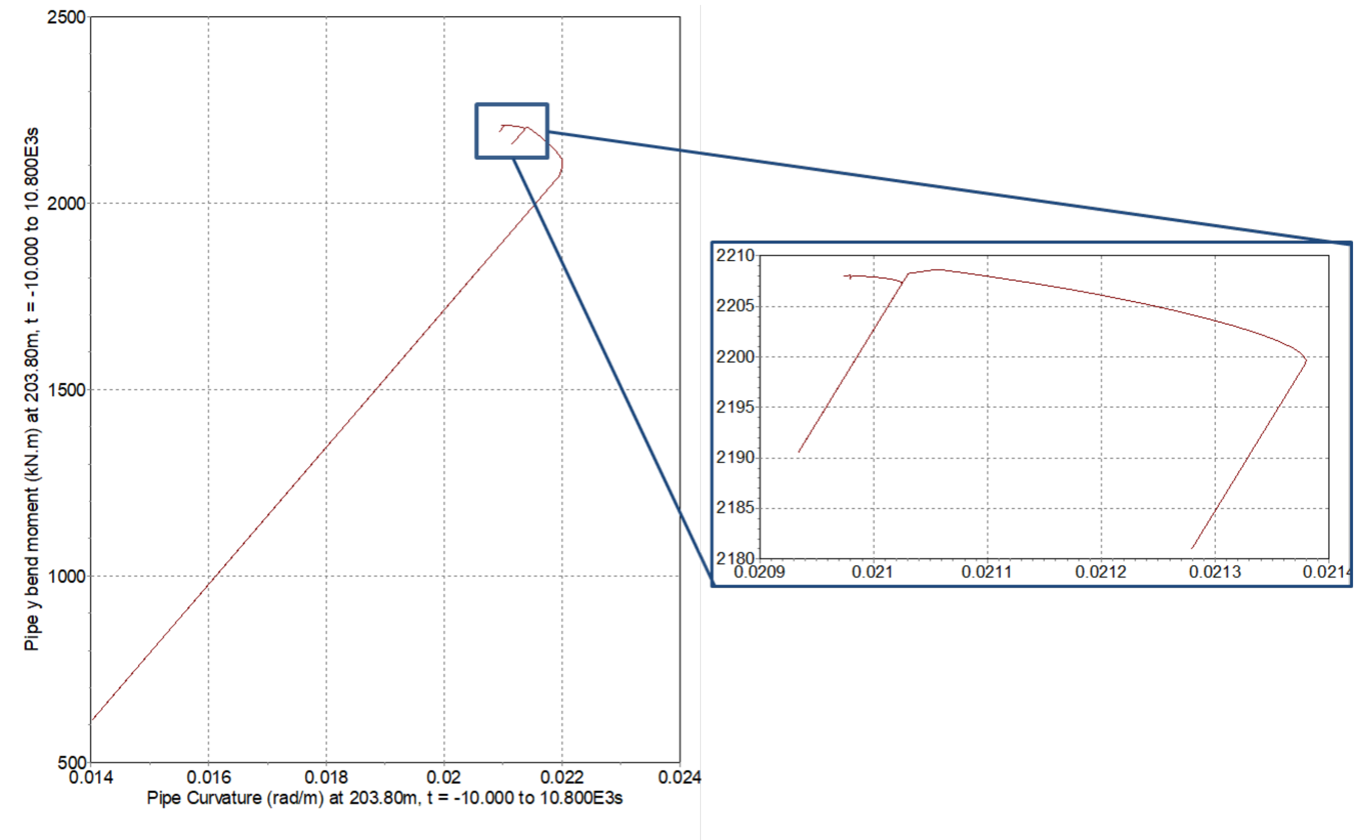

Figure C.2: 10 s duration of build up stage and regular curve.

Appendix D

Local buckling check- Load controlled conditions

Pipe members subjected to bending moment and effective axial force in the overbend should satisfy the following criterion [9].

$$\left[\gamma_m * \gamma_{SC,LB} * \frac{M_{Sd}}{\overline{M_k}} + \left(\gamma_m * \gamma_{SC,LB} * \frac{S_{Sd(p_i)}}{\alpha_c * S_p(t_2)}\right)^2\right]^2 \leq 1 \tag{D.1}$$

Where,
$\gamma_m = 1.15$, material resistance factor for Ultimate Limit State (Table 5-1 [9])
$\gamma_{SC,LB} = 1.04$, safety class resistance factor for low safety class (Table 5-2 [9])

- When allowing for a higher probability $\gamma_{SC,LB} = 1.0$, according to the Installation JIP [18]

$t_2 = t$, prior to operation (negligible corrosion)
$\overline{M_k} = \alpha_c * M_p$, the reduced bending moment capacity due to plastic strains

- If the pipeline also has a lateral point load (from a support) in addition to the axial load and moment, the design moment capacity should be modified:
  $\overline{M_k} = \alpha_c * \alpha_{pm} * M_p$,
  $\alpha_{pm} = 1 - \frac{D/t_2}{130} * \frac{R}{R_y}$,
  $R_y = 3.9 * f_y * t_2^2$
  $R =$ reaction force from point load

$M_{Sd} = M_F * \gamma_F * \gamma_c + M_E * \gamma_E + M_I * \gamma_F * \gamma_c + M_A * \gamma_A * \gamma_c$, the design moment load effect

- For static analysis, only the functional loads are considered, therefore only M_F (maximum bending moment) remains in the above relation. In a dynamic analysis, the environmental loads M_E are included as well.
- $\gamma_F = 1.1$ for local check
- $\gamma_c = 0.77$ *or* 0.8 for Load Controlled conditions [9]

$S_p = f_y * \pi * (D - T) * t$, the plastic capacity in the effective axial load (formula 5.22 [26])
$S_k = \alpha_c * S_p$, the effective axial load capacity
$S_{Sd} = S_F * \gamma_F * \gamma_c + S_E * \gamma_E + S_I * \gamma_F * \gamma_c + S_A * \gamma_A * \gamma_c$, the design effective axial force load effect

- For static analysis, only the functional loads are considered, while for dynamic analysis both functional and environmental loads are taken into account.

Static analysis results

As already discussed, the local buckling was examined for the pipe section located above the stinger hinge. It is the location of the final (16th) support of the vessel, after which the supports of the stinger start. The 16th vessel's support induces a point load on the pipe. Therefore, the effect of this load should be included in the local buckling criterion.

The analytical calculation of the local buckling check was based on the aforementioned formulas. The cases of 1.9 and 2 degrees stinger inclination were examined separately. The results are presented in Table D.1. It can be seen that the unity check is satisfied for both cases. The load controlled condition check was also performed in OrcaFlex. As depicted in Table D.1, there is an agreement between the results from

OrcaFlex and the analytical calculations.

Table D.1: Local buckling check in the pipe section above the stinger hinge, for load controlled condition, when the stinger inclination is 1.9 degrees and 2.0 degrees. Static analysis. Pipe exposed to point load from the V16 vessel rollerbox.

1.9 degrees			**2.0 degrees**	
Load Controlled conditions				
γ_m	1.15		1.15	
$\gamma_{SC,LB}$	1.04		1.04	
α_c	1.09		1.09	
γ_F	1.1	local check	1.1	local check
γ_c	0.8		0.8	
M_F	2208.01	kNm	2217.56	kNm
M_{Sd}	1943.05	kNm	1951.45	kNm
S_F	2971.42	kN	2971.22	kN
S_{Sd}	2614.85	kN	2614.67	kN
M_p	2346.55	kNm	2346.55	kNm
R_y	1419.16	kN	1419.16	kN
R	448.6	kN	497.53	kN
α_{pm}	0.96		0.96	
$\overline{M_k}$	2435.48	kNm	2432.65	kNm
S_p	17195.95	kN	17195.95	kN
$\overline{S_k}$	18743.59	kN	18743.59	kN
Local buckling check	**0.96**	**Satisfied**	**0.97**	**Satisfied**
OrcaFlex result	**0.95**	**Satisfied**	**0.96**	**Satisfied**

Dynamic analysis results

The results for Load Controlled (LC) conditions from dynamic analysis are presented in Table D.2. The effect of the lateral point load induced by the supports of the vessel is included. The local buckling check was performed for both 1.9- and 2.0-degrees proposed stinger inclination.

Table D.2: Local buckling check in the pipe section above the stinger hinge, for load controlled condition, when the stinger inclination is 1.9 degrees and 2.0 degrees. Dynamic analysis. Pipe exposed to point load from the V16 vessel rollerbox.

1.9 degrees			**2.0 degrees**	
Load Controlled conditions				
γ_m	1.15		1.15	
$\gamma_{SC,LB}$	1.04		1.04	
α_c	1.09		1.09	
γ_F	**1.1**	local check	**1.1**	local check
γ_c	0.8		0.8	
γE	1.3		1.3	
M_{Sd}	1810.71	kNm	1857.78	kNm
S_{Sd}	3197.36	kN	3209.01	kN
M_p	2346.55	kNm	2346.55	kNm
α_{pm}	0.94		0.94	
$\overline{M_k}$	2380.00	kNm	2393.24	kNm
S_p	17195.95	kN	17195.95	kN
$\overline{S_k}$	18743.59	kN	18743.59	kN
Local buckling check	**0.91**	**Satisfied**	**0.94**	**Satisfied**
OrcaFlex result	**0.85**	**Satisfied**	**0.90**	**Satisfied**

Appendix E

Stress results in OrcaFlex

In OrcaFlex manual it is stated that "the nonlinear behaviour breaks the assumptions of the stress results". This warning will be explained in this section. First of all, there are two types of line modelling in OrcaFlex: the "homogeneous" line type and the "general" line type. In short, the homogeneous line type is a suitable option for modelling an elastic material. If hysteretic bending is to be considered (as in this research study), the general line type must be used.

In case of general line type the stress calculation in OrcaFlex is the following:

- OrcaFlex creates the nonlinear bend moment- curvature diagram as already presented in Chapter 3.
- Tensile stress: linearly proportional to the wall tension $\sigma_T = T_w/A$
- Bending stress: Always calculated based on moments and not strains by using the linear relation $\sigma_B = M_{(k)} * y/I$

When defining a nonlinear material curve (i.e. Ramberg Osgood in this thesis), the stresses are nonlinear beyond the yielding point. However, OrcaFlex always calculates linear stresses when a general line type is used. This means that the stress results are erroneously enlarged. This is something that one should be aware of when uses a general line type loaded beyond the linear- elastic region.

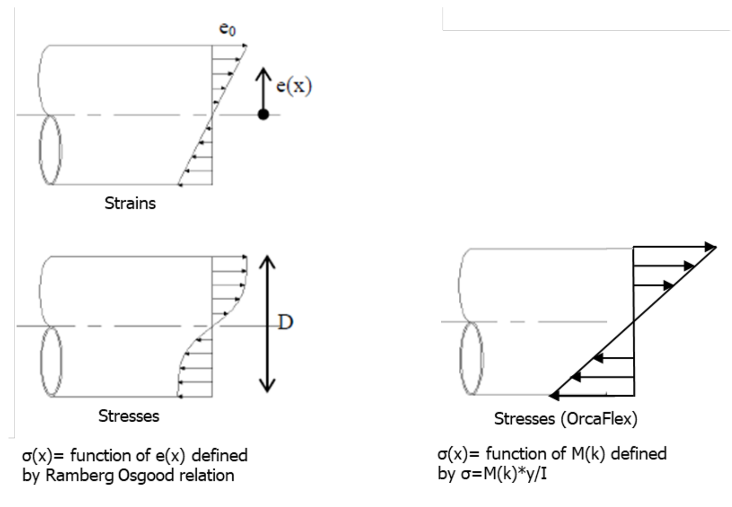

Figure E.1: Nonlinear (correct) stress distribution and stresses as calculated in OrcaFlex.

Appendix F

Post-processing fatigue calculation

To verify the expectations regarding the effect of the stinger rotation on the fatigue damage of the pipeline, a post processing tool was used for the fatigue analyses. This tool avoids the large forward and backward pipeline movement due to the tensioner, and uses linear bending stiffness. The results of fatigue damage during normal installation and installation with 1.9 degrees stinger angle are presented below.

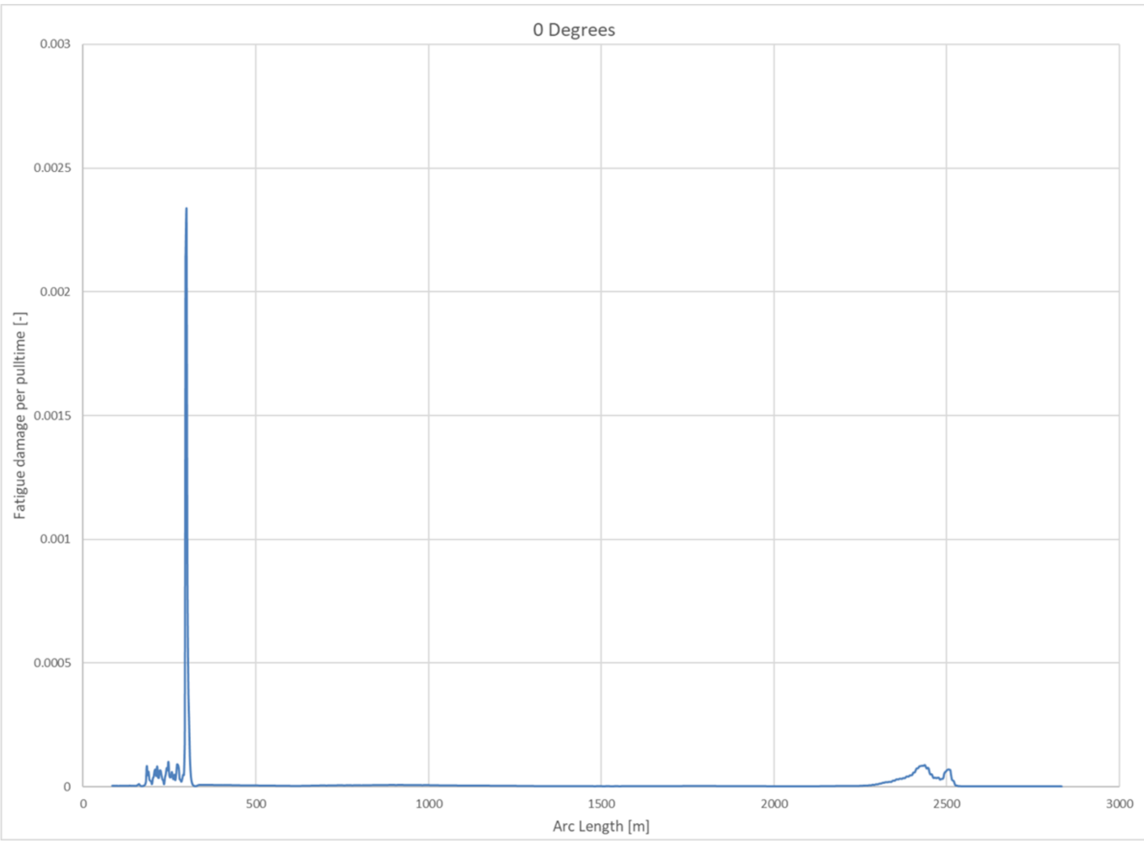

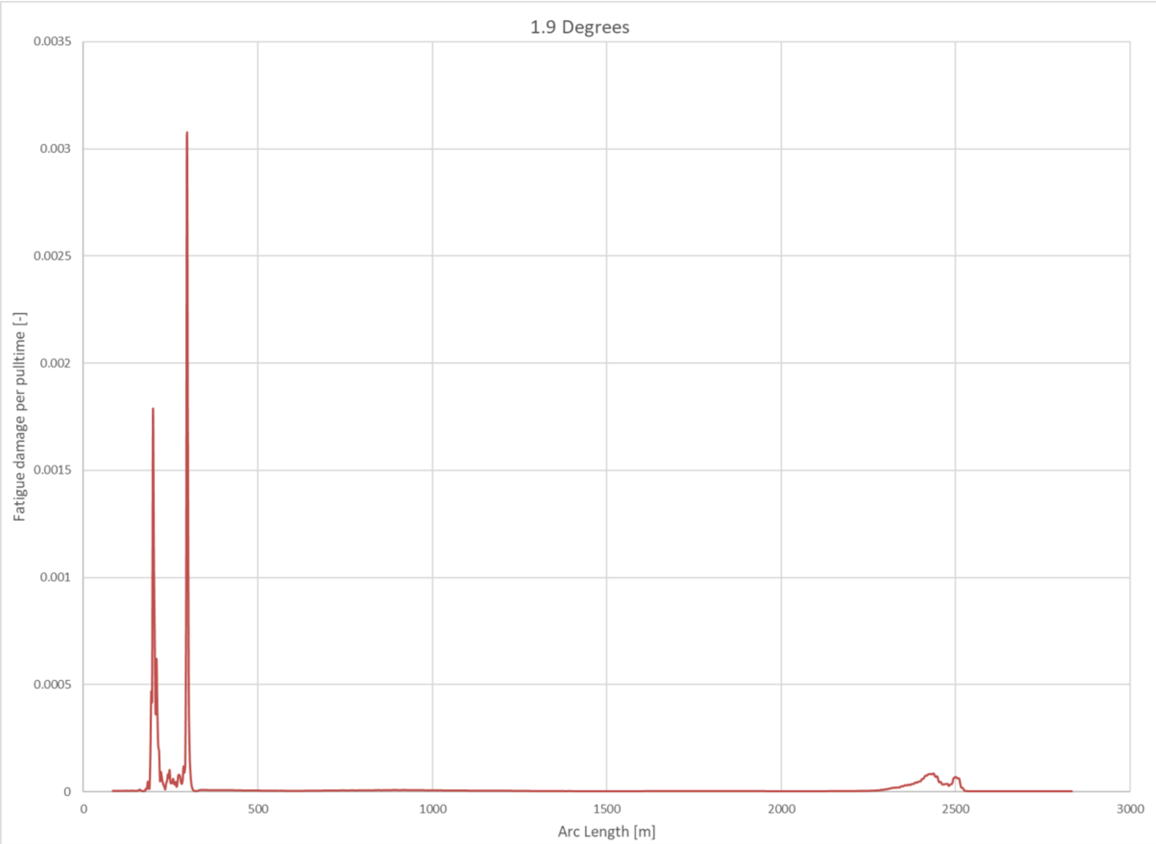

Figure F.1: Fatigue damage of the pipeline for the cases of 0 degrees and 1.9 degrees stinger angle, as calculated in the post-processing tool.

Appendix G

Rotational analysis

G.0.1 Impact of boundary conditions

In this section, the impact of the boundary conditions on the rotation of the pipeline will be examined. More specifically, the fixed End B of the pipeline is placed 300 meters approximately away from the touchdown point. To investigate if the presence of the fixed end influence the rotational behaviour of the pipeline, two new models were created in OrcaFlex, where the fixed End B was placed 1 km and 3 km away from its initial position. Dynamic analysis was performed during which there was line feeding so that the nodes from the overbend area reached the seabed. There are two possible scenarios. The rotation angles from the new models are either the same as the ones presented before, or larger because the boundary condition is moved further away from the location of rotation initiation.

Indeed, the analysis revealed that the rotation angle increases as the fixed End moves from 300 to 1300 to 3300 meters away from the touchdown point. For example, the final rotation angle of one node(at 196.3 meters arc length) increases from 109.6 degrees to 118.5 degrees (End B at 1300 meters) and finally to 126.5 degrees (End B at 3300 meters). The results of the final rotation angle of a particular node (196.3 m) when it lands on the seabed, can be seen in the Table G.1. Hence the resistance to rotation is weaken.

It can be concluded that there is an impact of the boundary condition on the rotation of the pipeline. The farther the boundary condition is, the more rotation is allowed. At some point the pipeline rotation should converge to a single value. For an accurate prediction of the angle of rotation, the effect of more factors should be taken into account. In reality, the position of the fixed end is not the only factor which influence the amount of rotation.The rotational resistance due to pipe-soil interaction is a parameter with significant influence on the pipeline behaviour on the seabed. Therefore, if one is interested to the specific amount of rotation, then a detailed analysis must be made, in which all factors will be encountered. For this research, it is enough to realise that the results depend on the modelling assumptions and that they do not refer to reality.

Table G.1: Magnitude of pipeline rotation with respect to the position of the fixed End B of the pipeline.

Location of End B [m]	-1500 (base case)	-2500	-4500
Max rotation angle (node at 196.3 m) [deg]	131	137	143
Difference [deg]	-	6	12

G.0.2 Extra results from rotational analysis

Case 1- Limit case: Elastic material

The Figure G.1 presents the time history of bending and total strain of the outer top fibre of the cross section in a node. The positive values correspond to extension and the negative to compression. It can be seen that the node experiences reverse bending (after 2000 s) and the top outer fibre that initially was extended, finally it is compressed.

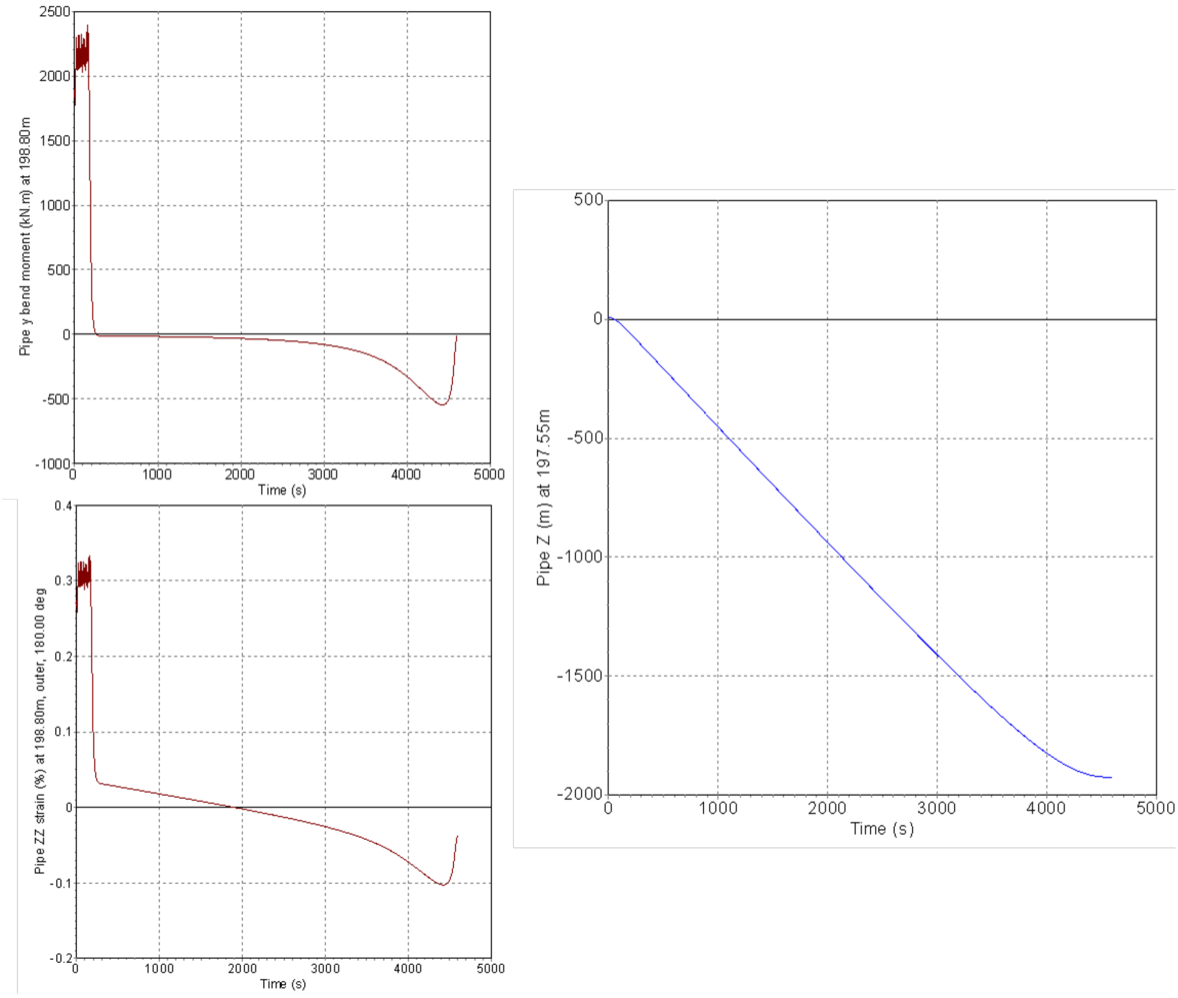

Figure G.1: Case 1- Limit case: Elastic material. Top: Bend moment time history graph for a node initially located at the beginning of the stinger. Positive bend moment values in the early seconds of the simulation corresponds to the overbend bending on the stinger. Negative bend moment corresponds to the reversed bending in the sagbend area. Bend moment is zero when the node touches the seabed. Bottom: Total strain time history graph of the top outer fibre of the cross section of the same node. The total strain is a result of bending strain and tensile strain. The outer top fibre is extended in the overbend while it is compressed in the sagbend. Right: The position of the node with respect to the global Z axis during simulation.

Case 2: Elastoplastic material- Normal Installation

The bending moment and total strain of the outer top fibre of the cross section of the same node (198.8) can be seen in Figure G.2. In contrast to Case 1, the diagrams follow an upward slope after the 3500 seconds. This happens due to the rotation of the pipeline at that moment, hence the top fibre is again extended and not compressed. In addition, the maximum bending moment in Case 2 is smaller than that from Case 1. This is plausible due to the non linear bending stiffness that is defined for the material. A final difference observed in the results of the two cases is that the total strains become zero later in the simulation (2300 s) for case 2 compared to case 1 (1800 s). The reason lies in the residual strains. These residual strains are not present in Case 1.

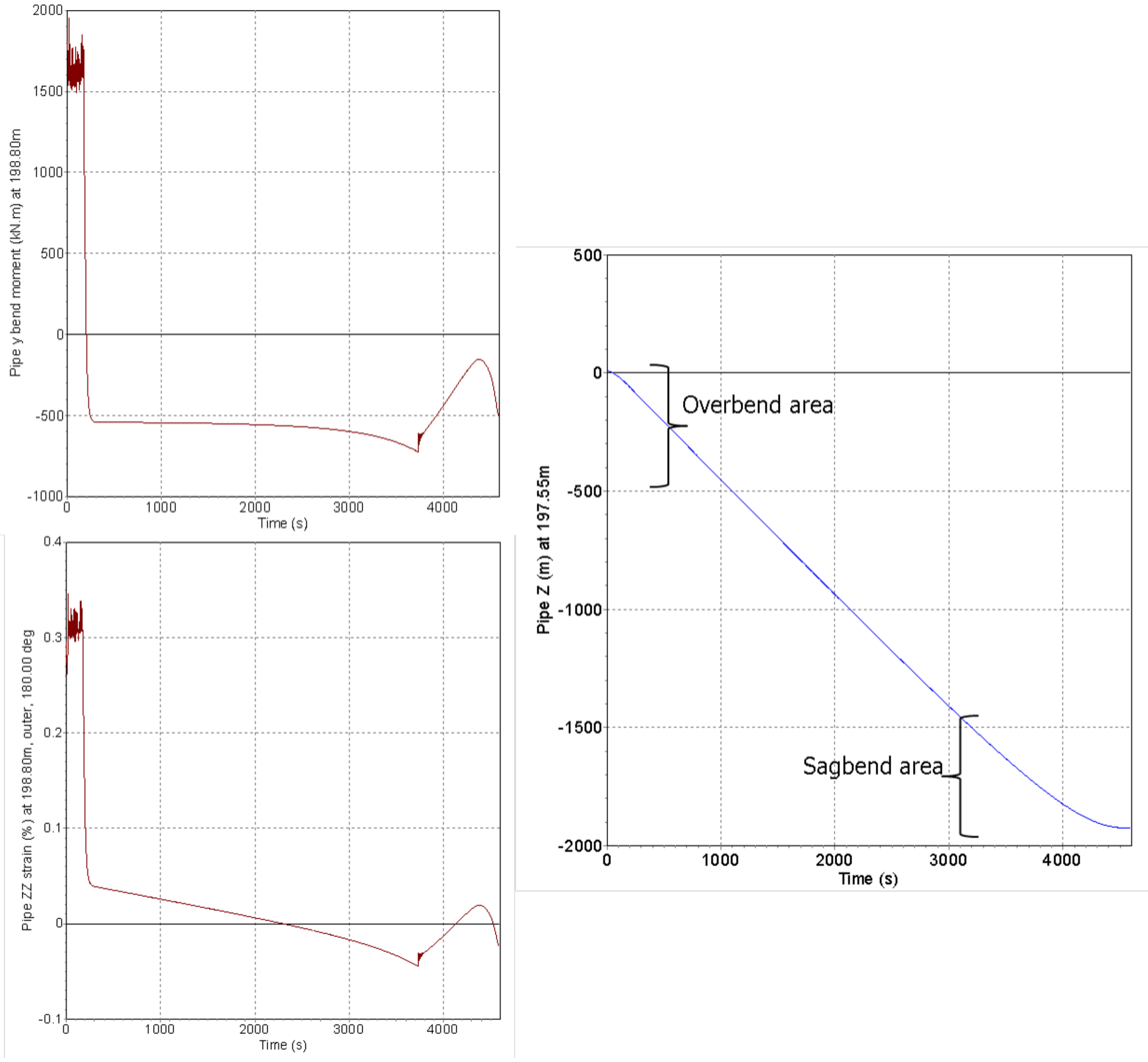

Figure G.2: Case 2- Elastoplastic material- Normal Installation. Top: Bend moment time history graph for the node 198.8, initially located at the beginning of the stinger. Positive bend moment values in the early seconds of the simulation corresponds to the overbend bending on the stinger. Negative bend moment after 3000 seconds of simulation time corresponds to the reversed bending in the sagbend area. Bend moment increases after 3500 seconds due to rotation. Bottom: Total strain time history graph of the top outer fibre of the cross section of the same node (198.8). The total strain is a result of bending strain and tensile strain. The outer top fibre is extended in the overbend and due to rotation after 3500 seconds, it is extended in the overbend as well. Right: The position of the node with respect to the global Z axis during simulation.

Case 3: Elastoplastic material- Residual curvature

In this case, the pipeline includes a pre-bent pipe section. The bending moment and total strain time history in the node 198.8 (m) can be seen in Figure G.3. This node belongs to the pre-bent section. The main differences compared to the plots of case-2 are highlighted here.

The initial bend moment and strain in the pipe cross section in the overbend are significantly decreased. That is due to the use of pre-bent curvature. The pre-bent section has smaller radius of curvature than the stinger radius of curvature. Therefore, the induced bending moment in the pre-bent section supported by the stinger, is reduced.

The curved section is pulled straight in the catenary area. Due to the plastic deformation of the pipe on the stinger, the top outer fibre of the cross section will be under compression when the section is pulled straight. Afterwards, due to the effect of the rotation, the magnitude of the moment and strain reduces. Before reaching the TDP, the node appears its maximum rotation, resulting into the minimisation of the bend moment. Finally, when the pipe section rest on the seabed, the top outer fibre is again under compression. This occurs due to the residual lay tension on the seabed. The residual lay tension results in an increase of the radius of the curvature in the pre-bent section. As a consequence, the top outer fibre is compressed.

The magnitude of the compressive strain (-0.17%) of the node at the end of the simulation (on seabed) is larger than that in case 2 (-0.03%). The larger residual curvature is responsible for the increase in the strains. When the residual lay tension is applied on the extra-curved pipe section, the induced compressive strain in the top fibre is more significant.

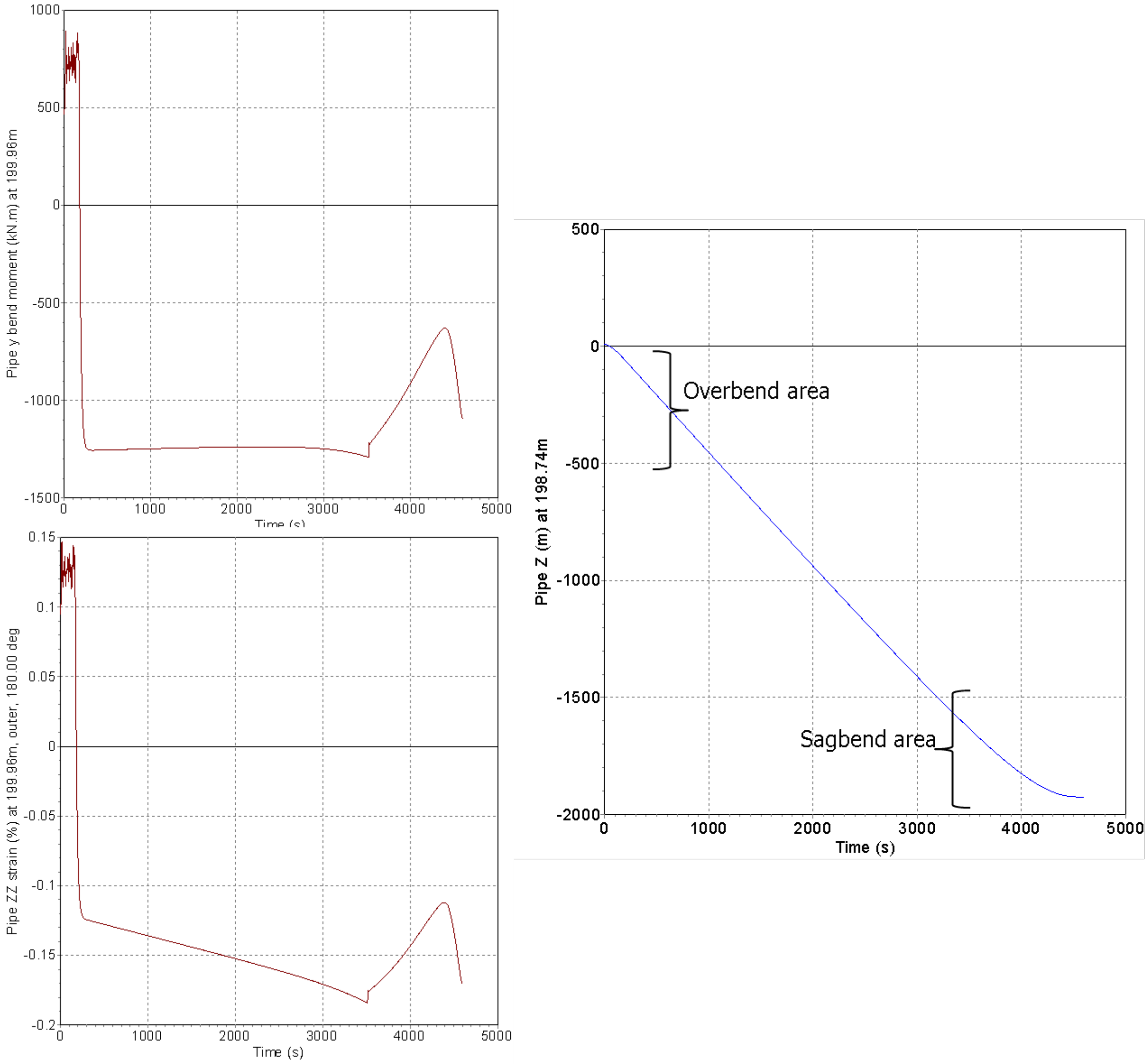

Figure G.3: Case 3- Elastoplastic material- Residual curvature. Top: Bend moment time history graph for the node 198.8, located at the beginning of the residual curvature. Positive bend moment values in the early seconds of the simulation corresponds to the overbend bending on the stinger. Negative bend moment after 3000 seconds of simulation time corresponds to the reversed bending in the sagbend area. Bend moment increases after 3500 seconds due to rotation. Bottom: Total strain time history graph of the top outer fibre of the cross section of the same node (198.8). The outer top fibre is extended in the overbend and due to rotation after 3500 seconds, it is extended in the overbend as well. Right: The position of the node with respect to the global Z axis during simulation.